Enzymatic Synthesis of Functional Polyesters and Their Modification by Grafting Reactions

Dissertation

Zur Erlangung des akademischen Grades

Doctor rerum naturalium (Dr. rer. nat.)

Vorgelegt der

Naturwissenschaftlichen Fakultät II-Chemie, Physik und Mathematik

der Martin-Luther-Universität Halle-Wittenberg

von

Herrn Dipl.-Chem. Toufik Naolou

geb. am 01. August 1979 in Aleppo, Syrien

Gutachter

1. Prof.Dr. Jörg Kreßler

2. Prof. Dr. Carmen Scholz

Halle (Saale), den 23.04.2014

DEDICATION

"To all who sacrificed for dignity, justice and equality in the Arab

world"

Table of Content

Abbreviations

AFM	Atom Force Microscopy
ATRP	Atom Transfer Radical Polymerization
Asp	Aspartic Acid
CAC	Critical Aggregation Concentration
CuBr	Copper bromide
CMC	Critical Micellization Concentration
CAL-B	Lipase B derived from Candida Antarctica
CRP	Controlled Radical Polymerization
CuAAC	Copper (I) Catalyzed Huisgen 1,3-Dipolar Azide-Alkyne Cycoloaddition, "Click" Chemistry
DCC	dicyclohexylcarbodiimide
DCM	Dichloromethane
DLS	Dynamic Light Scattering
DMA	Dimethy Adipate
DMAP	4-(Dimethylamino)pyridine
DMF	Dimethylformamide
DMSO-d_6	Deutrated dimethylsulfoxide
DP	Degree of Polymerization
DSC	Differential Scanning Calorimetry
DVA	Divinyl Adipate
FM	Fluorescence Microscopy
His	Histidine
HDA	Hetro-Diels-Alder
Et$_3$N	Triethylamine
EDCI	1-Ethyl-3-(3-dimethylaminopropyl)carbodiimide
FDA	Food and Drug Administration
FTIR	Fourier Transform Infrared
NMR	Nuclear Magnetic Resonance
mPEO-N$_3$	Azide-Terminal Poly(ethylene oxide)-Monomethylether
mmA	Mean Molecular Area
MWCO	Molecular Weight Cut Off
PAA	Poly(2-(azidomethyl)-2-methylpropane adipate)

PAA-*g*-PEO	poly(2-(azidomethyl)-2-methylpropane adipate)-*g*-poly(ethylene oxide)
PAA-*g*-PEO$_{op}$	poly(2-(azidomethyl)-2-methylpropane adipate)-*g*-poly(ethylene oxide) in "one pot"
PCL	Poly(ε-caprolactone)
PDI	Polydispersity
PEO	Poly(ethylene oxide)
PGA	Poly(glycerol adipate)
PMDETA	N,N,N′,N″,N″-pentamethyldiethylenetriamine
RAFT	Reversible Addition Fragmentation Chain Transfer
ROP	Ring Opening Polymerization
SEC	Size Exclusion Chromatography
SEM	Scanning Electron Microscopy
TEM	Transmission Electron Microscopy
TGA	Thermogravimetric Analysis
THF	Tetrahydrofuran

Symbols

π	Surface Pressure
δ	Chemical Shift
θ	Scattering Angle
λ	Wavelength
Γ	Decay Rate
$\Delta\widetilde{H}_m$	Specific Enthalpy of Melting
D_{app}	Apparent Diffusion Coefficient
q	Scattering Vector
n_0	Refractive Index
M_n	Number Average Molar Mass
M_w	Weight Average Molar Mass
T_C	Crystallization Temperature
T_m	Meting Temperature
γ	Surface Tension
T	Temperature
ΔH^0_{mic}	Standard Enthalpy of Micellization,
X_{DSC}	Degree of Crystallinity
ε_s	Static Elasticity

Chapter 1
General Introduction

1.1   Historical perspective

It is surprising that industry began to produce polymers before scientists even knew the fundamental understanding of structure and nature of polymers. During that time development of polymer materials was carried out by "trial and error" which might be described also as "Edisonian" fashion. Polymer products appeared during that time either by modification of natural polymers, such as modification of cellulose to produce *celluloid*, or via syntheses of new polymers such as *Bakelite* which was produced by the reaction of phenol and formaldehyde.[1] The concept of high molecular compounds "macromolecular chemistry" was first introduced by the German organic chemist Hermann Staudinger in 1917. The concept was further expanded to become "polymer science" by Hermman F. Mark in order to cover the organic chemistry and physical chemistry of polymers.[2] In the thirties of the last century, many synthetic polymer products, such as polystyrene, poly(methyl methacrylate), polyethylene, poly(vinyl chloride), polybutadiene, polychloroprene, nylon-6,6, and poly(ethylene terephthalate), were developed as a result of the urgent need to find alternatives for natur materials which were of short supply. Silicon rubber was produced during the forties of the last century, whereas polyolefins beside polycarbonate production started during 1950s. The year 1953 saw the development and production of polyethylene under low pressure using Ziegler catalyst whereas in 1954 Giulio Natta produced for the first time high molar mass polypropylene.[3] The anionic polymerization technique was also invented by Szwarc et al. in 1956.[4] This synthetic approach especially enabled polymer chemists for the first time to control for number average molar mass (M_n), the degree of polymerization (DP), and the polydispersity index (PDI). Additionally, this technique opened the door to synthesize block copolymers since macro-anions formed during the polymerization exhibit living properties. Living cationic polymerization was developed in the 1970s and 1980s.[5–7] The first report about enzymatic polycondensation was demonstrated in the middle of the 1980s. This technique was further applied to polymerize cyclic ester monomers (lactones) in 1993.[8] Enzymatic polymerization indeed enabled polymer chemists to prepare functional polyesters under mild conditions without the need of the protection/deprotection steps. The early 1990s saw the introduction and development of novel approaches to synthesize polymers called

controlled radical polymerization (CRP) was possible.[9] This approach covers three novel polymerization techniques, including reversible addition-fragmentation chain transfer polymerization (RAFT),[10] atom transfer radical polymerization (ATRP),[11,12] and nitroxide-mediated radical polymerization (NMP).[13]

In conclusion, substantial developments were indeed made in different fields of polymer science during the last century such as, finding new techniques to synthesize polymers with various architectures, understanding the mechanisms, kinetics of different polymerization techniques and or the physical properties of polymers with various architectures under different conditions.   In fact, our nowadays knowledge in organic synthesis and polymer chemistry enable scientists to prepare virtually any monomer and its associated polymer.[14] According to the new synthesis techniques which have appeared during the past twenty years, many polymers with complex architectures have been synthesized such as, cyclic, multicyclic, dendritic, hyperbranched, star, graft, and arborescent.[15] It should be noted that synthesis of such complex topologies before that time would not have been possible.

1.2   Synthesis and applications of graft copolymers

Graft polymers or copolymers belong to the family of nonlinear, branched segmented copolymers in which the polymer backbone has a number of side chains of different chemical nature.[16] Graft polymers have attracted increasing attention due to their unusual properties caused by confined and compact structures in comparison with the identical linear counterpart having similar molar mass.[17] Such unique structural characteristics make graft copolymers candidates for a lot of advanced applications, such as preparation nanostructures,[18] preparation of hybrid nanostructure,[19] biomedicine, [20] super soft elastomers,[21] and in photonics.[22]   The development of advanced synthetic techniques such as living/controlled polymerization, and "click" chemistry facilitate the synthesis of graft copolymers with well-defined structure and low molecular polydispersity. Graft copolymers can be synthesized *via* three main synthetic routes as shown in Figure 1.1.

1.2.1   "Grafting-through" strategy

This method is based on polymerization of macromonomers having a α-polymerizable group which offers the ability of controlling the grafting density by controlling the ratio between monomers and macromonomers during the polymerization process. Additionally, it is possible using this technique to synthesize graft copolymers having well-defined chemical structures since the characterization of the side chains occurs prior to the grafting reaction.
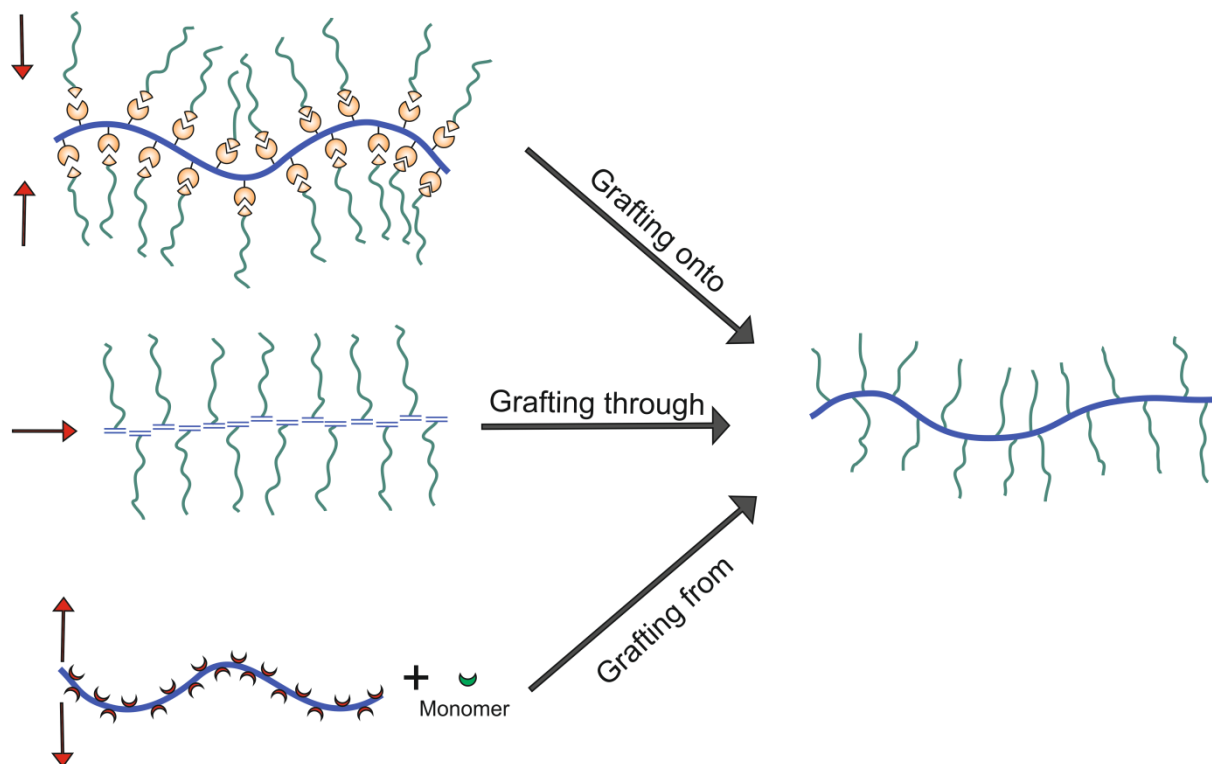
Figure 1.1   The main synthetic route to prepare graft copolymers.

Using the grafting-through method can also produce graft copolymers having 100% grafting density (every repeating unit has one side chain). Unfortunately, grafting reaction does not usually include all of the macromonomers exists in the reaction vessel. Even by using effective polymerization techniques such as ring-opening metathesis polymerization (ROMP), the complete conversion of macromonomers seems to be also not feasible, mostly due to the low reactivity of macromonomers and large hindrance between α-functionalized macromonomers and the reactive sites in the propagating graft copolymer. Thus, it is always necessary to purify the final product from unreacted macromonomers which is certainly time consuming.

Preparation of graft copolymers by "grafting through" strategy are carried out using three synthetic pathways [23]

1.2.1.1 Polycondensation reaction

Many scientists have reported the direct synthesis of comb-like polyesters having aliphatic alkyl side chains by utilizing monomers that can participate in condensation reactions and having *n*-alkyl chains within its structure. Lenz *et al.* reported the synthesis of poly(2-*n*-alkyl-1,4-phenylene terephthalate) through polycondensation processes between terephthalic acid

and 2-n-alkyl-hydroquinone.[24] Additionally, Watanabe *et al.* reported on the preparation of a series of rigid-rod polyesters having aliphatic side chains.[25]

1.2.1.2 Homopolymerization of monomers or macromonomers

Rehberg and Fisher have introduced the first comb-like polymer in 1944 based on poly(*n*-alkyl acrylate)s which was prepared radically.[26] Thereafter, many comb-like polymers were reported such as poly(α-olefine)s, poly(*n*-alkyl methacrylate)s, poly(*n*-alkyl acrylamide)s,[27] and poly(*n*-alkyl itaconate). However, controlling the molar mass and regularity of molecular chains always presents a difficult task when scientists utilize this conventional polymerization technique to prepare comb-like polymers.

1.2.1.3 Copolymerization of monomers and macromonomers

A series of graft copolymers having poly(ethylene glycol) (PEG) as a side chains have been synthesized by "grafting through" strategy by polymerize reactive monomers and *ω*-functional PEG*,* such as, poly(styrene)-g-PEG,[28] poly(methyl methacrylate)-g-PEG,[29] poly(butyl methacrylate)-g- PEG.[30]

1.2.2 "Grafting onto" strategy

Grafting-onto strategy is based on grafting the end-functional polymer onto a linear backbone through the reactive sites present on each monomer units.[23] Utilization of the "grafting-onto" route yields well-defined graft copolymers since precise characterization of side chains and the backbone can be carried out prior to the grafting reaction. However, this technique has also several drawbacks, including limited grafting density, and the necessity of purifying uncoupled side chains from the grafted copolymers. The grafting density varies in the case of "grafting-onto" technique according to the chemical structure of the utilized side chains where for the more bulkier side chains such as poly(styrene), poly(butyl acrylate), and poly-(n-butyl acrylate)-b-poly(styrene) grafting densities are smaller than 50%.[31] Such a result is the consequents to the steric hindrance caused by the attached side chains to the reactive side on the polymer backbone. In contrast, using relatively thinner side chains such as poly(ethylene oxide) (PEO) will result in brush polymers with grafting density up to 88%.[31] The main key for the successful preparation of graft copolymers *via* "grafting-onto" strategy is to use efficient coupling reactions between the end-functionalized macromonomer and the functional backbone. In general, graft copolymers using "grafting-onto" approach can be prepared using two methods:[23] i) covalent "grafting-onto" *via* chemical coupling reaction between the side chains and polymer backbone,[32] or ii) non-covalent "grafting-onto" by supramolecular

chemistry assembly processes through metal-ligand coordination,[33] π-π interaction, hydrogen bonding,[34] and or ionic interaction.[35]

1.2.3 "Grafting from" strategy

This method can be defined as the process of initiating the polymerization of side chains from the predetermined initiation sites on the polymer backbone (macroinitiator), which is either existing within the structure of monomers before polymerization or being introduced onto the backbone afterwards.[23] Many reports have appeared describing this technique to synthesize well-defined graft copolymer. [36,37] Graft copolymers prepared by this method are characterized by high grafting density and a narrow molar mass distribution. Using controlled radical polymerization such as ATRP or ROMP for grafting reaction, yield well-defined graft polymers since the low concentration of instantaneous propagating species decrease significantly the coupling and termination reactions. Furthermore, the gradual growth of the side chains could also decrease notably the steric effect which normally exists in the case of "grafting-onto" and grafting-through" routes.[17] Additionally, it is not necessary to use dialysis and fractionation methods to purify the resulting graft copolymers since there is no unreacted macroinitiator. Nevertheless, this technique also suffers from many drawbacks such as carrying out grafting reactions in highly diluted systems and/or the relatively low monomer conversion which is necessary to avoid crosslinking reactions between the macroinitiators. In fact, working under such conditions leads to a significant waste of monomers, solvent and also long reaction time.

It is worth mentioning here that the synthesis of amphiphilic graft copolymers having two different side chains have been previously reported , which can be obtained either by using only one type of grafting strategy[38] or by a combination of two types,[39] e.g. the combination of "grafting from" and "grafting onto".[40]

1.3 Biodegradable polymers and functional polyesters

Over the past century scientist have focused on inventing new materials to meet the needs of modern life and further to find alternative methods to decrease production costs. However, many environmental problem emerge as a result of using toxic catalysts during polymer production or due to difficulties of disposal plastic wastes.[41] Thus, researchers have developed over the last three decades eco-friendly reactions and materials in order to achieve sustainability. Biodegradable polymers came to the market as alternative products to nondegradable conventional polymers for packaging and biomedical applications.[42] Aliphatic

polyesters are considered to be the most of used biodegradable polymers especially for biomedical applications.[43] However, mechanical, biological, and physical properties of these polyesters are not always meeting the technical needs of many applications.[44] The presence of pendent functional groups on the polyesters backbone, however, can have a significant impact on properties for potential applications.[45–47] For instance, polyesters with pendant cationic groups could be used to make surfaces antibacterial and for gene therapy.[48,49] Furthermore, it has been demonstrated that the covalent conjugation of drug to the functional groups of amphiphilic block copolymers, which are designed to be used as nano-size drug carriers, is much better than the classic physical encapsulation as it prevents the leakage of drugs by diffusion from micelles.[50] Additionally, introducing functional groups onto the blocks that forms the core of micelle can enable adjusting the encapsulation and release properties of micelles or nanoparticles by some special interactions between the block forming the core and the drug, such as hydrogen bond,[51] π-π interaction,[52] electrostatic complexation,[53] and some chemical reaction.[54] Moreover, introducing pendent functional groups to the polyester can enhance its degradation properties,[55] offering opportunities to attach the polymer backbone with biological active components or increase the cell/matrix interactions in the tissue engineering field.[56] Despite these advantages, introduction of functional groups to the polyester backbone is still a challenge.[57] In general, functional polyesters can be synthesized *via*

    i) anionic activation of linear polyesters using non-nucleophilic bases such as lithium diisopropyl amide to form polycarbanion on which electrophiles can be easily attached. [58]

    ii) ring-opening polymerization of functional lactones and lactides.[59–62]

    iii) ring opening polymerization (ROP) of functional O-carboxyanhydrides.[63]

    iv) catalyzed polycondensation of polyfunctional monomers.[64,65]

In terms of limitations, using the first strategy (i) to synthesize functional polyesters could cause simultaneous main-chain degradation.[66] On the other hand, using ring opening polymerization of lactones to synthesize functional polyesters offers a lot of attractive advantages,[67] such as the reaction proceeds in one direction without generating leaving groups during the course of reaction,[68] high molar mass polyesters within short time, low polydispersity and it proceeds by chain growth mechanism which can control its telechelic functional groups.[69] Ring opining polymerization of O-carboxyanhydrides has the same advantages as lactones except that carbon dioxide is released during the polymerization reaction, readily to evaporate at reaction temperatures. However, it is not possible using ring

opening polymerization to synthesize polyesters with free hydroxyl, carboxylic acid or mercapto pendent functional groups in one step since these functional groups are considered as initiators for ring opining polymerization. Actually, polyesters with free hydroxyl, carboxylic acid or mercapto pendent functional groups can be synthesized *via* ring opining polymerization either by polymerization of protected cyclic monomers (lactones, lactides and O-carboxyanhydrides) followed by deprotection reaction, [55,63,70–74] or by synthesizing polyesters which contain ketone groups within the polyester backbone followed by hydrogenation reaction of the ketone bond to form hydroxyl groups.[57,75,76] The protection steps of monomers prior to polymerization, in addition to possible degradation of the polyester backbone during the deprotection step are considered the major disadvantages of this synthetic route. In contrast, functional polyesters can be synthesized in one step by enzymatic polycondensation reactions without the need of protecting monomers.

1.4 Enzymatic polymerization

Enzymatic polymerization is defined as " the *in vitro* polymerization of artificial substrate monomers catalyzed by an isolated enzyme *via* nonbiosynthetic (nonmetabolic) pathways".[77] *In vitro* enzymatic catalysis was first reported by a Polish chemist in the 1930s for the synthesis of esters in organic media.[78] However, these results did not attract much of the attention of scientists, until Klibanov et al. reported similar reactions in 1984.[79] Since then, more interest has been given for this novel technique in the field of organic synthesis due to its ability to control the rigioselectivity and stereochemistry of the products, major limitation in organic synthesis techniques.[77] The enzymatic polymerization, however, was introduced in the late 1980s and extensively investigated in the following two decades. Lipase-catalyzed polyester synthesis is considered to be one of the most extensively investigated topics in enzymatic polymerization. Enzymatic polycondensation route, especially lipase/esterase-catalyzed polymerization, has many advantages compared to conventional chemical routes, [80–82] such as

i)   mild reaction conditions which can reduce the energy consumption of the overall process and the possibility of polymer chain degradation that might occur by working at high temperatures.

ii)   It does not require protection-deprotection steps due to the high ability of enzymes to control chemo-, enantio-, and regioselectivity of the products.

iii) high catalytic activity.

iv)   fewer byproducts (considered as clean process).

v)   the enzyme is recyclable when it is immobilized, which reduces the catalyst costs.

vi) sustainability of the enzyme.

vii) enzymes are derived from renewable resources.

In principle, lipases are responsible to catalyze the hydrolytic cleavage of fatty acid triacyl glycerol ester *in vivo*. However, lipases can *in vitro* form ester bond instead of breaking it when the reaction is carried out in anhydrous media and the resulting by-products are removed. Lipases are considered to be the most popular biocatalysts for enzymatic reactions.[83] In particular, lipase derived from *Candida Antarctica* lipase B (CAL-B) is considered to be one of the most commonly used enzyme in the field of enzyme-catalyzed condensation polymerization for polyesters.[77,80] This enzyme is commercial available under the trade name Novozyme 435, which consists of physically adsorbed CAL-B within the macropores of poly(methyl methacrylate-co-butyl methacrylate) resin. In general, the immobilized enzymes can facilitate their removal from the final product, allowing for its reuse. Additionally, immobilization of enzymes can also improve their properties like stability, activity, their selectivity to non-natural substrates, and enantioselectivity.[84]

1) Ring-opening polymerization of lactones

2) Polycondesatios polymerization of

i) Carboxylic acids or their esters with alcohols
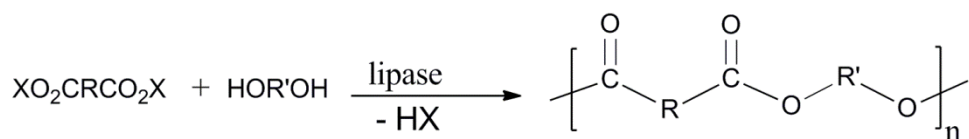
ii) Hydroxyacids or their esters
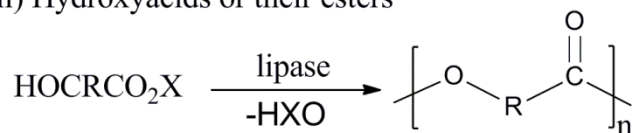
X: H, alkyl, vinyl, alky etc

Figure 1.2 Main synthetic routes to prepare polyesters using enzyme as a catalysts. [77]

There are two main routes for enzymatic synthesis of polyesters which are shown in Figure 1.2.[77]

1.4.1 Lipase-catalyzed ring opening polymerization

This synthetic technique was first introduced in 1993 by Kobayashi et al. by carrying out ring opening polymerization of ε-caprolactone and δ-valerolactone.[85] Utilizing this route to produce polyesters has been extensively investigated and high molar mass polyesters were produced under relatively mild conditions. Additionally, this polyaddition reaction is performed with no or very limited amounts of side-reactions which makes it possible to control the polymer properties such as molar mass, molar mass distribution, and polymer end groups.[43] Interestingly, it has been illustrated that reaction kinetics and the achievable molar mass in lipase–catalyzed ROP increase by increasing the ring size of lactones in contrast to traditional chemical methods which has led to the polymerization of macrolactones that are derived from natural sources.[86] For instance, poly(pentadecalactone) was enzymatically synthesized using ω-pentadecanolide as a monomer with a molar mass of up to 150 000 g mol^{-1}. Controlling the end-group of a polymer is considered as a critical issue in polymer chemistry especially in the case of synthesizing amphiphilic polymers. Thus, this topic has been extensively investigated in the lipase-catalyzed ROP of lactones. Using functional alcohol as initiator was applied in this technique to incorporate functional groups into the polymer chain. However, a mixture of cyclic species, water initiated polymer chains and polymer chains with desired functional groups were obtained. Actually, the maximum degree of obtained functionality was 95% even when stringent drying conditions were applied.[87]

1.4.2 Lipase-catalyzed polycondensation

Enzymatic polycondensation is defined as "enzyme catalyzed esterification and transesterification between diacids or their activated esters with diols or self-polycondensation of hydroxyacids in non-aqueous media". Like any condensation reaction, enzymatic polycondensation is usually a reversible reaction since it is accompanied by low molar mass compounds as byproduct. Removal of this byproduct is considered as a critical factor to shift the equilibrium towards the products. Monomers having activated acyl donors, such as oxime ester, thioester, and anhydrides, have been used instead of traditional carboxylic acids in order to increase the activity of the monomers towards enzymatic polymerization and to facilitate removing byproducts. Using enol esters , however, such as vinyl esters seems to be the most efficient synthetic route since they release unstable enols as a byproduct which tautomerizes readily to give the corresponding aldehydes or ketones.[83]

CAL-B is composed of 317 amino acid residues and its structure was determined in 1993.[88] Its active center has a catalytic triad, serine (Ser105)-histidine (His224)-aspartic acid

(Asp187). A large hydrophobic pocket exists above the Ser105-His224-Asp224 triad whereas a medium-sized pocket exists below it. The accepted mechanism by which CAL-B catalyzes transesterification reaction to yield polyester is illustrated in Figure 1.3. The catalyst site in the active center of CAL-B is the –CH$_2$OH of the Ser residue. The imidazole group of the His residue pulls a proton from –CH$_2$OH which augments the nucleophilicity of the oxygen in order to attack the carbonyl group in the substrate.
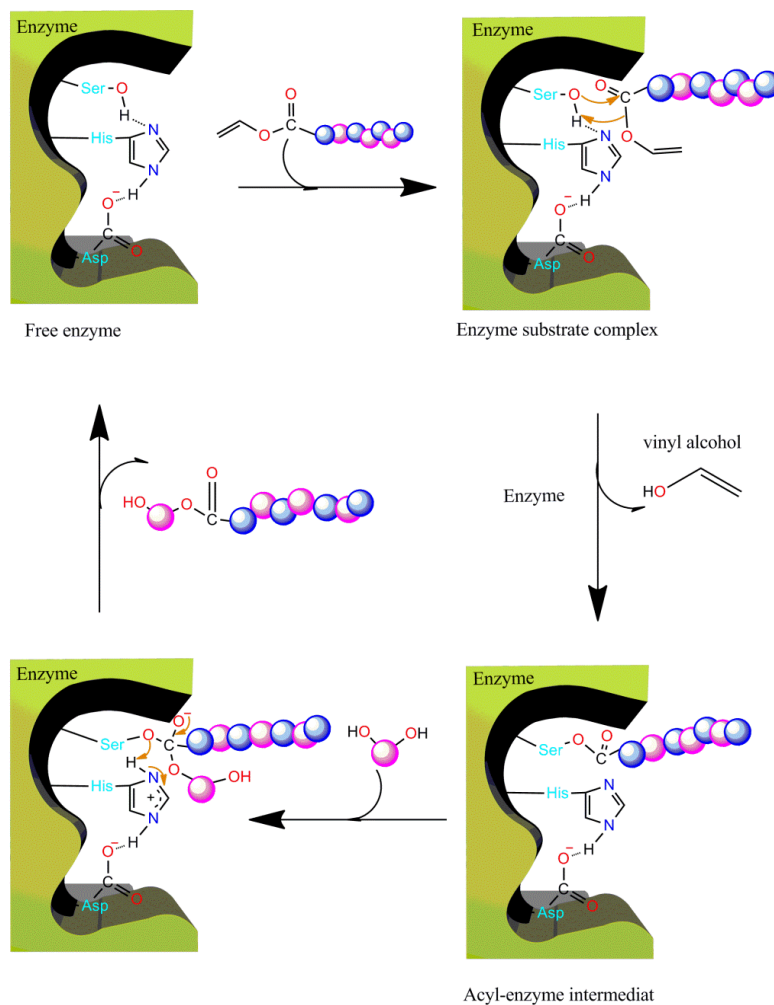
Figure 1.3 Illustration of lipase-catalyzed transesterification mechanism.[89]

Meanwhile, the carboxylate group of the aspartic acid residue helps the imidazole group to pull a proton of the Ser residue and trasnlocate it to the substrate and subsequently the corresponding alcohol will be released from the substrate. As a result, a covalent bond will be formed between the enzyme and the substrate to get the acyl-enzyme intermediate.

In the deacylation step, the nucleophile (which is generally water, or alcohol, or amine) will attack the acyl-enzyme carbonyl group. In this process the proton of the nucleophile is

transferred to the His residue of the enzyme. This hydrogen is transferred again to the Ser alkyl oxygen which causes the weakness of the enzyme-product complex bond which ultimately releases the reaction product from the enzyme allowing for its regeneration.[89,90]

Nevertheless, using the enzymatic polycondensation route to prepare polyesters also suffers from several drawbacks including[43]

i) Like any conventional polycondensation, enzymatic polycondensation requires a precise stoichiometric balance between the hydroxyl groups and reactive acids with high conversion ratio in order to obtain high molar masses.

ii) The need to remove resulting by-product(s) in order to shift the reaction equilibrium.

iii) The inability to control of the telechelic functional groups since polycondensation proceeds *via* step-growth mechanism.

In contrast to lipase-catalyzed ROP, using the enzymatic polycondensation route has a great benefit for the preparation of polyesters with free pendant functional groups in one step without the need of the protection/deprotection steps which might otherwise cause degradation of the polymer backbone. The chemo-, and regio-selectivity of lipase are considered to be the main reason behind their use. Accordingly, functional polyesters have been enzymatically synthesized with free pendent groups, such as alcohol [91,92], mercapto,[93] and carboxylic acid,[94] which cannot be synthesized in one step by enzymatic ROP. Furthermore, this technique allows for the production of polyesters form renewable resources as e.g. glycrol of sugars.

1.5 "Click" chemistry

In 2001, Sharpless introduced the concept of "click" chemistry and defined it as a "set of powerful, highly reliable, and selective reactions for rapid synthesis of useful new compounds and combinatorial libraries".[95] Any chemical reaction can be classified as a "click" reaction if it is characterized by the following features: modular and wide in scope, highly efficient with high yield, resulting in no or unoffending byproduct, stereospecific, its starting materials and reagents are readily available, insensitive to the type of solvent, and easily to be purified.[96] A particular interest has been paid during the last decade to the applications of "click" reactions in polymer synthesis since it can solve many of the critical problems which encounter this field.[97] Accordingly, utilization of "click" reaction in polymer synthesis facilitates the preparation of many novel polymers with complex chain topologies (ie, graft, star, dendrimers, and cyclic) or block copolymers which cannot be synthesized by conventional polymerization pathways.
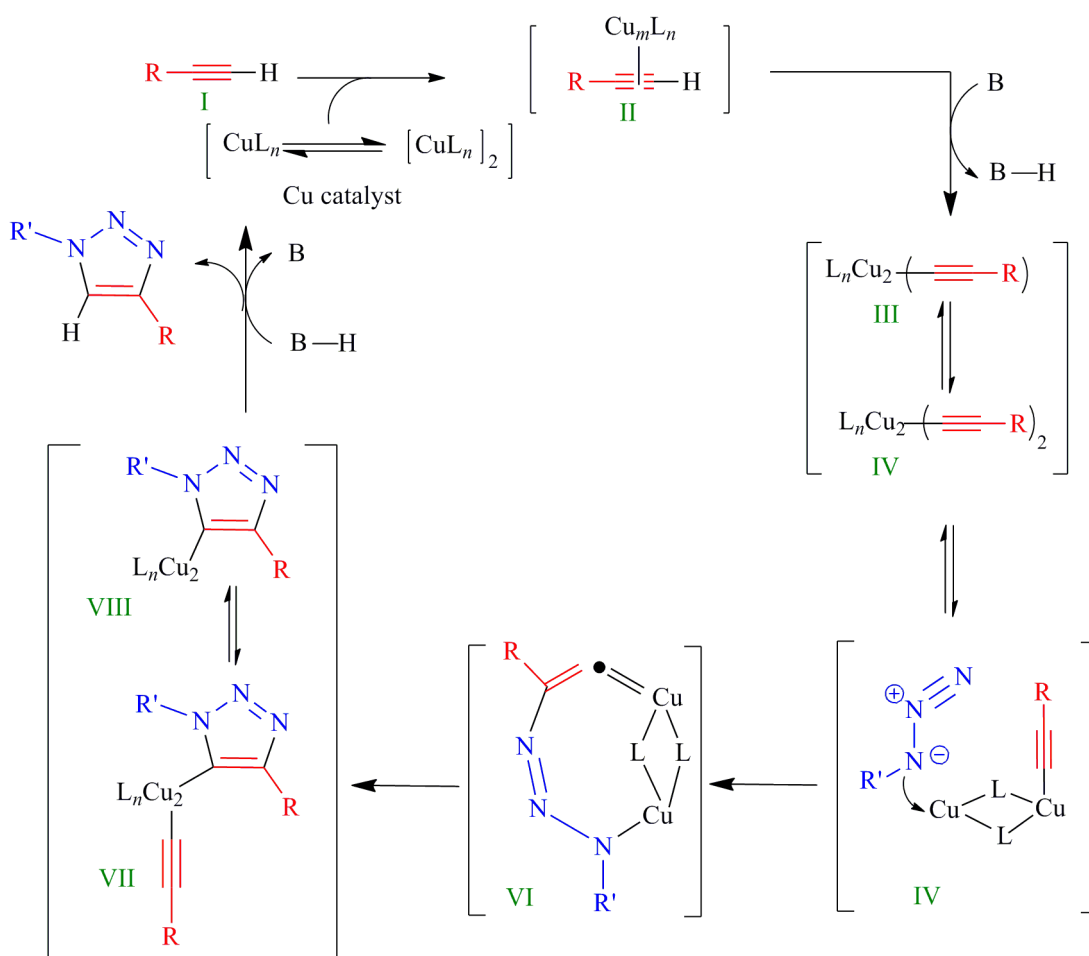
Figure 1.4 The mechanism proposed for CuAAC "click" reaction.[98]w here L is ligand, B is a base.

Copper(I) catalyzed 1,3-dipolar azide-alkyne cycloaddition (CuAAC) was introduced shortly after 2001.[99] This reaction has become within a few years the most important "click" reaction as it plays a particular important rule in organic and macromolecular synthesis. Azide and alkyne groups are stable in the presence of electrophiles or nucleophiles and they are almost completely unreactive towards biological molecules.[99] Additionally, both groups are not able to form a significant hydrogen bonds and they are relatively nonpolar, and thus are unlikely to change significantly the properties of compounds onto which they are attached.

The mechanism proposed for CuAAC click reaction is shown in Figure 1.4. The mechanism is explained as a stepwise process which begin with the formation of Cu(I) acetylide species *via* the π complex followed by azide complexation and cyclization. Finally, the triazole-copper derivative becomes protonated and subsequently dissociates to yield the final product beside the catalyst. Different compounds have been used as a ligand in this reaction to

dissolve the catalyst, such as amines, phosphines, triazoles, and pyridine. It has been reported that the type of ligand has a significant effect on the kinetics of the "click" reaction explained by decreasing the oxidation of Cu(I), and promoting the formation of the copper-acetylide complex.[100] However, the product which participates in CuAAC reaction is not suitable for biological applications due to the presence of transition metal traces. Significant interest has been made in the last couple of years in developing new "click" reactions that do not require metal catalysts while still exhibiting all "click" chemistry criteria.[101] One elegant approach is the reaction between azide and strained cycloalkynes developed by Bertozzi et al.[102] However, the reaction rate is relatively low in comparison with the CuAAC reaction. Thus, electron withdrawing substituents are added at the α-position of this triple bond (Figure 1.5a). Cycloaddition reactions of unsaturated species have been proposed also as alternative "click" reactions to the CuAAC reaction. As an example, Diels-Alder [4+2] cycloaddition between maleimide and anthracene derivatives has been proposed and used successfully in the polymer synthesis as metal free "click" reaction (Figure 1.5b).[103] The necessity of high temperature application, however, for the coupling reaction limits the usage of this synthetic pathway to polymeric structures that are thermally unstable. The groups of Kowollik and Stenzel reported recently an alternative hetero-Diels-Alder (HDA) route as a coupling reaction between terminal electron-deficient thiocarbonylthio group of polymers which are produced by RAFT polymerization technique and an appropriate diene (Figure 1.5c). The dienophilicity of the dithioester end group is further increased in HDA by utilization of trifluoroacetic acid or zinc chloride as a catalyst which enhances the electron-withdrawing effect of the Z-group. This reaction proceeds to a high conversion at reaction temperature of 50 °C and reaction time between 2 and 24 h.[104] An efficient and ultrafast hetero-Diels-Alder reaction has also been reported by the utilization of more reactive cyclopentadiene compared with linear dienes (Figure 1.5d).[105] Surprisingly, a high coupling yield was obtained within just a few minutes at ambient temperature without the need of any catalyst addition. Thus, this type of "click" chemistry is expected to become an important synthetic route in polymer synthesis.

(a)

(b)

(c)

(d)

(e)
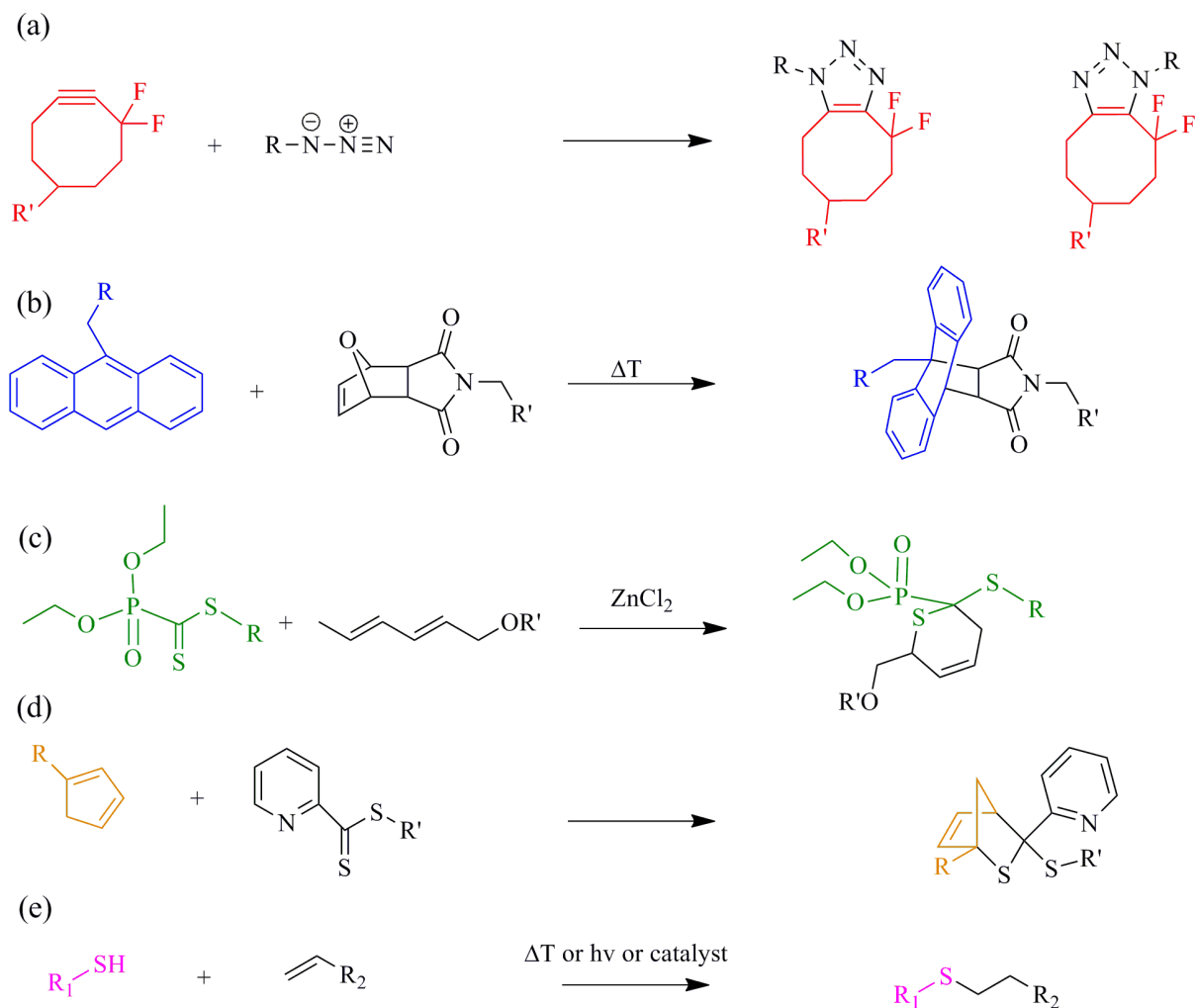
Figure 1.5 Examples of click reactions employed commonly in polymer synthesis. (a) strain-promoted azide-alkyne cycoloaddition. (b) Diels-Alder [4+2] cycloaddition between maleimide and anthracene derivatives. (c) Hetero-Diels-Alder HDA. (d) Ultra hetero-Diels-Alder reaction. (e) Thiol-ene click reaction.[15]

A series of thiol-based reactions with unsaturated bonds have highlighted recently as a powerful coupling chemistry (Figure 1.5e). Typically, these reactions can be classified into two main categories depending on the chemical nature of unsaturated bond and reaction conditions: i) thiol-ene reaction by ionic mechanism (Michael-type addition) or ii) by free radicals (thermally initiated or by UV-light). Thiol based "click" reactions are considered as simple, highly reactive, need short reaction times and can be performed at ambient temprature.[106]

1.6   Motivation and objective of this work

As already mentioned at the beginning of this chapter, there is currently a great interest to investigate the potential applications of macromolecules which have complex topologies, particularly graft copolymers. Actually, many reports have recently appeared showing superior properties of graft copolymers compared to the classical linear block copolymers, considering their ability to form more stable micelles with low critical micelle concentration (CMC), high drug loading, low melting point T_m and small crystallization degree.[107–110] Such features suggest the use of graft copolymers in the field of drug delivery systems instead of the classical block copolymers. To achieve such target the biodegradability and the biocompatibility of the synthetic graft copolymer should also be considered.

The main objective of this work is to synthesize well-defined graft copolymers that are suitable for drug delivery applications and to investigate their properties. In order to achieve this goal, a series of novel graft copolymers is synthesized where their main backbones are composed of biodegradable aliphatic polyesters. In fact, the presence of free pendent functional groups on the polyester backbone used in this study is found critical as it facilitates the grafting process using different coupling reactions. Thus, several approaches are suggested and applied to obtain functional polyesters with functional groups in each repeat unit. CAL-B is used as a catalyst for the polyester preparation, found suitable for products that can be used in the biomedical field. Poly(ethylene oxide) (PEO) chains are mainly attached as side chains in these reactants   since PEO are water soluble polymer that can form a hydrophilic shield protecting it from the immune system recognition and thus prolonging its *in vivo* circulation time.[111] Additionally, a comparison is made between the differences in properties achieved by synthesizing graft copolymers that have hydrophobic/hydrophilic block copolymers as a side chains versus synthesizing linear block copolymers that have identical chemical composition as the grafted chains. The comparison reveals the difference of the polymer properties in water and at the air/water interface. Such a comparison is aimed to find the potential applications for using graft copolymers instead of conventional linear block copolymers.

Chapter 2

Synthesis of Well-Defined Graft Copolymers by Combination of Enzymatic Polycondensation and "Click" Chemistry

2.1   Introduction

Linear aliphatic polyesters represent one of the most important groups of biocompatible and biodegradable polymers having a huge versatility with respect to physical, chemical, and biological properties.[112] The presence of pendant functional groups at the polyester backbone can be used for further modification of polymer properties. Anionic activation of linear polyesters using non-nucleophilic bases to form polycarbanion on which electrophiles can easily be attached,[113–115] ring-opening polymerization of substituted lactones,[59–61,64,116–121] and catalyzed polycondensation of polyfunctional monomers[65,91,92,122,123] is the main strategy used to synthesize aliphatic polyesters with pendant functional groups. When carrying out the polycondensation of glycerol with derivatives of dicarboxylic acids, it is necessary to use a chemoselective catalyst to obtain linear poyesters.[80] Using, for example, lipase from *Candida antarctica* type CAL-B as a chemoselective enzyme can result in linear polyesters because the enzyme favors the condensation process of primary alcohols rather than secondary alcohols.[124]

When polyesters with pendant groups are used to synthesize well-defined graft copolymers, functional groups should meet strict requirements such that

(i) They must be reactive enough to attach other polymer (oligomer) chains quantitatively under large steric restrictions.

(ii) They should undergo the coupling reaction in one step under mild conditions to avoid any degradation of the polyester backbone.

(iii) The coupling reactions should be selective only for this functional group, which means that protection/deprotection steps are not required for other functional groups present on the polymer backbone.

Recently, the concept of copper-catalyzed azide−alkyne cycloaddition CuAAC, "click" reaction, which was first introduced by Meldal et al.[125] and Sharpless et al.,[126] meets exactly the previously described requirements to synthesize graft copolymers using the "grafting onto" protocol.[31] It seems reasonable to use monomers containing clickable functional groups for enzymatic polycondensation rather than introducing clickable groups by polymer analogous reactions, which might also attack the sensitive ester groups of the polymer

backbone.[127] Therefore, this approach is based on the polycondensation of a N_3-containing diol that is used for polycondensation with divinyl adipate (DVA). This polymer is then used for "click" reaction with monoalkyne-functional poly(ethylene oxide) (alkyne-PEO, $M_n = 750$ g/mol). This reaction is based on the Huisgen 1,3-dipolar cycloaddition chemistry.[128] According to the properties of PEO such as biocompatibility and water solubility [61] and for applications of aliphatic polyester in bioresorbable medical applications,[129] connecting both species to graft copolymers should lead to potential biomedical materials. Here the aggregation behavior of the polymers in water is analyzed by dynamic light scattering (DLS), and the behavior at the air/water interface is studied by surface tension measurements and by Langmuir trough experiments.

2.2   Experimental section

2.2.1   Materials

All chemicals were purchased from Sigma-Aldrich unless otherwise stated. Hydrobromic acid, *n*-hexane, sodium azide, dimethyl sulfoxide (DMSO), tetrahydrofuran (THF), dichloromethane (DCM), dimethylamino pyridine (DMAP), *N*-(3-dimethylaminopropyl)-*N'*-ethylcarbodiimide hydrochloride (EDCI), copper bromide CuBr, *N,N,N',N'',N''*-pentamethyldiethylenetriamine (PMDTA), 5-hexynoic acid, hydrochloric acid, and poly(ethylene oxide) monomethyl ether $M_n = 750$ g/mol were used as obtained. Novozym 435 (derived from *Candida antarctica* type B and immobilized on an acrylic macroporous resin) was dried under vacuum at 4 °C over P_2O_5 for two days prior to use. DVA was purchased from TCI-Europe. 3-Methyl-3-oxetanemethanol was purchased from Alfa Aesar. The membranes used for dialysis were bought from Spectrum Laboratories (regenerated cellulose) and had an MWCO of 1000 g/mol.

2.2.2   Measurements

Weight-average molar mass (M_w), number-average molar mass (M_n), and molar mass distribution (M_w/M_n) were measured by gel permeation chromatography (GPC) Viscotek GPCmax VE 200 using DMF or THF as eluent with a flow rate of 1 mL/min through column set H_{HR} + GMH_{HR}-N (Viscotek, mixed bed). The GPC was equipped with a refractive index detector (VE 3580 RI detector, Viscotek). Polystyrene standards were used for calibration. In the case of using THF, the temperature of the column was adjusted to 22 and to 60 °C for DMF.

^{1}H NMR and ^{13}C NMR spectra were recorded using a Varian Gemini 2000 spectrometer operating at 400 MHz for ^{1}H NMR and 200 MHz for ^{13}C NMR spectroscopy.

The surface tension γ of the aqueous polymer solutions was measured by the Wilhelmy plate method using an automated DCAT tensiometer (Data Physics Instruments). A solution of 0.036 g/L of the polymer in bidistilled water was filtered through a 0.45 μm pore-size PTFE filter prior to use. Following each injection, the surface tension was measured after 10 min of stirring and a 2 h waiting period. Measurements were carried out at 25 °C.

DLS measurements were performed using an ALV/DLS-5000 instrument (ALV GmbH). As a light source a 20 mW He−Ne gas laser was used (Uniphase, 632.8 nm). The DLS instrument was equipped with a goniometer for automatic measurements between scattering angles θ of 30 and 140°. The correlation functions were analyzed by the CONTIN method, which gives information on the distribution of decay rate (Γ). Apparent diffusion coefficients were obtained from $D_{app} = \Gamma/q^2$ (where $q = (4\pi n/\lambda)\sin(\theta/2)$, λ is the wavelength of the light, n is the refractive index, and θ is the scattering angle). Finally, apparent hydrodynamic radii were calculated via Stokes−Einstein equation. The polymers were dissolved in bidistilled water at a concentration of 1.25 g/L and directly filtered into the light scattering cells through a 0.45 μm pore size PTFE filter. The hydrodynamic radii were determined at 10 to 12 different angles and averaged for each concentration.

The surface pressure (π) as a function of mean molecular area (*mmA*) was measured using a Langmuir trough system (KSV, Helsinki, Finland) with a Teflon trough and a microroughened platinum Wilhelmy plate. The temperature of the water of the subphase was maintained at 20 °C. The compression and expansion rate for all experiments was 750 mm^2/min. In the case of relaxation experiments, after expansion, a waiting period of 20 min was included.

2.2.3   Preparation of 2-(azidomethyl)-2-methylpropane-1,3-diol (AMD)

2-(Bromomethyl)-2-methylpropane-1,3-diol was synthesized according to the procedure described by Lugo-Mas et al.[130] For AMD synthesis, a mixture of 2-(bromomethyl)-2-methylpropane-1,3-diol (5 g, 27.3 mmol), sodium azide (7.1 g, 109 mmol), and 100 mL of DMSO was added to a 250 mL round-bottomed two-necked flask. The mixture was stirred for 2 days at 80 °C. Then, DMSO was removed at 80 °C by rotary evaporation under reduced pressure. The organic residue was cooled using an ice bath. Distilled water (50 mL) was added gradually under stirring, and the solution was extracted three times using DCM. The organic phase was dried overnight using magnesium sulfate. The solvent was removed under reduced pressure. The synthetic route to prepare this monomer is revealed in Figure 2.1. The

NMR data were as follows. ^{1}H NMR (400 MHz, CDCl$_3$) δ = 3.60 (d, 4H, 2 CH$_2$OH), 3.45 (s, 2H, N$_3$−CH$_2$), 2.26 (s, 2H, 2 −OH), 0.86 (s, 3H, −CH$_3$). ^{13}C NMR (200 MHz, CDCl$_3$) δ = 68.08 (CH$_2$−OH), 55.56 (CH$_2$−N$_3$), 40.93 (C), 17.52 (−CH$_3$).
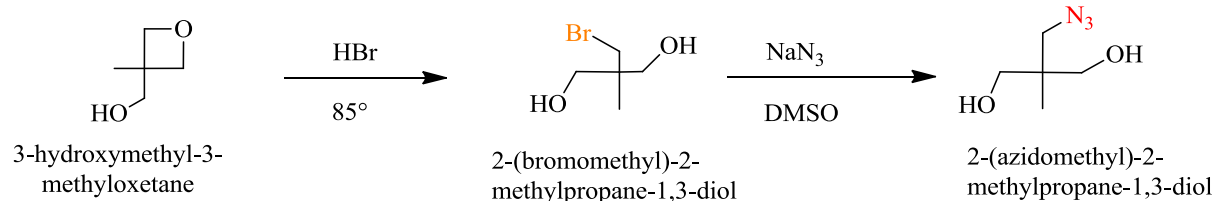
Figure 2.1 Synthesis of 2-(azidomethyl)-2-methylpropane-1,3-diol

2.2.4   Typical enzymatic polycondensation procedure

A mixture of 2-(azidomethyl)-2-methylpropane-1,3-diol (713 mg, 4.9 mmol), DVA (974 mg, 4.9 mmol), and CAL-B (61 mg) was added to a Schlenk tube, and the mixture was stirred under nitrogen at 60 °C for 3 days. Then, the reaction was quenched by the addition of ~30 mL of DCM, followed by filtration to remove the acrylate beads carrying the enzyme. The organic layer was washed with distilled water three times and then dried using magnesium sulfate overnight. The solvent was removed under reduced pressure. The polymer was precipitated from THF into *n*-hexane and dried. The resulting polymer is called PAA. M_n was 3100 g/mol and M_w/M_n was 1.6. ^{1}H NMR (400 MHz, CDCl$_3$) δ = 4.43 (s, 1H, −OH), 3.96 (s, 2H, 2C−CH$_2$−O), 3.43 (s, 2H, N$_3$−CH$_2$−C at the end group), 3.34 (s, 2H, N$_3$−CH$_2$−C), 2.36 (s, 4H, 2CH$_2$−CO), 1.74 − 1.58 (m, 4H, 2CH$_2$−CH$_2$−CH$_2$), 1.00 (s, 3H, CH$_3$), 0.96 (m, 3H, CH$_3$ at the end group). PAA had a glass-transition temperature of about −43 °C without the presence of any melting peak

2.2.5   Typical procedure for synthesis of poly(2-(azidomethyl)-2-methylpropane adipate)-*g*- poly(ethylene oxide)   (PAA-*g*-PEO)

Alkyne functional poly(ethylene oxide) monomethyl ether (alkyne-PEO) was synthesized according to Gao et al.[131] PAA (100 mg, 0.39 mmol with respect to azide groups) of M_n = 3100 g/mol, alkyne-PEO (363 mg, 0.429 mmol), and anhydrous THF (3 mL) were placed in a Schlenk tube. The mixture was agitated using a magnetic stirrer and sealed using rubber septum. Degassing was carried out by bubbling nitrogen for 15 min. This was followed by the addition of 11 mg (0.08 mmol) CuBr and 0.018 mL (0.9 mmol) of PMDTA. The solution was stirred for 24 h at room temperature. At the end, the reaction solution was diluted using ~30 mL of THF, followed by passing it through a silica gel column. The solvent was removed

using rotary evaporation at 40 °C. The residue was dissolved using 10 mL of distilled water, followed by dialysis against distilled water for 4 days using regenerated cellulose membrane with MWCO of 1000 g/mol. The polymer was freeze-dried to obtain PAA-*g*-PEO with yield of 40%, M_n = 13750 g/mol, and M_w/M_n = 1.6. ^{1}H NMR (400 MHz, D$_2$O) δ = 7.68 (s, 1H, triazol-CH-C), 4.33 (s, 2H, CH$_2$-O-CH$_2$−CH$_2$−O-CO), 4.10 (s, 2H, C−CH$_2$-triazol), 3.80 (d, 4H, 2 C−CH$_2$−O-CO), 3.71 (m, 68H, O−CH$_2$-CH$_2$−O), 3.24 (s, 3H, O−CH$_3$), 2.60 (s, 2H, CH$_2$−CH$_2$−CH$_2$−COO), 2.40 (m, 6H, 3 CH$_2$−CH$_2$−COO), 1.80 (s, 2H, triazol-C−CH$_2$), 1.45 (s, 4H,2 CH$_2$−CH$_2$−COO), 0.81 (s,3H, C−CH3).
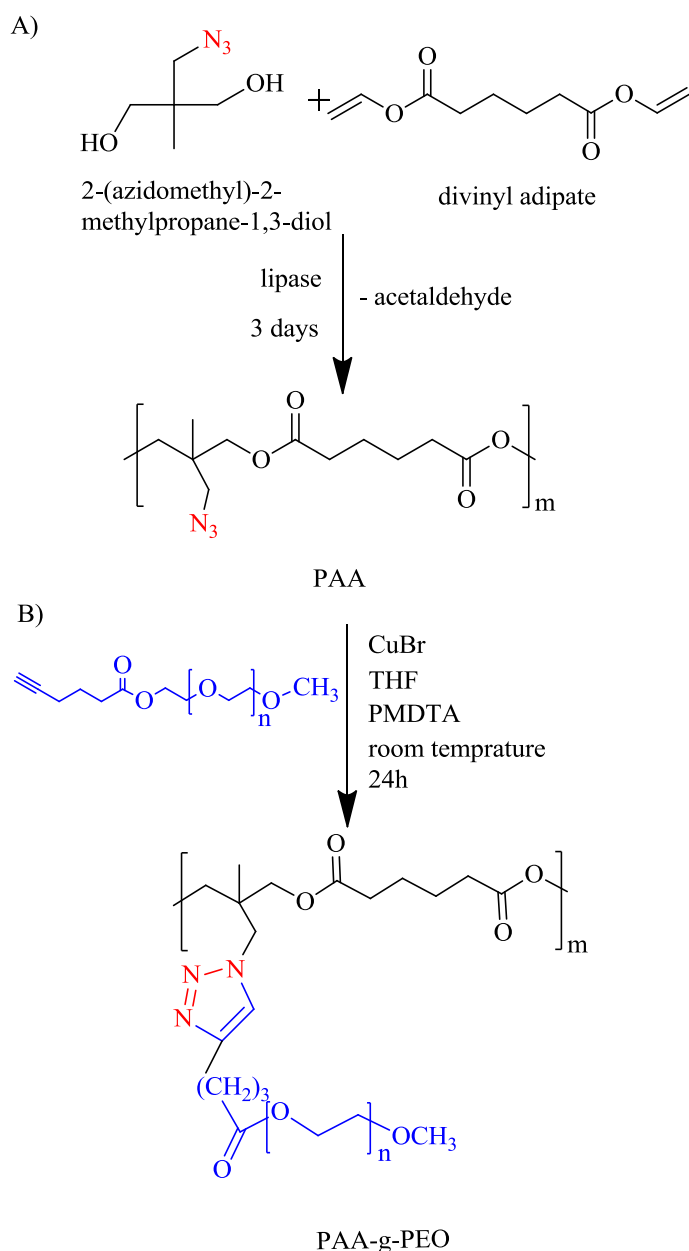
Figure 2.2 A) Enzymatic synthesis of polyester with pendant azide aroups (PAA) and B) Grafting reaction to PAA using alkyne-PEO

2.2.6   Synthesis of PAA-*g*-PEO using enzymatic polymerization and "Click" chemistry in   one-pot process

2-(Azidomethyl)-2-methylpropane-1, 3-diol (285 mg, 1.97 mmol), DVA (390 mg, 1.97 mmol), and immobilized lipase CAL-B (14 mg) were charged into a Schlenk tube, and the mixture was stirred for 3 days at 60 °C. At the end, a solution of alkyne-PEO (1.831 g, 2.17 mmol), CuBr (56 mg, 0.39 mmol), PMDTA (0.094 mL, 0.45 mmol), and 5 mL of anhydrous THF was added to the Schlenk tube, which contained the polyester and the enzyme. The mixture was then degassed by bubbling nitrogen for 15 min. The solution was stirred for 24 h at room temperature, then diluted with THF and purified first by filtration to remove the enzyme beads, followed by passing it through a silica gel column to remove the CuBr. The solvent was removed by rotary evaporation at 40 °C under reduced pressure. Further purification was carried out using dialysis against distilled water for four days using regenerated cellulose membrane with MWCO of 1000 g/mol. The polymer was freeze-dried to obtain PAA-*g*-PEO$_{op}$ with M_n = 11100 g/mol and polydispersity of M_w/M_n = 2.1. The ^{1}H NMR spectrum of this polymer shows the same peaks as the previously discussed graft polymer.

2.3   Results and discussion

2.3.1   Enzymatic polycondensation of poly(2-(azidomethyl)-2-methylpropane adipate) (PAA).

Figure 2.2 shows the enzymatic polycondensation of DVA with AMD, which yields poly(2-(azidomethyl)-2-methylpropane adipate) (PAA). Table 1.1 summarizes the polycondensation results using different conditions. As described above, the polymer is synthesized using CAL-B as catalyst, and it is generally considered that polycondensation of diols and activated esters does not occur in the absence of enzyme in the temperature range up to 60 °C,[132] which is also confirmed by our results. All polycondensation of DVA with AMD show a significantly lower activity compared with the use of DVA and glycerol. This is indicated when doing the polycondensation under identical conditions, as described in literature, but replacing glycerol by AMD.[124] This can be explained by (i) the increased steric hindrance when the substituents at the C2 carbon of glycerol (H and OH) are replaced by CH_3 and CH_2N_3 in AMD and (ii) the fact that AMD is a prochiral monomer. At the moment, there is no comprehensive view on the influence of substituents on the reaction kinetics of

enzymatic polycondensation. Peeters et al[133] studied the influence of sterical hindrance in the ROP of 4-substituted caprolactones. It was shown that deacylation becomes rate-determining upon increasing the substituent size. This fact might play the same role in enzymatic polycondensation reaction. Mahapatro et al. found that using monomers as diacids and diols having more CH_2 groups in lipase-catalyzed polycondensation results in higher molar mass polyesters compared with shorter chain-length species.[134]

Table 1.1 Enzymatic polycondensation of DVA and AMD.

Condition	Temperature (°C)	Time (days)	M_n[1] (g/mol)	M_w/M_n
bulk	50	3	2,000	1.7
bulk	60	3	3,100	1.6
bulk	90	3	2,200	1.9
Toluene[2]	60	3	2,100	1.8
bulk[3]	60	3	---	---

1) M_n and M_w/M_n results were obtained by GPC.
2)   The concentrations of DVA and AMD were 1.97 mol/L.
3)   The experiment was performed in the absence of CAL-B.

For bulk polycondensation at different temperatures and keeping all other parameters constant, the highest M_n value is obtained at 60 °C. These results are in agreement with enzymatic ring-opening polymerization of ε-caprolactone at different temperatures. Also, in this case an increase in M_n with temperature is observed until 60 °C, followed by a decrease at higher temperatures.[135] For another lipase-catalyzed polycondensation, the highest M_n value is obtained at 50 °C.[136] For comparison, one polycondensation is carried out using toluene as a solvent because a higher activity can be achieved by CAL-B in ring-opening polymerization of ε-caprolactone when using toluene as solvent instead of bulk conditions.[135] This is different for the system under consideration where the enzyme shows more activity when performing

the reaction in bulk compared with solution polycondensation in toluene. The PAA samples are characterized by ^{1}H NMR spectroscopy as shown in Figure 2.3.

All peaks can be assigned to the structure of PAA. A minor side reaction indicated by the peaks z, u, and v is observed, which is most prominent at a reaction temperature of 90 °C. The side reaction occurs between vinyl end groups and azide groups.
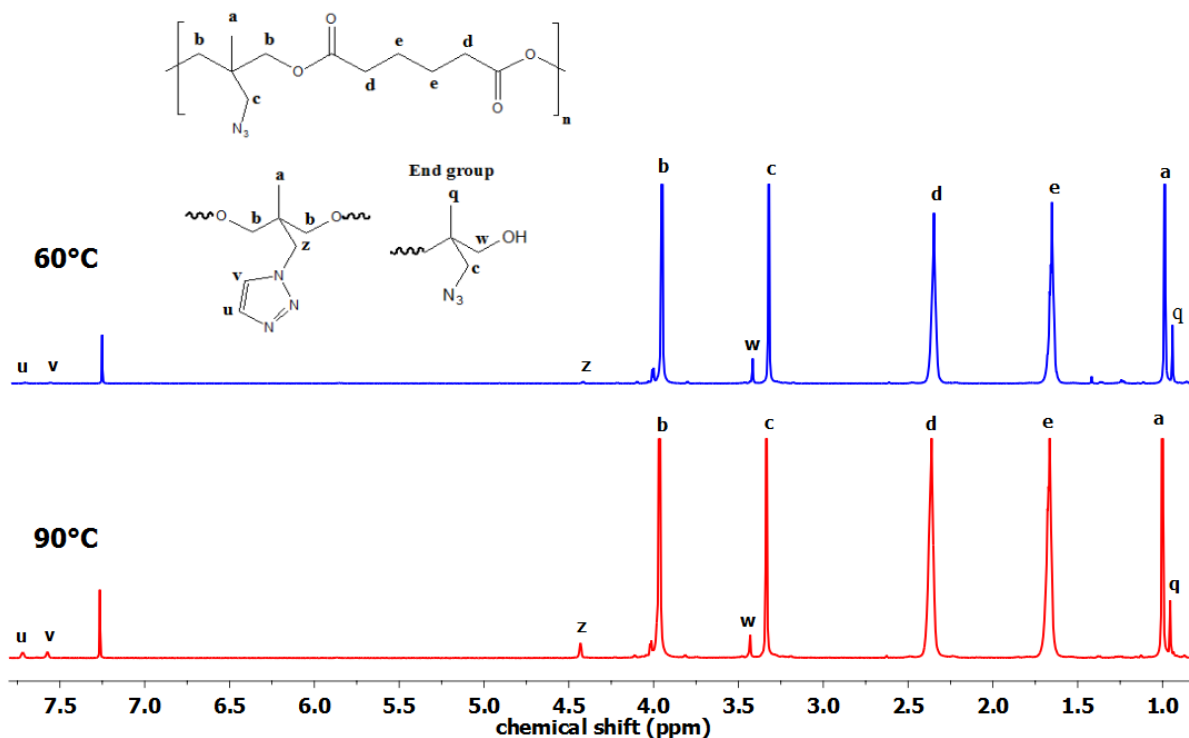
Figure 2.3 ^{1}H NMR spectra of PAA synthesized at 60 °C and at 90 °C in CDCl$_3$.

This type of reaction has been previously reported for activated olefins and azides.[137] The reaction is proposed to proceed according to Figure 2.4. First, an azide group will react with a vinyl group according to Huisgen 1,3-dipolar cycloaddition,[138] and second, an elimination reaction[139] occurs to form a 1,2,3-triazole ring and a carboxylic acid group. The amount of repeating units that has a 1,2,3-triazole ring instead of an azide group is calculated by the ratio between peaks u and d and is 1.4 mol % and 6.7 mol % for the PAA synthesized at 60 and 90 °C respectively. Signals from vinyl end groups do not appear, which indicates hydrolysis of these end groups during the polycondensation reaction.[136]
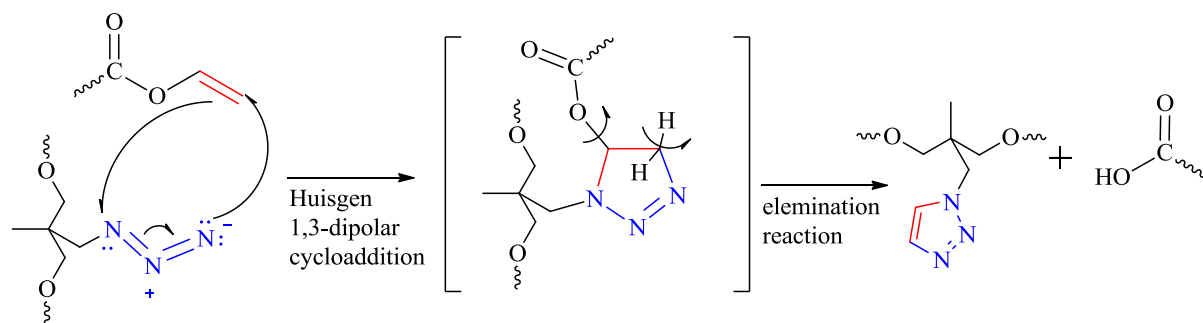
Figure 2.4 Proposed side reaction mechanism between vinyl ester end groups and pendant azide groups during polycondensation reaction.

2.3.2   Synthesis of PAA-*g*-PEO using CuAAC "Click" chemistry

The synthesis of PAA-g-PEO is carried out by "grafting onto" strategy using CuAAC "click" reaction. The reaction is performed under mild conditions in the presence of 10 mol % excess of alkyne-PEO. Figure 2.2B shows the grafting reaction that is carried out in anhydrous THF. This "click" reaction is fastest when using PMDTA as ligand to dissolve CuBr.[100] The GPC traces of Figure 2.5 show that PAA-*g*-PEO has a higher molar mass than PAA, indicating the successful grafting reaction. Both traces have a small aggregation peak at small retention volume. This peak disappears when THF is used as a solvent for GPC.
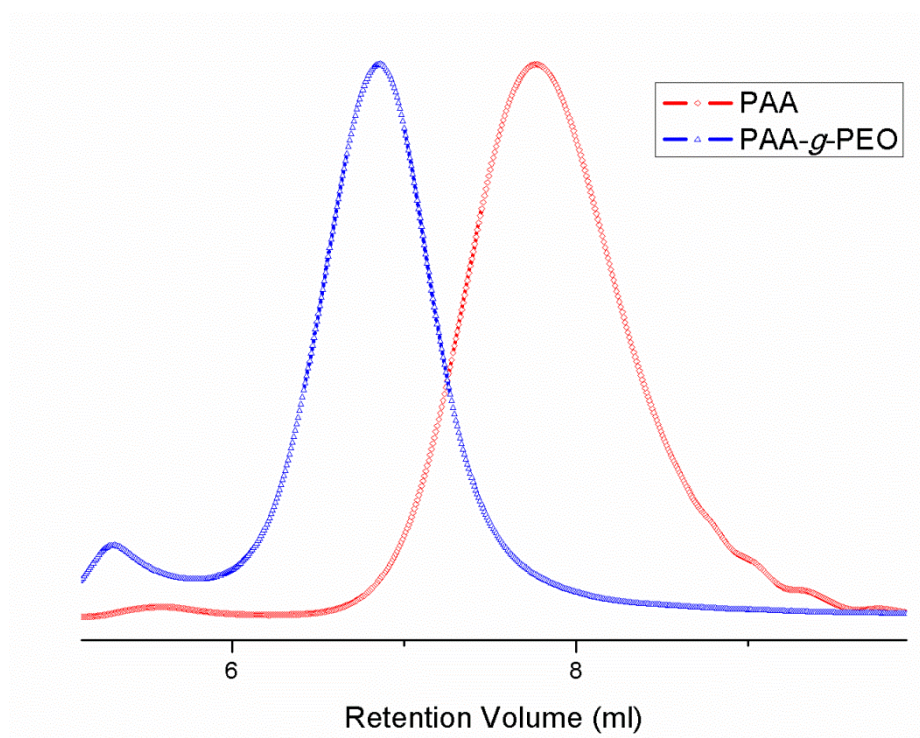
Figure 2.5 GPC traces of PAA and PAA-g-PEO in DMF at 60 °C.

Usually, the molar masses of PAA are determined by GPC employing THF. Unfortunately, using THF for PAA-*g*-PEO results in nonsymmetric peaks in the GPC traces because PEO chains obviously interact with the column material, which has been reported in the literature.[140] Figure 2.6 shows the ^{1}H NMR spectrum of PAA-*g*-PEO in D_2O. The ratio between peak a and peak p is 3:2.9 which indicates that there is approximately one PEO chain for each repeating unit.

Furthermore, Figure 2.7 depicts the complete disappearance of the vibration of the azide group in the FT-IR spectrum at 2100 cm^{-1} as a result of the coupling reaction, which is also an indication of quantitative reaction.
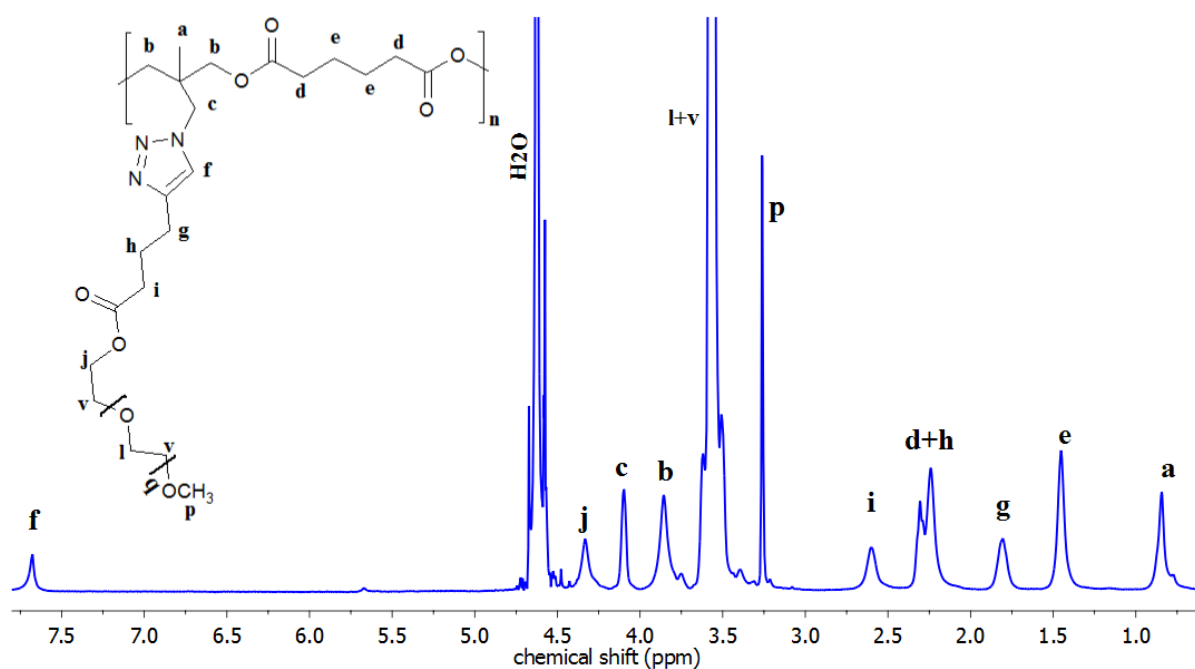
Figure 2.6 ^{1}H NMR spectrum of the PAA-*g*-PEO in D_2O at room temperature.

Usually, in polymer analogous reactions, the polymer reactivity is sterically hindered when the functional group is close to the polymer backbone.[141] Even by using "click" reactions for the "grafting onto" route, the reactions are not always quantitative.[142] In fact, to increase the density of graft chains on the polymer backbone, steric hindrance must be lowered by increasing the spacer length between the repeating azide or alkyne units and the polymer backbone and by using reactive oligomers to be grafted with less bulky structures, such as, for example, PEO. Also, an excess of the oligomer grafted to the backbone improves the grafting density.[131] Additionally, ligand, solvent, and temperature also affect the yield of

the click reaction.[100] In the case under investigation, only one CH_2 group separates the azide group and the polymer backbone. Nevertheless, the grafting reaction is quantitative.
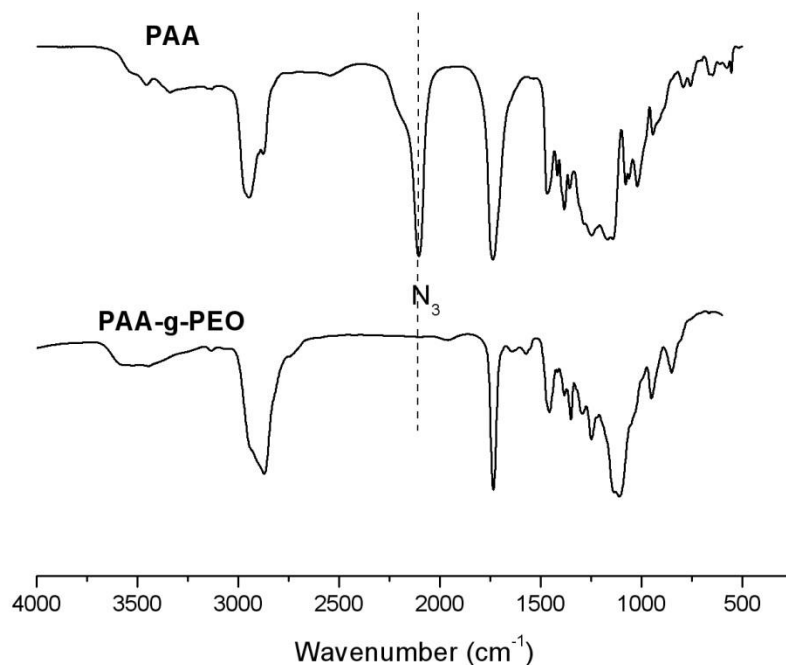
Figure 2.7 FT-IR spectra of PAA and PAA-*g*-PEO.

2.3.3   Synthesis of PAA-*g*-PEO in sequential one-pot reaction (PAA-*g*-PEO$_{op}$)

The graft copolymer is also synthesized by polycondensation of DVA and AMD in the presence of the CAL-B as catalyst, followed by the addition of alkyne-PEO, ligand, CuBr, and the solvent to the same pot. The solution then undergoes bubbling with nitrogen for 15 min. Carrying out the chemical reactions in one pot has the advantage of accelerating the synthetic procedures by reducing the number of purification steps, therefore leading to more ecofriendly products.[143] The reaction must be carried out sequentially for two reasons. First, the presence of copper ions in the reaction vessel can inhibit the lipase during polycondensation.[144] Second, any AMD converted with alkyne-PEO might be unable to undergo enzymatic polycondensation with DVA because of steric hindrance caused by the attached PEO chains. One-pot lipase-catalyzed ring-opening polymerization and ATRP polymerization in the presence of CuBr as catalyst for ATRP polymerization was carried out successfully in one step but by using super critical carbon dioxide as a solvent. Other solvents suitable for this procedure could not be identified.[145,146] Both ¹H NMR and FT-IR spectra of

the PAA-*g*-PEO$_{op}$ are identical to that of PPA-*g*-PEO, which means that the reaction also performs quantitatively, but as shown in Figure 2.8, when the GPC traces of the two polymers are compared, it is obvious that the PAA-*g*-PEO$_{op}$ has a broader molar mass distribution than PAA-*g*-PEO, simultaneously, the sequential one-pot synthesis leads to a polymer with a smaller molar mass.
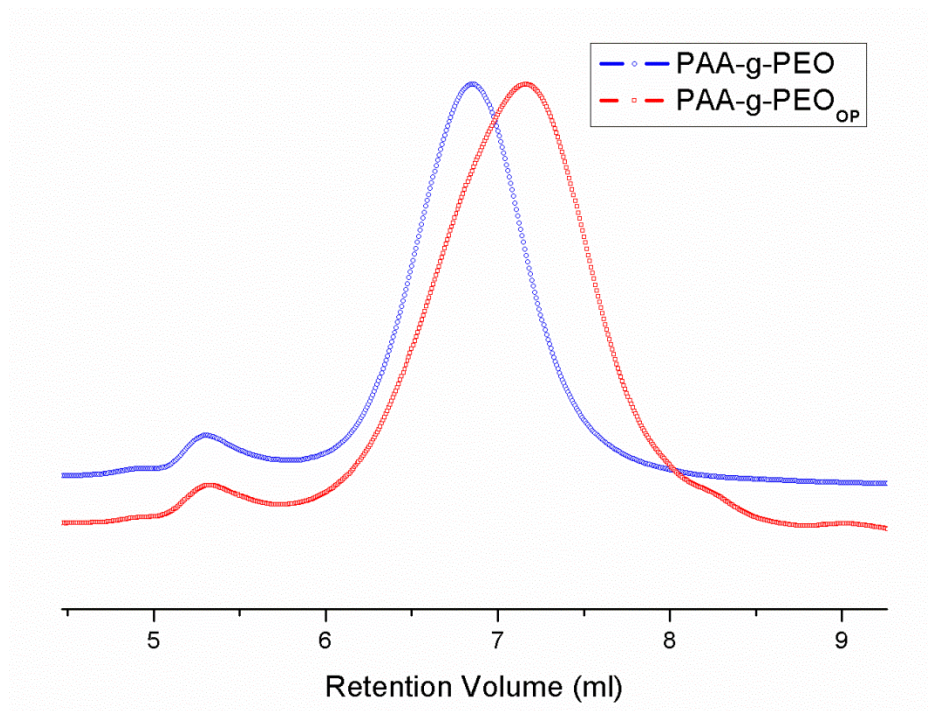
Figure 2.8 FT-IR spectra of PAA and PAA-*g*-PEO.

The reason for this difference is the fact that PAA-*g*-PEO is synthesized from PAA without oligomers because it is purified prior to grafting. In the case of PAA-*g*-PEO$_{op}$, the click reaction was carried out directly after the polycondensation without carrying-out any purification step, which means the remaining oligomers will react with PEO to yield a larger number of graft copolymers with lower molar mass.

2.3.4   Surface tension measurements

The surface tensions γ of aqueous solutions of PAA-*g*-PEO are measured as a function of polymer concentrations at 25°. Plotting γ versus polymer concentration (log C) yields the critical aggregation concentration (cac) indicated by the intersection of the extrapolation of the two linear regimes where the curve shows an abrupt change in slope. (See Figure 2.9) The value obtained by this method is surprisingly low at 3×10^{-2} μM.

Amphiphilic graft and brush copolymers usually have low cac values.[147] This value is lower than that for conventional surfactants and block copolymers.[110] Small cac values will

strongly nominate the polymer for drug delivery application because the in *vivo* stability after injection is improved.[107]
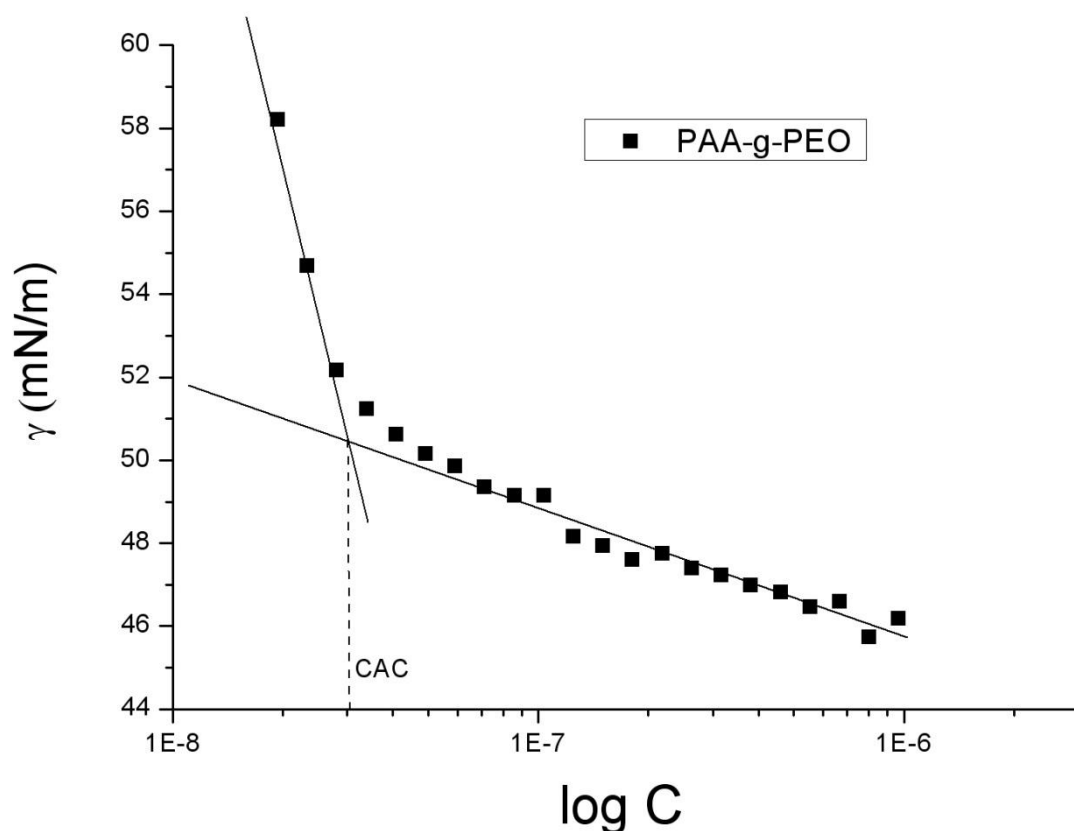
Figure 2.9 Surface tension of PAA-g-PEO in water as a function of polymer concentration at 25 °C.

2.3.5 ^{1}H NMR spectroscopy in water and in THF

THF is a good solvent for the polyester backbone and the grafted PEO chains. For that reason, a comparison between the ^{1}H NMR spectra of PAA-*g*-PEO in water (which is a nonsolvent for the polymer backbone but a good solvent for PEO) and THF is carried out. (See Figure 2.10.) Actually, a broadening of the polyester backbone peaks in the spectrum obtained in D_2O can be recognized easily in contrast with the same peaks in the spectrum obtained in THF-d_8. Such broadening is the result of a decreased mobility of protons of the polymer chains with hindered motion.[148] In fact, the ^{1}H NMR spectrum of PAA-*g*-PEO in D_2O confirms the formation of large polymer aggregates in water, as will be discussed below.
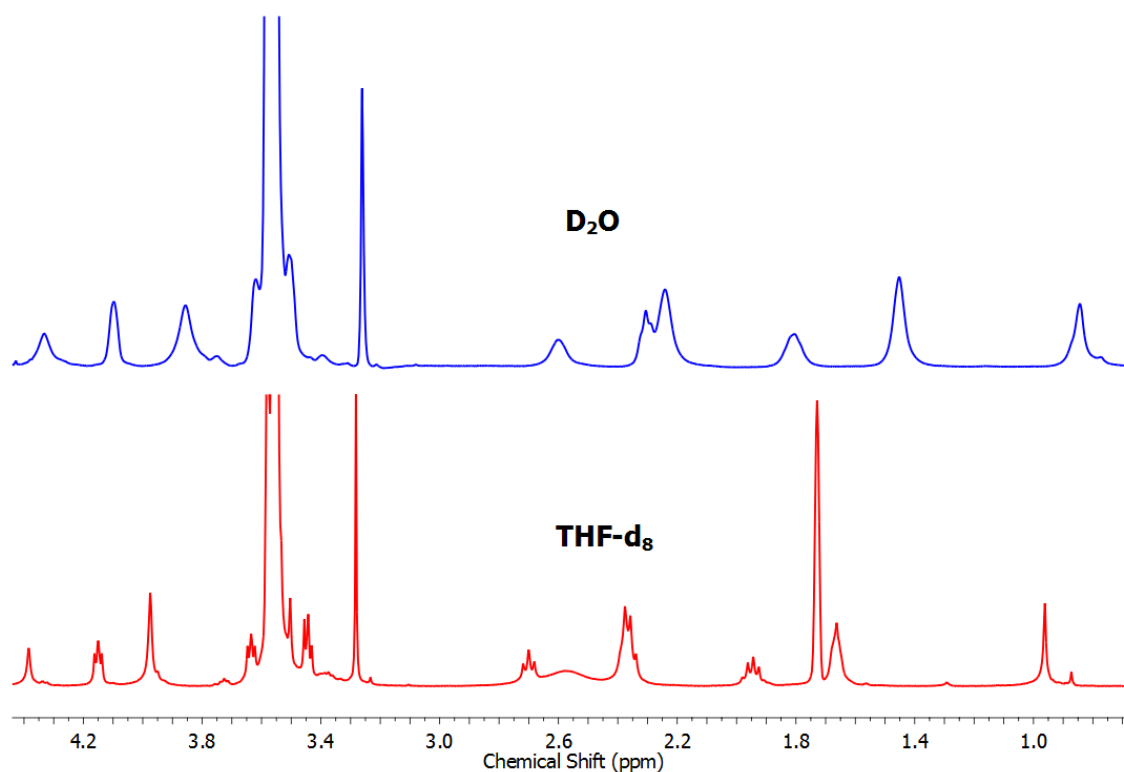
Figure 2.10 Comparison between the ^{1}H NMR spectra of PAA-*g*-PEO in D_2O and in THF-d$_8$.

2.3.6   Dynamic light scattering

In DLS measurements of PAA-*g*-PEO in water, for all angles and concentrations above cac, two different species have always been observed. The corresponding hydrodynamic radii can be attributed to single chains with a typical value of 6 nm and larger aggregates of 75 nm. Figure 2.11 shows the hydrodynamic radius R_h distribution obtained at the polymer concentration of 1.25 g/L and scattering angle $\theta = 80°$ measured at 25 °C. Furthermore, the average hydrodynamics radii for both species at different polymer concentrations are depicted. The error bars indicate the standard deviation of the averaging over all measurements at different angles. No significant increase in aggregate size can be observed with increasing polymer concentration. The hydrodynamic radii of both species vary only weakly with concentration.
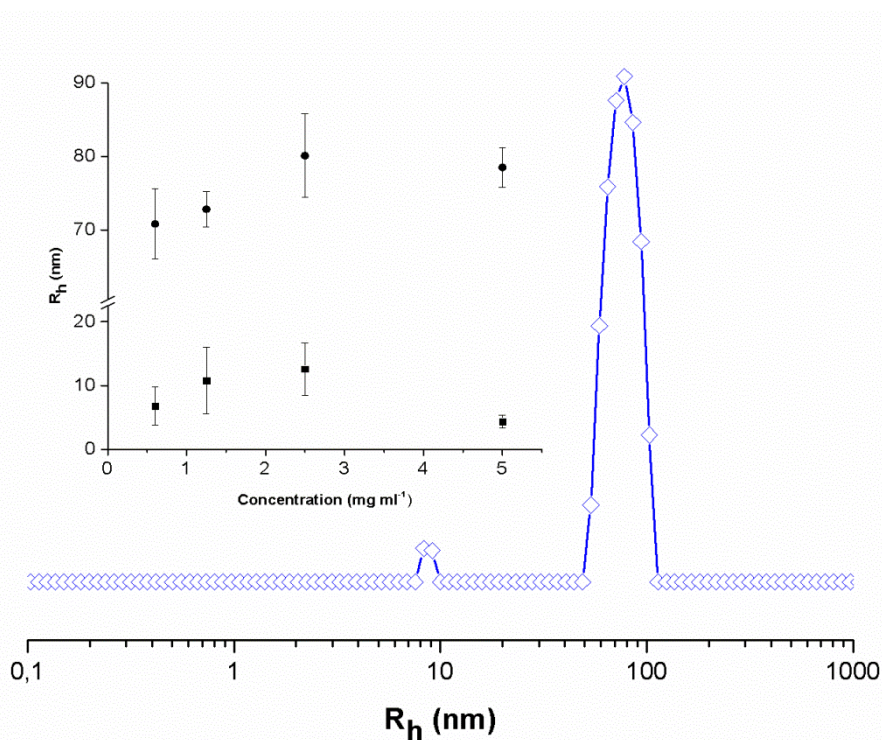
Figure 2.11 Hydrodynamic radius distribution of PAA-*g*-PEO in water at a concentration
of 1.25 g/L, scattering angle of 80°, and temperature of 25 °C. The inset
shows the concentration dependence of R_h for the two species identified by
DLS.

2.3.7   Langmuir trough measurements

Figure 2.12 shows the Langmuir isotherm of PAA (M_n = 3100 g/mol) at the air/water
interface. The isotherm shows a horizontal region at a surface pressure π of 13 mN/m without
having a further increase prior to final collapse. This indicates a weak anchoring of the
molecules at the air−water interface. Two different mechanisms can occur in this case: One is
according to a gradual formation of "giant folds" or "multiple folds" with an extension into
the subphase.[149] The other mechanism is according to a multilayer formation of the PAA on
the water surface.[150,151] To investigate the mechanism, a reversibility experiment for PAA is
performed by compression−expansion steps. In the case of PAA, no significant differences of
the isotherms can be observed. This indicates that all chains remain flexible and stay at the
water surface. The isotherm of PAA-*g*-PEO shows a typical isotherm for amphiphilic block or
graft copolymers that contain PEO as water-soluble part.[152,153] The isotherm has a significant
pseudoplateau indicating the phase transition from pancake to brush.[154] At the end of the
plateau, the hydrophilic chains form brush domains, and the hydrophobic parts anchor them to
the water surface. Typically, the surface pressure at which the pseudoplateau appears for

grafted copolymers is 16 mN/m slightly larger than that in the case of PEO block copolymers (between 9 and 13 mN/m depending on the length of PEO chains).[155,156] With further compression, the surface pressure increases again until at 29 mN/m the slope of the isotherm changes significantly, which can be assigned to the monolayer collapse. To investigate the mechanism of this collapse, a reversibility experiment is performed. Because of the limited trough size, *mmA* values between 200 and 10 Å^2 are chosen for this experiment to cover the range between phase transition (pseudoplateau) and collapse region.
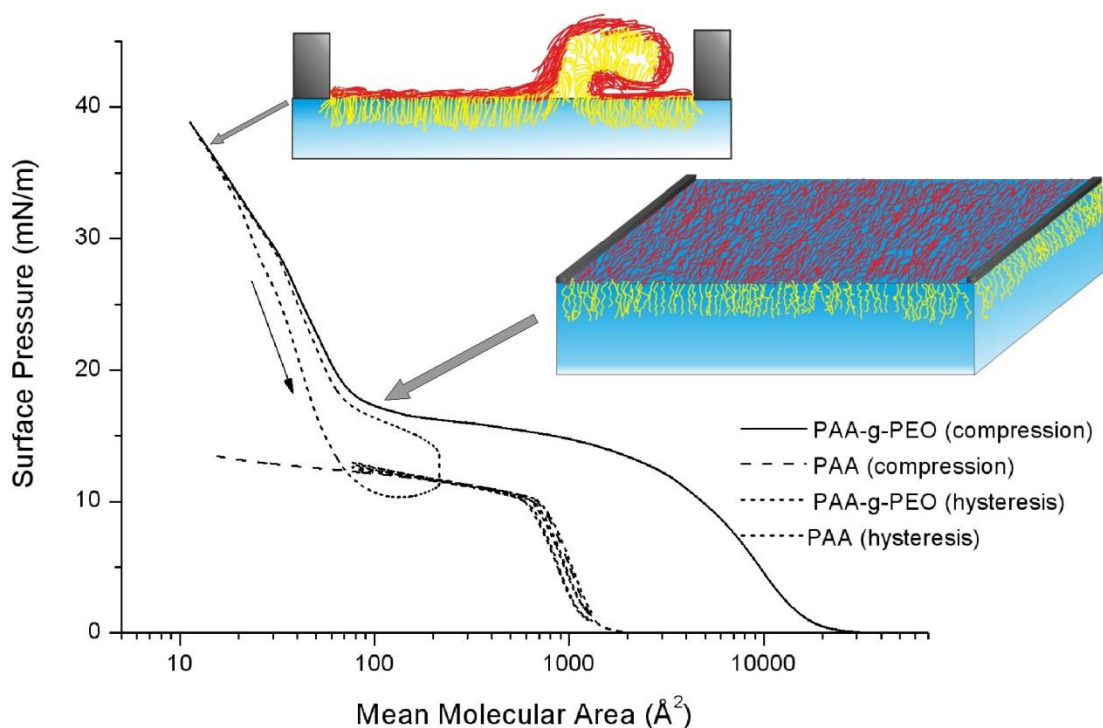
Figure 2.12 *π-mmA* isotherms of PAA and PAA-g-PEO at tthe air-water interface at 20°C.

During expansion, the surface pressure is lower compared with the compression curve at identical *mmA* values, but the course is similar. During relaxation after expansion, the surface pressure approaches the initial isotherm, and starting from the end of the pseudoplateau during the following compression, the initial behavior is reproduced. This behavior can be explained according to the long relaxation time needed for PEO chains to move from the water subphase to the water surface. Beyond the end of the pseudoplateau, the hydrophobic parts are dominating the shape of the isotherm, which are, as in case of neat PAA, fully relaxed. The reproduction of the isotherm in this higher pressure regime indicates that no chains are lost in the subphase during collapse. This suggests that the collapse point indicates

a multilayer formation. The PAA-*g*-PEO has a higher surface activity compared with PAA because the PEO chains anchor the polymer backbone at the water surface effectively during compression, resulting in a larger collapse pressure, but their hydrophilicity is not sufficient to remove the PAA backbone of PAA-*g*-PEO from the air−water interface to the water subphase.

2.4 Conclusions

Aliphatic polyesters with pendant azide groups were successively synthesized using enzymatic polycondensation of 2-(azidomethyl)-2-methylpropane-1,3-diol and DVA. The enzymatic reaction was performed at different temperatures. The highest molar masses were obtained at 60 °C by polycondensation in bulk. A side reaction between azide groups and vinyl end groups was observed to a minor extent, which becomes more pronounced at higher polycondensation temperatures (90 °C). The mechanism suggested is based on the Huisgen 1,3-dipolar cycloaddition, followed by elimination reaction resulting in a 1,2,3-triazole ring. The polyester was quantitatively modified using alkyne-PEO. The reaction to the corresponding graft copolymer was quantitative. Both enzymatic polymerization and "click" reaction were successfully carried out in sequential one-pot synthesis. Surface tension measurements show that the graft copolymer had a very small cac. Above cac, stable aggregates with a size of 75 nm are formed at different concentrations, as revealed by DLS. The aggregate formation was obviously the result of the amphiphilic character of the graft copolymer. The polyester backbone was hydrophobic, whereas the PEO graft chains were hydrophilic. This was also confirmed by ^{1}H NMR spectroscopy. Langmuir trough experiments showed that the isotherm of the graft copolymer had a pancake-to-brush transition. The PEO anchored the PAA onto the water subphase, and by relaxation experiments, it was found that the PAA layer remains flexible at the surface, even after monolayer collapse. The polyester backbone of the new polymer can be considered to be biodegradable, and the remaining PEO parts have a sufficiently low molar mass, so the graft copolymer can be excreted *in vivo* via kidneys. Therefore, advantages compared with the use of poloxamers can be expected in the field of biomedical applications.[157]

Chapter 3

Utilization of Poly(glycerol adipate) to Synthesize Graft Copolymer and Polymeric Analogues of Glycerides

3.1 Introduction

Synthetic polyesters are one of the most widely used polymers in modern life. Their biodegradability and low cost of production are considered to be the main factors for their wide global demand. Nevertheless, many physical, biological and mechanical properties of polyesters are not always meeting the crucial requirements for some applications. Therefore, synthesizing new polyesters with functional groups able for post-polymerization functionalization is a challenging task.[158] Many routs have been developed to synthetize polyesters with functional groups such as ring opening polymerization of substituted lactones,[61,119,121,159] or by polycondensation of multifunctional monomers.[62,64,80,160,161] Utilization of enzymes as a catalyst to synthesize functional polyesters has been attracting many interests for two decades due to advantages that enzymes can provide over conventional chemical catalysts.[162] Enzymatic polymerization can be performed under mild reaction conditions and does not require protection-deprotection steps due to the regio- and chemoselectivity of enzymes.[82] This will protect the polyester from possible degradation that might occur to the polyester backbone during deprotection processes. Poly(glycerol adipate) (PGA) was enzymatically synthesized first by Kline et al. [124] using glycerol and divinyl adipate as monomers and lipase enzyme from *Candida Antarctica* type B (CAL-B) as catalyst to yield linear polyesters with free pendent hydroxyl groups. The enzyme is immobilized on an acrylic macroporous resin which facilitates the processes of separating it from the final polymer. The overall synthesis process could be described as a simple, clean, easy to conduct, easy to purify the final product, and easy to scale up to 500 g.[163] Using glycerol as a monomer has a big advantage since it is cheap, widely used, and biocompatible compound. On the contrary, the utilization of divinyl adipate as monomer for synthesis is not appropriate for commercial purposes. Using dimethyl adipate (DMA) instead of divinyl adipate to synthesize poly(glycerol adipate) (PGA) is more appropriate since it is a large-scale and cheap commodity chemical compound. In the previous chapter, a graft copolymer was synthesized by utilization of a polyester called PAA which has free pendant azide group on every monomer unit. Utilization of PGA instead of PAA to synthesize identical graft copolymers seems reasonable for both commercial and environment-friendly purposes. The conversion of glycerol with different fatty acids may result in mono-, di- or triglycerides.[140] Triglycerides

are usually hydrophobic and the mono- or diglycerides can be considered as amphiphilic molecules due to remaining OH-groups.[164] Thus, they are surface active and reduce the surface tension of water or they are effective emulsifiers.[165] Additionally, they are able to form lyotropic liquid crystalline phases.[166] Especially, the monoolein/water system is interesting since it can form cubosomes when stabilized by poloxamers.[167] These nanoparticles can dissolve both hydrophilic and lipophilic drugs and additionally they can be used as scaffold for therapeutic proteins.[168] It is reasonable to assume that polyesters based on glycerol can achieve similar properties as low-molar mass glycerides discussed above. They would have the advantage of higher mechanical stability and longer *in vivo* circulation times. Esterification of the hydroxyl pendant groups at the PGA backbone with fatty acids has been found to yield promising materials for application in the field of nano-drug carriers.[122,169–171] However, further characterization for these polymers and corresponding nanoparticles is necessary in order to tune their properties and to ensure their ability to be applicable *in vivo*. Furthermore, additional applications in pharmacy and medicine can be envisioned due to biocompatibility and biodegradability.

3.2 Experimental section

3.2.1 Materials

All chemicals were purchased from Sigma-Aldrich and used without further purification unless otherwise stated. Lauroyl chloride 98%, stearoyl chloride 97%, behenoyl chloride ≥99%, copper bromide 99.99%, N,N,N′,N″,N″-pentamethyldiethylenetriamine (PMDETA), dichloromethane ≥99.5% (DCM), N-(3-dimethylaminopropyl)-N′-ethylcarbodiimide hydrochloride (EDC), 4-(dimethylamino)pyridine (DMAP) dimethyl adipate (DMA) (99.5%) are used as received. Tetrahydrofurane is dried over sodium under anaerobic conditions. Pyridine (99%) was dried over calcium hydride overnight, distilled under atmospheric pressure and stored over molecular sieve (3Å). Solvents for column chromatography and precipitation were distilled prior to use. CAL B (lipase B from *Candida Antarctica* immobilized on an acrylic macroporous resin) is dried under vacuum at 4 °C over P_2O_5 for two days prior to use. Divinyl adipate (DVA) is obtained from TCI-Europe. The synthesis of azide-terminal poly(ethylene oxide) monomethylether (mPEO-N$_3$) was performed as described by Gao et al.[31] The number-average molar mass was M_n = 2000 g/mol

3.2.2 Synthesis of poly(glycerol adipate) (PGA)

Ploy(glycerol-adipate) was synthesized at 50°C from glycerol and DVA as described by Kallinteri et al.[122] A typical procedure for the synthesis of PGA backbone using DMA and glycerol as monomers was as follows: (11.5 g, 0.12 mol) glycerol, (21.7g, 0.12mol) DMA, and 13 ml anhydrous THF were charged into an oven dried two-necked 250 ml round bottom flask.

Figure 3.1 Synthesis of (a) poly(glycerol adipate) backbone by using glycerol and either DVA or DMA as monomers and CAL-B as a catalyst. (b) Esterification reaction to obtain PGA-alkyne, (c) "Click" reaction to synthesize PGA-*g*-PEO.(d) Esterification reaction between acyl chloride of fatty acids.

35

The flask was equipped on the top with soxhlet extractor (150 ml) attached to a condenser. The soxhlet extractor was charged with 105 g of molecular sieve 5Å and then filled with about 100 ml anhydrous THF. The mixture was stirred by magnetic stirrer to allow reactants to warm up to the bath's temperature (60°C) for about 30 min. The reaction was started by adding (0.73 g) of enzyme. The pressure was then reduced gradually to 300 mbar in order to allow for the evaporation process. The azeotropic mixture of THF and methanol was collected gradually into the soxhlet extractor and became into contact with the molecular sieve. As a result the methanol was entrapped gradually by the molecular sieve. The conditions (temperature and pressure) were adjusted to allow one cycle of soxhlet filling to be 20 min. The enzyme was removed at the end of polymerization by filtration followed by washing with 35 ml THF. The solvent was removed by rotary evaporation at 60°C under vacuum. Finally, the temperature was raised up to 95°C for 10 min in order to deactivate any remaining free enzyme. The polymer was used for the next step without further purification.

3.2.3 Acylation of PGA backbone with fatty acid chains

Acylation reaction is carried out between hydroxyl groups on PGA backbone and acyl halide of lauroyl, stearoyl and behenoyl acids. The acylation reaction is performed also using the procedure described by Kallinteri et al.[122] However, further purification step is necessary in order to remove unreacted fatty acid. The purification is carried out by precipitation into cold n-hexane in the case of acylation with lauroyl chloride or for low substitution degrees in the case of the other fatty acids. Whereas, dialysis against THF for 5 days, using regenerated cellulose membrane of a MWCO of 1000 g/mol, is performed in case of higher substitution degrees. PGA with molar mass 3700 g/mol is used for acylation reaction. The acylation degrees (given in mol% of converted OH-groups of PGA) were as the following:

lauroyl chains: 30%, 50%, 75% called L30, L50 L75.

stearoyl chains: 8%, 20%, 45%, 65%, 85% called S8, S20, S45, S65, S85.

behenoyl chains: 45%, 65% called B45, B65

3.2.4 Synthesis of alkyne modified poly(glycerol adipate) (PGA-Alkyne).

A solution of PGA (1.5 g, 7.41 mmol with respect to OH groups), 5-hexynoic acid (2.1 mL, 18.5 mmol) dissolved into 20 mL DCM were added to an oven dried 100 mL two-necked round bottom flask. The mixture was cooled with an ice bath. Afterwards, DMAP (293 mg, 0.96 mmol) and DCC (3.44mL, 14.85 mmol) dissolved into 10 mL of DCM were dropwise added to the polymer solution over 20 min. The mixture was stirred at the room temperature for 24 h to yield a brownish solution. The solution was then filtered to remove the resulting

precipitate. The organic solution was then extracted three times using distilled water. The resulting organic layer was dried by anhydrous sodium sulfate. The polymer was further purified by precipitation into cold n-hexane two times followed by drying at 40°C.

3.2.5   Synthesis of poly(glycerol adipate)-*g*-poly(ethylene oxide) PGA-*g*-PEO.

PGA-alkyne (150 mg, 0.51 mmol with respect to alkyne groups) and azide-terminated poly(ethylene oxide) monomethylether (1.2 mg, M_n=2000 g/mol, 0.56 mmol) were dissolved in 3.5 mL anhydrous DMF and then added to a 10 mL oven dried Schlenk flask. The mixture was agitated using magnetic stirrer and sealed using rubber septum. Degassing was carried out by bubbling nitrogen for 15 min. This was followed by addition of CuBr (21 mg, 0.15 mmol) and PMDETA (0.031 mL, 0.15 mmol). Further degassing was carried out using nitrogen for 10 min. The solution was kept for 37 h at room temperature. The reaction was quenched by open the rubber septum for 30 min. The solution was then diluted using THF, and purified using a silica gel column to remove copper bromide. This was followed by removing solvent using rotary evaporation at 40 °C under vacuum. The residue was redissolved using 10 mL methanol followed by dialysis against water for four days using regenerated cellulose membrane MWCO= 3500 Da. The polymer was finally dried using freeze drying.

3.2.6   Polymer nanoparticle preparation

Nanoparticles are prepared according to the optimized interfacial deposition method.[47] Shortly, 10 mg of polymer were dissolved in 1 mL of acetone which is then injected slowly into 15 mL of 60 °C water using a glass syringe under rapid magnetic stirring. The hot nanoparticle dispersion is subsequently poured into an empty iced beaker under magnetic stirring. The remaining solvent and some water are then removed by a rotary evaporator to obtain finally an 1% dispersion (10 mg polymer/g solution).

3.2.7   Differential scanning calorimetry

Differential scanning calorimetry (DSC) experiments are carried under continuous nitrogen flow using a Mettler Toledo DSC 823e module. Aluminum pans were filled with about 10 mg of sample. Every sample is heated up to 100 °C and kept at this temperature for 20 min. The sample is then cooled until -50°C with a cooling rate of -1 K/min. The sample is kept at -50°C for further 20 min, afterwards the sample is heated up again to 100°C with a heating rate 1 K/min. DSC traces were baseline-corrected. The maximum of the endothermal peak during the second heating is taken as the melting temperature T_m, whereas the minimum of the

exothermal peak is taken as a crystallization temperature T_c. Specific enthalpy of melting $\Delta\widetilde{H}_m$ is obtained from integration of the endothermal peak divided by the weight of alkyl side chains of the sample. The degree of crystallization $X_{DSC}= \Delta\widetilde{H}_m/ \Delta\widetilde{H}_m^0$ where $\Delta\widetilde{H}_m^0$ is the enthalpy of melting of the respective fatty acid.

3.2.8   Transmission electron microscopy (TEM)

The samples are negatively stained using aqueous solution of uranyl acetate. The samples for freeze-fracture were cryofixed using a propane jet-freeze device JFD 030 (BAL-TEC, Balzers, Liechtenstein). Thereafter, the samples were freeze-fractured at −150 °C without etching with a freeze-fracture/freeze-etching system BAF 060 (BAL-TEC). Cryo-TEM grids were prepared in the same way as the TEM, measurements were carried out immediately after preparation of the grids with a Zeiss 902 A microscope operating at 80 kV.

3.3   Results and Discussion

3.3.1   Synthesis of poly(glycerol adipate) (PGA) backbone

PGA is an amphiphilic, water insoluble, yellowish, and highly viscous polymer. The overall synthesis route for the PGA backbone is shown in (Figure 3.1a). The polymer is enzymatically synthesized using two strategies. In the first one glycerol is enzymatically polymerized with DVA in the presence of CAL-B as catalyst.
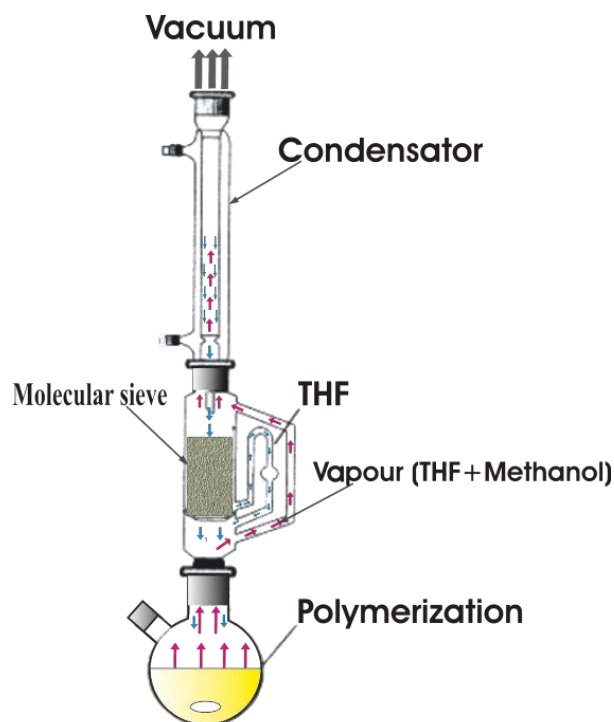

Figure 3.2 Experimental setup to prepare poly(glycerol adipate) using DMA and glycerol
in the presence of CAL-B as a catalyst and THF as solvent.

 The rigioselectivity of lipase towards primary alcohols of the glycerol will yield linear polyesters with free pendent hydroxyl groups at its backbone. The absence of enzyme, on the other hand, results in cross-linked products.[172] The vinyl alcohol produced as by-product, beside PGA during the enzymatic reaction, is directly converted into acetaldehyde by tautomerization and will finally evaporate at the reaction temperature. This will shift the equilibrium of the polycondensation reaction towards the products. The second strategy to synthesize PGA is using DMA instead of DVA. Utilization of DMA will cause some problems of shifting the direction of the equilibrium towards the polymer since methanol will be the by-product of this reaction which has to be removed. Actually, methanol and tetrahydrofurane (THF) form an azeotropic mixture which makes their separation impossible by distillation during the enzymatic reaction. Thus the polymerization reaction would be ceased at low conversions. Therefore, the polymerization reaction is carried out in the presence of molecular sieves placed into a soxhlet apparatus attached on the top of the reaction vessel as depicted in Figure 3.2. Both methanol and THF evaporate together during the enzymatic polymerization and condense again by the condenser to be collected finally into soxhlet extractor where the mixture becomes in contact with the molecular sieve. The molecular sieve has a pore size of 5Å. This size will allow only methanol to be captured by the molecular sieve and thus only pure THF will reflux to the reaction vessel. The capacity of the molecular sieve to entrap methanol is around 14 wt% of its weight. An excess of about 80 *wt*% of molecular sieve is added in order to prevent the system to reach a state of saturation of the molecular sieve with methanol. The procedure described above to remove the resulting by-product has many advantages, e.g. easy to scale-up by increasing the amount of molecular sieve and the molecular sieve is not in contact with the polymer formed. Many strategies have been suggested to remove the resulting by-product in order to shift the reaction equilibrium towards the products in polycondensation processes.[173] However, not all of these strategies are convenient for both laboratories and industrial applications.[174–176] Using the solvent route instead of bulk route for the polycondensation provides a better distribution for both enzyme beads and temperature within the reaction vessel. Furthermore, Juais et al. [177] proved that carrying out enzymatic polymerization in solvents gives a higher M_w than in bulk. The procedure can be extended to be suitable for large scale processes. Table 3.1 shows the results of enzymatic polymerization of divinyl adipate or dimethyl adipate with glycerol at different reaction times. Increasing M_n of the polymer causes also an increase of its polydispersity *D*.

Table 3.1 SEC of PGA synthesized using either DVA or DMA and glycerol.

Kind of adipate	Time [h]	M_w (g/mol)	M_n (g/mol)	D
Divinyl adipate	4	5,070	2,700	1.9
Divinyl adipate	8	7,650	3,500	2.1
Dimethyl adipate	18	1,660	890	1.8
Dimethyl adipate	48	4,800	1,950	2.4

The number-average molecular weights M_n obtained from the reaction of DVA are higher than that of DMA within a shorter time of reaction. The small reactivity of alkyl esters towards alcohols in lipase-catalyzed transesterification could be the reason for these results.[82]
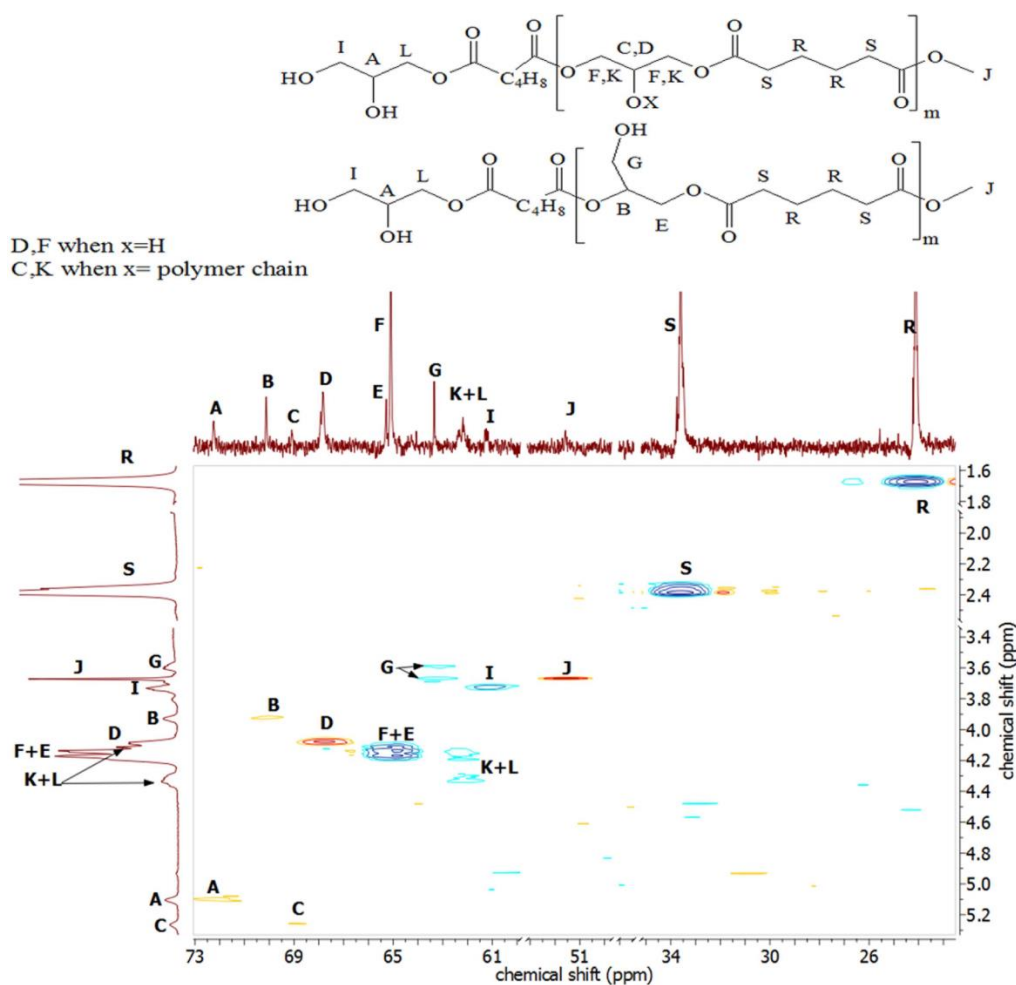

Figure 3.3 ^{1}H-^{13}C COSY NMR spectrum of PGA measured in CDCl$_3$ at room temperature.

PGA (M_n is 1950 g/mol) is characterized first by ^{1}H-^{13}C COSY NMR carried out in CDCl$_3$ and shown in Figure 3.3. The APT NMR spectrum reveals that the peaks at 51.1, 66.1, 68.6, 69.2, 71.9 ppm have a negative value which indicates that they are related to methine (CH) and methyl (CH$_3$) groups. The peak at 51.1 ppm is well known to be related to the methyl group of dimethyl adipate. This essentially means that the other peaks are related to the methine group of glyceride units within the PGA backbone. The peaks in the ^{1}H-^{13}C COSY NMR spectrum are assigned to the polymer structure as shown in Figure 3.3. The presence of many peaks for methine groups indicates some imperfections of the enzyme regioselectivity during polymerization towards primary alcohols. This imperfection causes the formation of 1,2-disubstituted and 1,2,3-trisubstituted glyceride units within the backbone whereas only 1,3-disubstituted and 1-substituted species should appear in the case of ideal regioselectivity of the enzyme during polymerization. The presence of some imperfections of the regioselectivity has been noticed before.[124,178] Actually, the presence of 1,2,3-trisubstituted glyceride has the worst effect on the properties of the backbone since it decreases the number of hydroxyl groups on PGA backbone and will effect also the linearity of the total polymer backbone. The ratio of trisubstitution is calculated using the integral ratio between the peaks R or S and the peak C and it is equal to about 8 mol%.

3.3.2   Temperature dependence of rigioselectivity

Two enzymatic reactions are carried between divinyl adipate and glycerol but at different temperatures (60°C and 40°C) in order to investigate the influence of reaction temperature on the rigioselectivity of the CAL-B. The corresponding ^{13}C NMR spectra of both reaction products are shown in Figure 3.4. The comparison between both spectra shows a complete disappearance of the peaks related to 1,2-disubstituted and 1,2,3-trisubstituted glycerides for the polymer synthesized at 40°C. This indicates a perfect rigioselectivity of the enzyme at 40°C. These results are matching the results reported before for the enzymatic polymerization of divinyl sebacate with glycerol at different temperatures.[179]
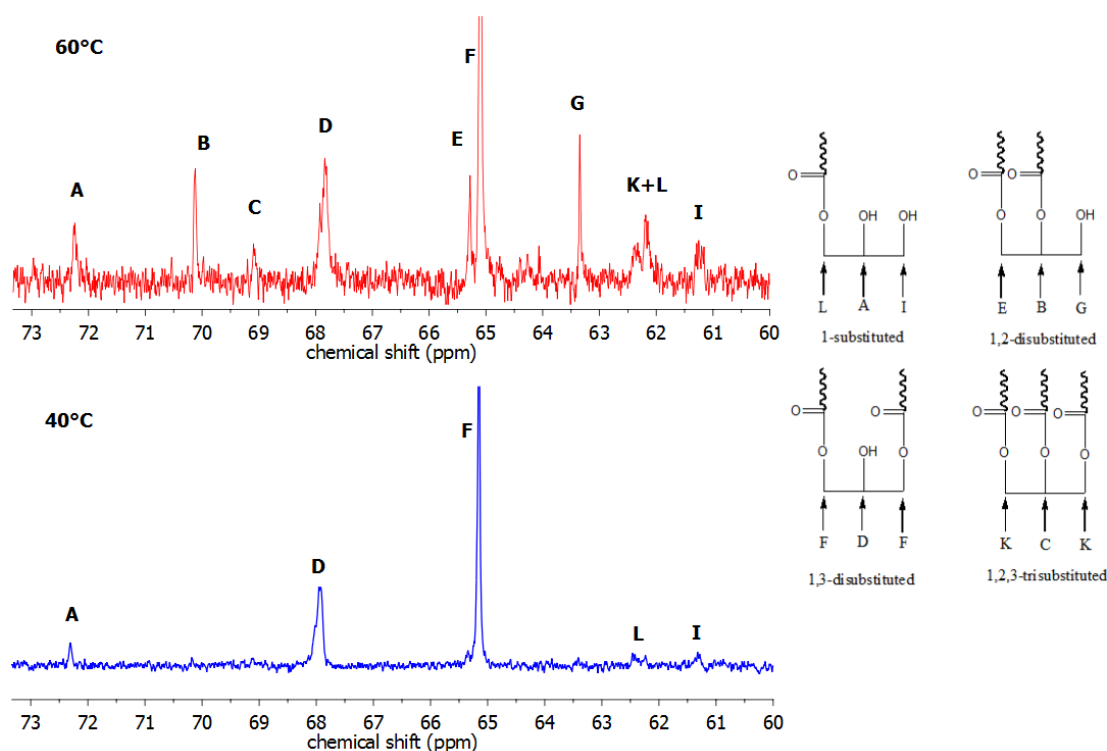
Figure 3.4 Expanded ^{13}C NMR spectra of PGA obtained from glycerol and DVA at 40°C, and at 60°C.

3.3.3   Synthesis poly(glycerol adipate)-*g*-poly(ethylene oxide) (PGA-*g*-PEO)

The synthetic pathway for PGA-*g*-PEO from PGA is shown in (Figure 3.1a and b). Alkyne groups are introduced to the PGA backbone by the esterification reaction between the hydroxyl groups of the PGA backbone and 5-hexynoic acid in the presence of DMAP and EDCI as a catalyst. The ^{1}H NMR spectrum of PGA-alkyne in CDCl$_3$ is given in (Figure 3.5a). The integral ratio between peak a and peak d is 4 : 0.97. This reveals nearly quantitative coupling. The synthesis of PGA$_{17}$-*g*-PEO$_{44}$ is carried out under mild conditions in order to prevent any type of degradation to the polymer backbone. Actually, an excess of 1.1 eq (with respect to alkyne groups) of mPEO-N$_3$ is added. Additionally, (Figure 3.5b) shows the ^{1}H NMR spectrum of PGA$_{17}$-*g*-PEO$_{44}$ in CDCl$_3$. The grafting efficiency is calculated by the integration of the ratio between peak w and peak d which is 3 : 0.97. Thus, the reaction is quantitative within the experimental error. Furthermore, the comparison between the FT-IR spectra of PGA$_{17}$-alkyne and PGA$_{17}$-*g*-PEO$_{44}$ reveals the complete disappearance of the alkyne vibrations of PGA$_{17}$-alkyne at 650, 2115, and 3290 cm^{-1} as a result of the coupling reaction as seen in Figure 3.6. The resulting PGA$_{17}$-*g*-PEO$_{44}$ is water soluble. The polymer structure is similar to the structure of a graft copolymer synthesized using DVA and azide functional diols followed by "click" chemistry.[62]

42
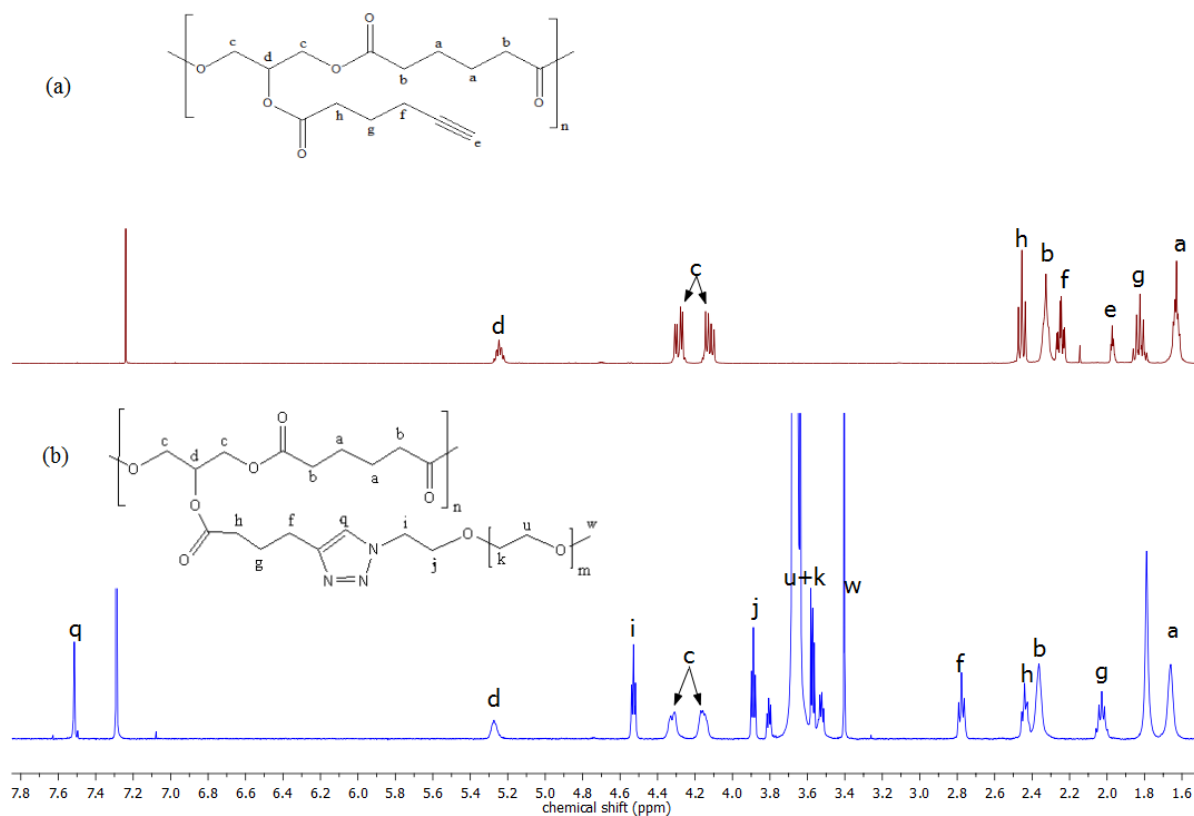
Figure 3.5 ^{1}H NMR spectrum of (a) PGA$_{17}$-alkyne, (b) PGA$_{17}$-*g*-PEO$_{44}$ in CDCl$_3$ at room temperature and 400 MHz.
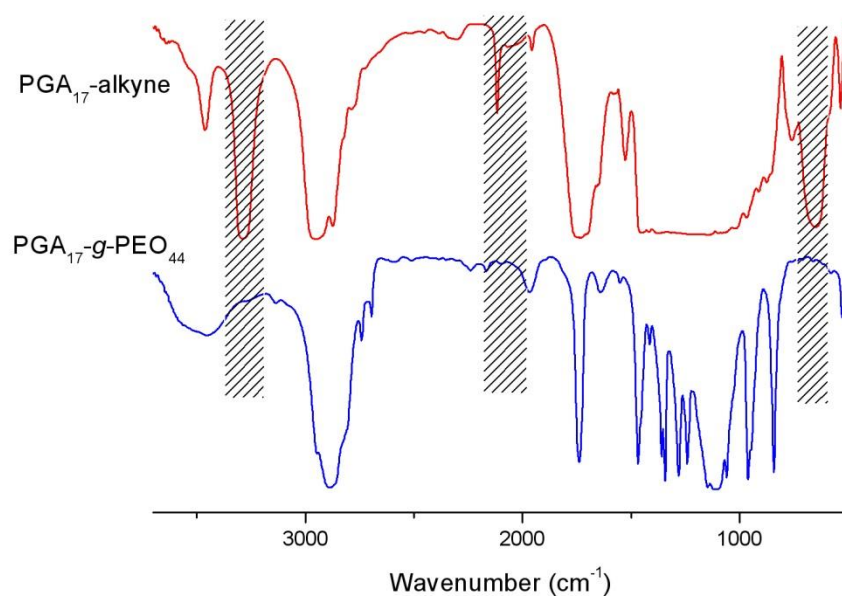
Figure 3.6 FT.IR spectra of PGA$_{17}$-alkyne and PGA$_{16}$-*g*-PEO$_{17}$. Shaded areas represent alkyne peaks.

3.3.4 Modification of PGA backbone with fatty acids

PGA backbone was acylated with aliphatic acid chlorides of lauric acid, stearic acid and behenic acid. Pyridine was added to polymer solution as acid scavenger. The molar mass of polymer backbone was estimated using SEC using THF as eluent and poly(styrene) as a standard. The absence of unreacted fatty acid chains was confirmed by mono-modal distribution of their SEC traces. The ratio of esterification and total molar mass of the modified polymers were determined using the corresponding ^{1}H NMR spectrum.
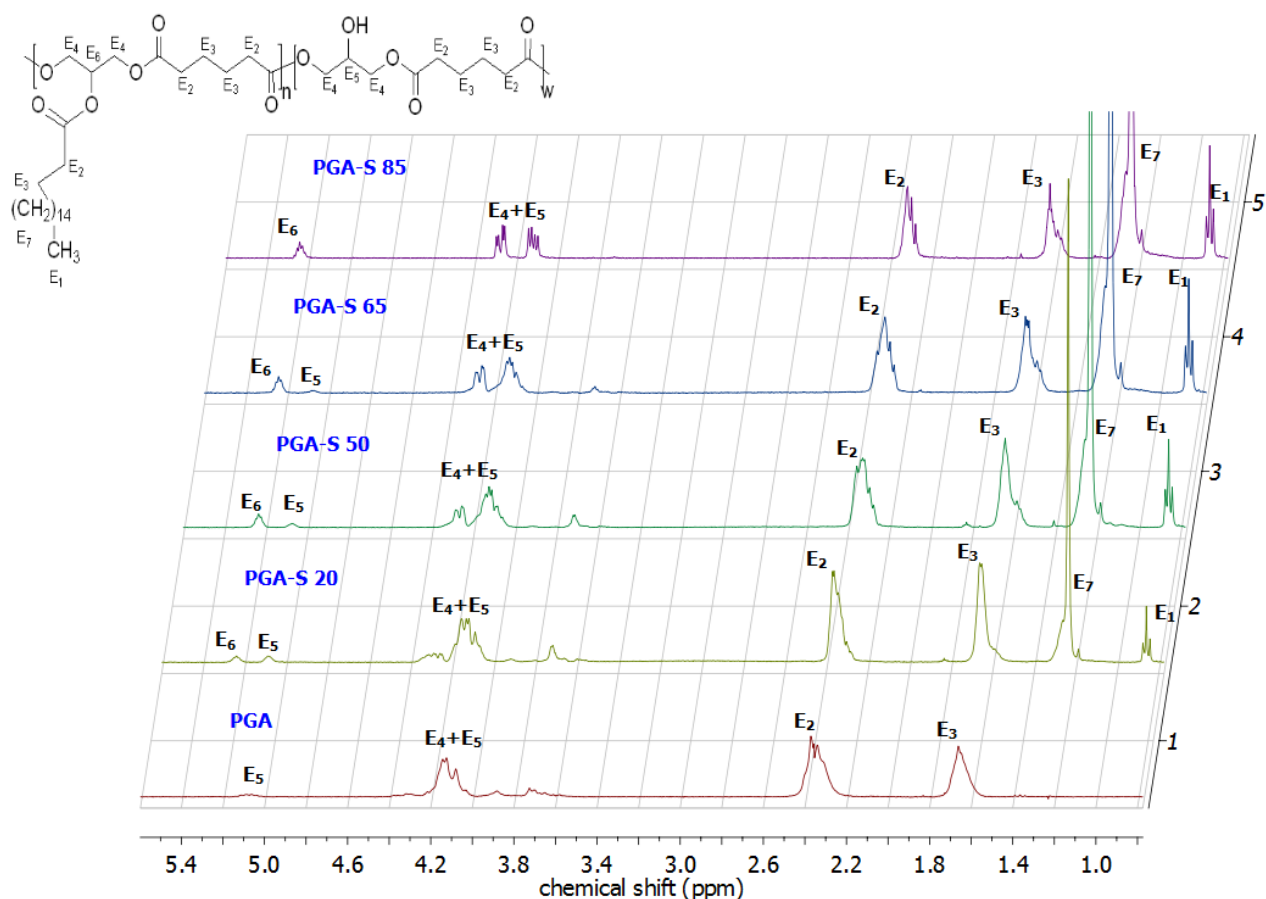
Figure 3.7 ^{1}H NMR spectra (400 MHz, CDCl$_3$) of the comb-like derivatives of PGA with stearoyl side-groups with esterification degrees from 20 mol% (PGA-S20) to 85 mol% (PGA-S85). Peaks and protons used for the calculation of the esterification degree are indicated.

The degree of esterification of OH-groups of poly(glycerol adipate) was calculated from the integrals of the peaks indicated in the ^{1}H NMR spectra according to the equation:

Esterification degree (%) = [1.33×E$_1$/(E$_2$-(0.67×E$_1$))]×100

3.3.5 DSC Measurements

Table II shows the results obtained by DSC. The PGA backbone is an amorphous polymer which means that the crystallization of the substituted polymer is related only to the alkyl side chains. The results reflect an increase of T_m and $\Delta\tilde{H}_m$ with increasing degree of substitution and with increasing length of alkyl side chains.

Table 3.1 Melting temperature T_m, crystallization temperature T_c, specific enthalpy of melting $\Delta\tilde{H}_m$, degree of crystallinity X_{DSC}

Sample	T_m (°C)	T_c (°C)	$\Delta\tilde{H}_m$ (J/g)	X_{DSC} (%)
L30	-37	--[a]	16.4	8.4
L50	-22	-25	61.3	26.4
L75	-20.6	-32	56.8	29.1
Lauric acid	45.3	-41	195.2	100
S8	29.1	21	34	14.6
S20	33.9	29.7	29.9	12.8
S45	36.9	35.4	100.7	43.2
S65	39	36.9	159.7	68.5
S85	38.7	34.8	162.9	69.9
Stearic acid	69.7	66.6	233	100
B45	57.9	57.3	145.2	59.6
B65	51.9	51.18	158.1	64.9
Behenic acid	80.1	76.1	243.7	100

[a] No DCS peak is present under the measurements conditions.

The increase of T_m and $\Delta\tilde{H}_m$ with increasing side chain length is mainly related to the thicker crystalline lamellae, which causes an increase of the energy required for melting the polymer.[180] The decrease of T_m with decreasing degree of substitution must be related to thinner or more imperfect crystals, whereas the decrease in $\Delta\tilde{H}_m$ indicates also a higher amount of amorphous alkyl chains. The results show also a decrease of the degree of

crystallinity with decreasing degree of substitution. Nevertheless, the degree of crystallinity is always lower than the crystallinity of the free fatty with identical chain length alone.

3.3.6 Thermogravimetry

The thermal decomposition temperatures of the stearic acid, PGA, S20, and S45 are investigated using thermo-gravimetric analyses in an air stream with a heating rate of 5°C/min. The results are shown in Figure 3.8. The comparison between the thermograms shows that the stability of S45 is higher than stearic acid or PGA. On the other hand, no big effect of substitution on the stability of the overall polymer is noticed in the case of S20 which has a low degree of substitution.
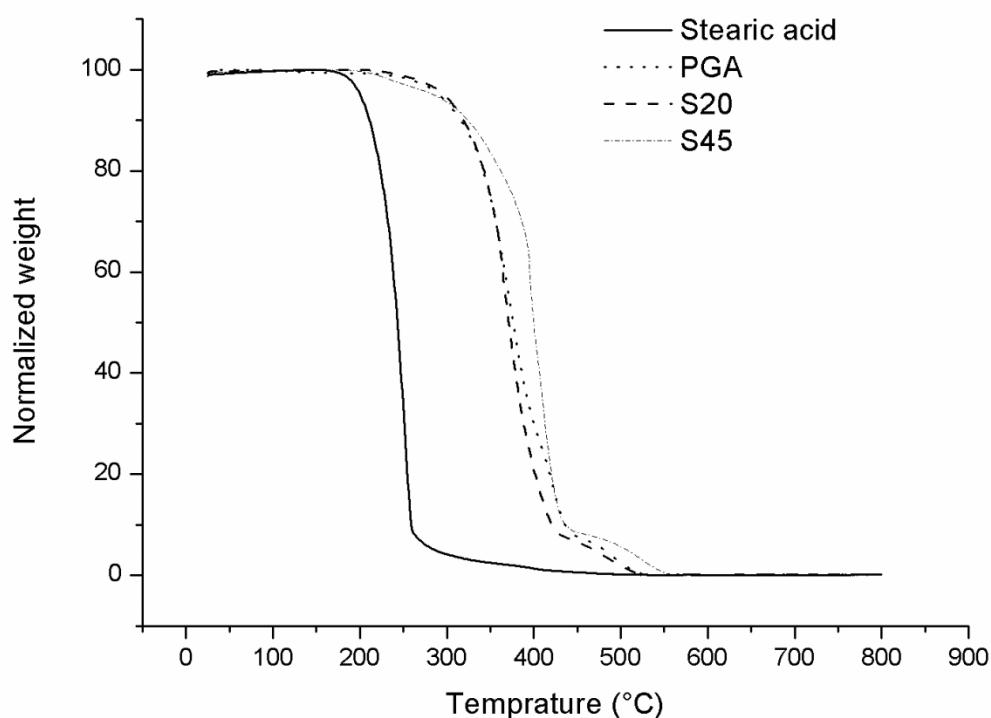
Figure 3.8 Thermal gravimetric analysis (TGA) thermograms of stearic acid, PGA, S20, and S45 using a heating rate of 5 K/min in air.

3.3.7 Transmission electron microscopy

It has been reported by Kallinteri et al.[122] that PGA substituted with stearoyl chains forms spherical nanoparticles. However, our investigation shows that the shape of these nanoparticles is strongly depend on the ratio of substitution. The cryo-TEM and negative

stain-TEM images (Figure 3.9a,b) show various non- spherical shapes of nanoparticles with linear boarders and defined geometries such as hexagons, pentagons, squares, and triangles.
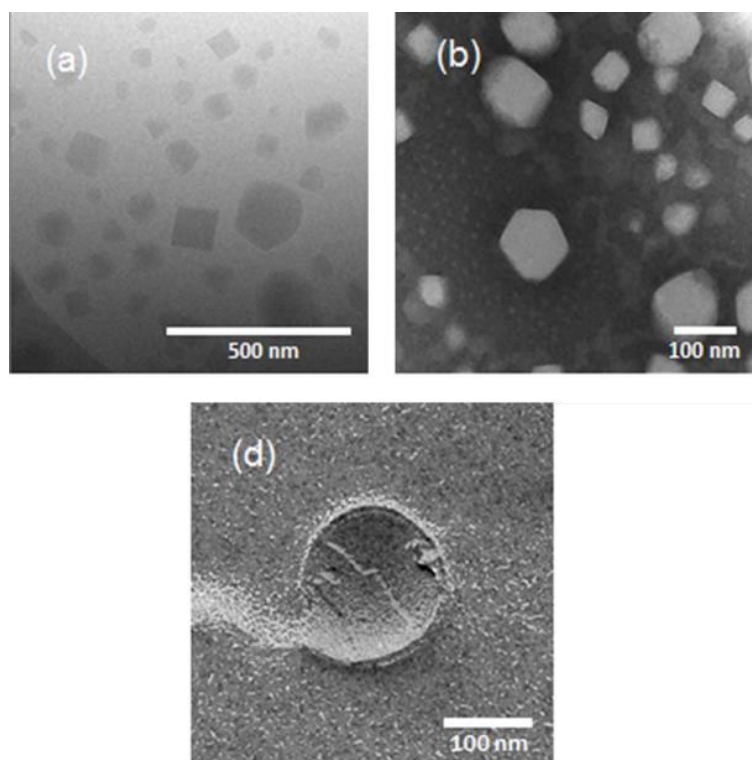
Figure 3.9 (a) Cryo-TEM image of S20 nanoparticles prepared in aqueous suspension. (b) Negative-stain TEM of S20 nanoparticles. (d) Internal structure of S85 nanoparticles after freeze fracture showing a layered morphology**.**

Further investigations into these nanoparticles show the presence of well-ordered pseudo-hexagonal structures.[46] A freeze fracture image of S85 (Figure 3.9d) reveals the presence of internal lamellar structure inside the nanoparticles which is explained as onion-like morphology. Such onion structure is suggested to be as results of alternating crystalline and amorphous phases within the body of the nanoparticles.[46]

3.4 Conclusions

This report describes the synthesis and characterization of poly(glycerol adipate) (PGA), PGA-*g*-PEO and fatty acid modified poly(glycerol adipate). PGA is synthesized by enzymatic polymerization using glycerol and either divinyl adipate or dimethyl adipate. Methanol which is produced as a by-product during the enzymatic polymerization in the case of using DMA is removed by molecular sieves packed into a soxhlet extractor on the top of the reaction vessel. DMA shows a slower enzymatic polymerization rate compared with DVA. The

rigioselectivity of CAL-B is affected by reaction temperature. It has been found that comb-like PGAs with branching are produced when the enzymatic polymerization is carried out at 60°C because of the rigioselectivity imperfection of CAL-B at this temperature. On the other hand, linear PGA can be produced when the reaction is carried out at 40 °C. The OH pendent groups on PGA were quantitatively attached to alkyne groups by esterifying them with 5-hexynoic acid to get PGA-Alkyne. Azide-terminated poly(ethylene oxide) monomethylether was grafted onto PGA-Alkyne by "click" reaction at room temperature to yield PGA-*g*-PEO. The synthetic route described here is considered as alternative strategy to synthesize graft copolymers similar to PAA-*g*-PEO as described in the previous chapter.

In the case of fatty acid modified PGA, both T_m, $\Delta \widetilde{H}_m$ increase with increasing the ratio of substitution and/or by increasing the length of alkyl side chains. This is explained as a result of improvement of the compact packing of the complete comb-like polymers. Substitution is also found to increase the stability of the polymers against thermal decomposition. Transmission electron microscopy images of the nanoparticles depict shapes of the resulting nanoparticles depending on the degree of substitution. S20 is found to form nanoparticles with linear boarders with polyhedral geometries whereas S85 forms onion-like spherical nanoparticles.

Chapter 4

Synthesis and characterization of graft copolymers able to form polymersomes and worm-like aggregates

4.1 Introduction

Graft copolymers have attracted interest of polymer scientists over several decades due to their existing commercial and potential applications.[110,181] Actually, a strong tendency has appeared to use them in the field of drug delivery instead of classic block copolymers due to some superior properties.[107,108] Biodegradability and biocompatibility of any polymer play an important role when used for drug delivery systems. Poly(ethylene oxide) (PEO) is the synthetic standard polymer in the field of pharmacy and medicine due to such properties as e.g. low costs, water-solubility, biocompatibility.[182] PEO is mainly attached to hydrophobic polymers, proteins, and DNA in order to form a water coordination sphere protecting them from being recognized by the immune system thus prolonging the *in vivo* circulation time.[111] Introducing oligo-PEO (sometimes called) as graft segments to a hydrophobic polymer chain can yield thermo-responsive polymers.[183,184] Furthermore, such type of comb-like polymer can form stable micelles with smaller cmc and melting point T_m compared to conventional amphiphilic block copolymers.[110] Using aliphatic polyesters as hydrophobic polymer backbone is an elegant strategy to obtain graft copolymers that are candidates for pharmaceutical applications.[48,159] Poly(glycerol adipate) (PGA) is synthesized by enzymatic polymerization of glycerol and divinyl adipate (DVA) to yield aliphatic linear polyesters with pendent free hydroxyl groups.[124] The process becomes even cheaper when DVA is replaced by dimethyl adipate (DMA).[185] The polymer has potential applications in the field of delivery of nano-carriers after modification of its backbone using fatty acids with different lengths and different degrees of substitution.[47,122]

One drawback of most synthetic comb-like polymers is the small ratio of hydrophobic to hydrophilic entities. Increasing this ratio results in an increase of the loading capacity of hydrophobic drugs.[186] One way to increase the hydrophobicity of graft copolymers is to synthesize amphiphilic graft copolymers with two blocks on its side chains where one of them is hydrophobic. Again, the hydrophobic part of the side chain should also be biodegradable when used for drug delivery.[61,187] Poly(ε-caprolactone) (PCL) is semi-crystalline, biodegradable, biocompatible with many drugs and has the ability of being fully excreted form the body.[188,189] Furthermore, amphiphilic linear block copolymers of PCL and PEO (PCL-*b*-PEO) have been investigated widely for potential applications as micellar drug-

delivery systems.[190,191] The self-assembly of PCL-*b*-PEO in water can vary according to the weight fraction of PEO and to the way of preparation.[192,193] One important form of these aggregates is worm-like micelles that show strong potential for applications as nano-carriers for hydrophobic drugs.[194] Preparation of worms are usually problematic since their phase occupies usually a narrow region of the block copolymer phase diagram.[195,196]Attention has been drawn recently to worm-like micelles caused by the fact that they have compared to typical spherical micelles such properties as higher drug-loading capacity, longer *in vivo* circulation time, and they help to shrink tumors more effectively.[197,198] Nevertheless, worm-like micelles show a relatively rapid degradation to spherical micelles as a result of hydrolytic degradation of PCL chains initiated mainly at the hydroxyl end groups.[199,200] The degradation rate changes dramatically by end capping of the hydroxyl groups. In addition, introducing only 10 mol% of DL-lactide within the PCL block can eliminate the rigidity of the micelles.[192] These results suggest that small modifications of the polymer composition cause significant changes of the properties of worm-like micelles.

Generally, three strategies are applied to synthesize graft copolymers: i) "grafting from",[36,37,201,202] ii) "grafting through"[203,204], and iii) "grafting onto". [31,32,62,142] Amphiphilic graft copolymer with two different side chains can be obtained either by using only one type of grafting strategy[38,205] or by a combination of two types,[39,206] e.g. the combination of "grafting from" and "grafting onto".[40,207]

This chapter describes the synthesis of biodegradable graft block copolymers using PGA as a backbone. PCL-*b*-PEO is attached to PGA by ring opening polymerization of ε-caprolactone using the pendent OH groups of PGA as initiator to synthesize PGA-*g*-PCL with three different lengths of the PCL chains. Then, PEO is added to PGA-*g*-PCL using again CuAAC to obtain finally PGA-*g*-(PCL-*b*-PEO). For comparison, PCL-*b*-PEO is also synthesized with molar masses similar to the grafted chains on the PGA backbone. The aggregation properties of all polymers in water are extensively characterized using scattering and microscopic techniques.

4.2 Experimental section

4.2.1 Materials

All chemicals were purchased from Sigma-Aldrich unless otherwise stated. Tetrahydrofuran (THF) 99.5% was distilled from calcium hydride and stored over molecular sieve 3Å.

Novozym 435 was dried under vacuum at 4°C over P_2O_5 for two days prior to use. Tin octoate was distilled under reduced pressure and stored over molecular sieve 4Å. Pyridine and ε-caprolactone (99%) were dried over calcium hydride overnight, distilled under atmospheric pressure and stored over molecular sieve (3Å). Poly(ethylene oxide) monomethyl ether = 2000 g/mol, , p-toluenesulfonyl chloride 99%, chloroform 99.9% HPLC grade, n-hexane ≥99.0%, dichloromethane 99.5%, copper bromide 99.99%, N,N,N′,N″,N″-pentamethyldiethylenetriamine (PMDETA), dichloromethane ≥99.5% (DCM), N-(3-dimethylaminopropyl)-N′-ethylcarbodiimide hydrochloride (EDC), N,N′-dicyclohexylcarbodiimide (DCC), 4-(dimethylamino)pyridine (DMAP) were used as received. Divinyl adipate (98%) was purchased from Fluorochem, U.K. and used as received. The synthesis of azide-terminal poly(ethylene oxide) monomethylether (mPEO-N_3) was performed as described by Gao et al.[31] The number-average molar mass was M_n = 2000 g/mol. Ploy(glycerol adipate) was synthesized from glycerol and DVA as described by Kallinteri et al.[122]

4.2.2   Synthesis of poly(glycerol adipate)-g-poly(ε-caprolactone) PGA-g-PCL

The PGA used for this reaction had M_n= 3400 g/mol determined by SEC. PGA (1.06 g, 5.5 × 10^{-3} mol with respect to OH group) was charged into a 50 mL Schlenk tube equipped with magnetic stirrer. This was followed by addition of ε-caprolactone (15.7 mL, 0.137 mol), 0.15 mL tin octoate, and 25 mL of anhydrous THF. The solution was degassed using three freeze-pump-thawing cycles. The resulting solution was stirred at 80°C for 20 h. Finally, the solution was diluted with THF and precipitated in 400 mL of methanol. Precipitation in methanol was repeated many times to remove the inevitably generated homopolymer poly(ε-caprolactone).[36] The resulting polymer was dried under vacuum at room temperature. Yield=46%.

4.2.3   Synthesis of alkyne-modified poly(glycerol adipate)-*g*-poly(ε-caprolactone), PGA-*g*- (PCL-alkyne)

PGA-g-PCL (1 g, M_n= 32000 g/mol, 0.52 mmol) and 5-hexynoic acid (0.13 mL, 1.15 mmol) were dissolved in 25 mmol of anhydrous DCM and charged into 250 mL two neck round bottom flask. The solution was cooled using an ice bath. Then a solution of EDCI (220 mg, 1.15 mmol) and DMAP (28 mg, 0.23 mmol) dissolved in 7 mL DCM was added dropwise. The mixture was agitated using a magnetic stirrer and sealed using rubber a septum for 24 h at ambient temperature. The solution was filtered to remove the precipitate. This was followed by a concentration of the solution using rotary evaporation. The polymer solution was then

precipitated two times into cold diethyl ether and dried under vacuum at room temperature. Yield=72%.
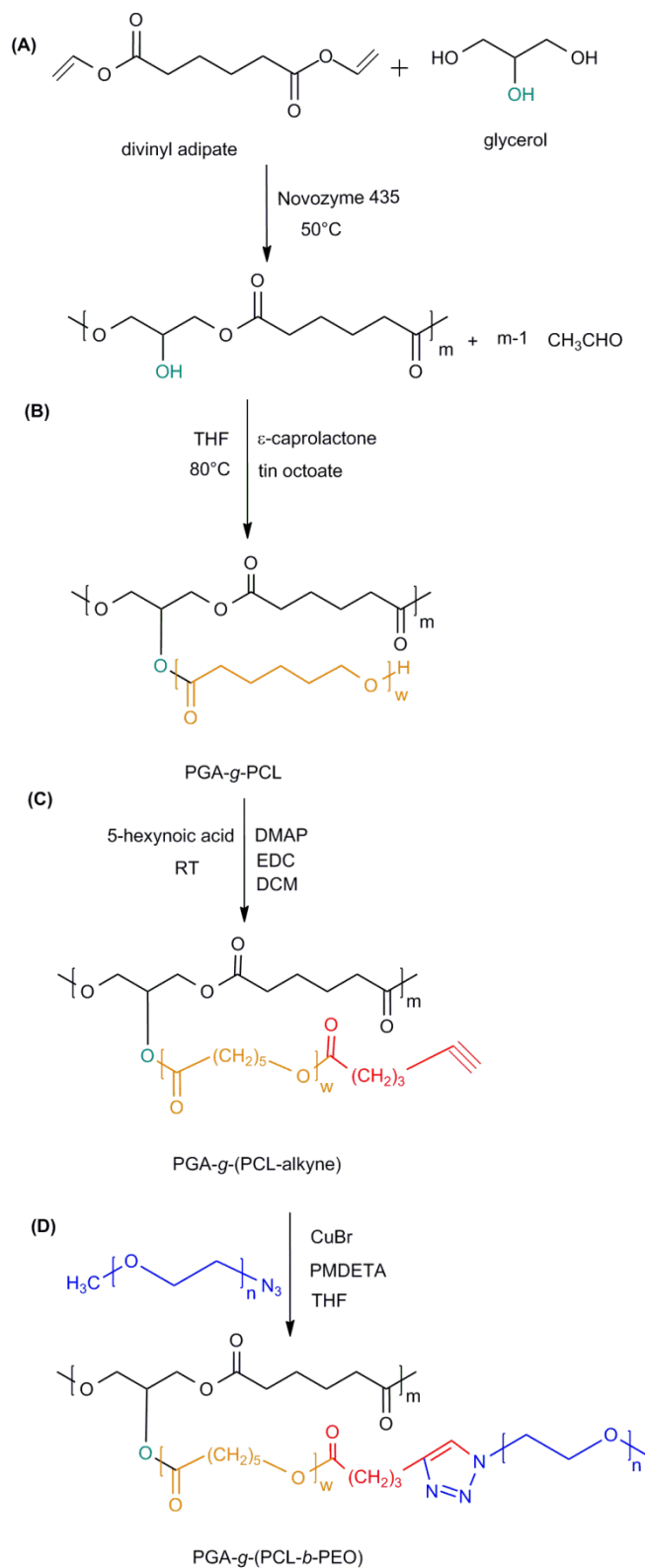

Figure 4.1 (A) Enzymatic synthesis of PGA, (B) Ring opening polymerization of ε-caprolactone at 80°C using OH of PGA,(C)Esterification reaction to prepare PGA-*g*-(PCL-alkyne), (D) CuAAC to obtain PGA-*g*-(PCL-*b*-PEO).

4.2.4 Synthesis of PGA-*g*-(PCL-*b*-PEO) using CuAAC

The typical procedure for the polymer synthesis can be described as the following; PGA-*g*-PCL (0.550 g, M_n=32000 g/mol, 0.289 mmol), mPEO-N$_3$ (0.618 g, M_n= 2000 g/mol, 0.301 mmol), and PMDETA (0.042 mL, 0.202 mmol) were dissolved in anhydrous DMF, and added to 25 mL Schlenk tube. The tube was degassed by bubbling nitrogen into the solution for 20 min. This was followed by addition of CuBr (29 mg, 0.202 mmol). Further degassing was carried out for 10 min. The solution was kept at room temperature for 48 h. The reaction was quenched finally by addition of 10 mL THF. The polymer solution was passed through an alumina column to remove CuBr. The resulting solution was concentrated and then dialyzed against water for 4 days using a dialysis membrane of MWCO= 3500 g/mol. The polymer was dried by freeze-drying. Yield=66%.

4.2.5 Synthesis of α-hydroxy-ω-alkyne end functional poly(ϵ-caprolactone) (Alkyne-PCL)

The polymer was synthesized according to the procedure described by Hoogenboom et al.[208] The reaction was carried out at 85 °C.

4.2.6 Synthesis of poly(ϵ–caprolactone)-*b*-poly(ethylene oxide) PCL-*b*-PEO

Alkyne-PCL (0.5 g, M_n=2900 g/mol, 0.172 mmol) and mPEO-N$_3$ (0.141 g, M_n= 2000 g/mol, 0.206 mmol) were dissolved in 20 mL anhydrous DMF and added to an oven dried Schlenk tube. The tube was sealed by rubber septum and purged with nitrogen for at least 10 min. CuBr (15 mg, 0.1 mmol) and PMDETA (0.02 mL, 0.1 mmol) were then added. The solution was further purged with nitrogen for 10 min. The solution was kept at room temperature for 2 days. At the end of reaction the solvent was removed under vacuum using rotary evaporator, then 20 mL of THF was added and the solution was passed through an alumina column in order to remove copper bromide. The solution was dialyzed against acetone for 2 days using a dialysis membrane of MWCO=2000 g/mol. Finally, the solvent was removed and the resulting polymer was dried in an oven at 50°C under vacuum. Yield=58%.
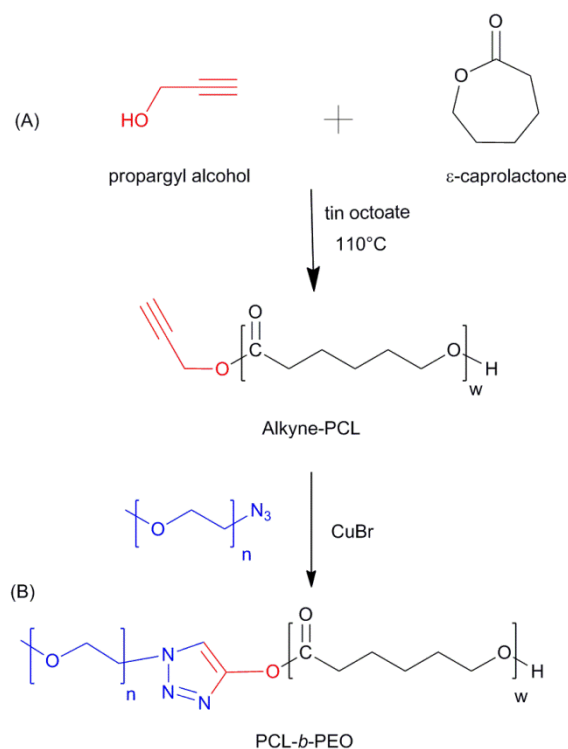
Figure 4.2 Synthesis of PCL-*b*-PEO. (A) Synthesis of alkyne-PCL by ring opening polymerization in the presence of tin octoate at 100°C. (B) Coupling reaction using CuAAC.

4.2.7 Procedures

The weight-average molar mass (M_w), number-average molar mass (M_n), and molar mass distribution (M_w/M_n) were measured by size-exclusion chromatography (SEC) using tetrahydrofuran (THF). The measurements were performed at room temperature using ViscotekGPCmax VE2001 and RI detector Viscotek 3580. For calibration PS standards were employed. ^{1}H and ^{13}C NMR spectra were recorded using a Varian Gemini 2000 spectrometer operating at 400 MHz or 500 MHz for ^{1}H NMR and 200 MHz for ^{13}C NMR spectroscopy. CDCl$_3$ was used as solvent. The surface tensions γ of the aqueous polymer solution at different concentrations were measured by the Wilhelmy plate method using an automated DCAT tensiometer (Data Physics Instruments). The tensiometer worked automatically by injecting predetermined volumes of micelle solution into milli Q water. The surface tension was measured after 10 min of stirring and 3 h waiting period. Measurements were carried out at 25° C. Dynamic light scattering (DLS) measurements were achieved using an ALV/DLS-5000 instrument (ALV GmbH, Langen). The DLS instrument was equipped with a goniometer for automatic measurements between scattering angles θ of 30 and 140°. The correlation functions were analyzed by the CONTIN method, which provide information on the distribution of decay rate (Γ). Apparent diffusion coefficients were obtained from

$D_{app} = \Gamma/q^2$ (where $q = (4\pi n/\lambda) \sin(\theta/2)$, λ is the wavelength of the light, n was the refractive index, and θ was the scattering angle). Finally, apparent hydrodynamic radii were calculated via Stokes-Einstein equation. The solutions of polymer micelles were prepared with a concentration of 1 g/L and directly filtered into the light scattering cells through a 0.45 µm pore size PTFE filter. The hydrodynamic radii were determined at 12 different angles and averaged for each concentration.

4.2.8   Micelle preparation

The typical procedure for the preparation of spherical micelles was as the following. 8 mg of polymer was dissolved in 1.8 mL acetone. The solution was stirred for 5 h using a magnetic stirrer. Afterwards, 3 mL of milli Q water was added to the organic solution within 3 h using a syringe pump (KD Scientific, Holliston). The resulting solution was then transferred into a dialysis bag (MCWO=1000 g/mol) and dialyzed against milli Q water for 24 h. On the other hand, the micelle solutions for temperature-dependent ^{1}H NMR experiments were prepared as the following. 20 mg of polymer was dissolved in 0.75 mL acetone (HPLC grade) and then stirred for 2 h. Afterwards, 2 mL of D_2O was added slowly to the polymer solution under vigorous stirring. The resulting solution was then gently stirred for 20 h at room temperature in order to evaporate the acetone. Finally, the volume of the solution was adjusted to 1 mL by rotary evaporator at room temperature.

4.2.9   Worm-like aggregates

The solution of worm-like aggregates was prepared by the cosolvent/evaporation method.[199] Briefly, 2 mg of the graft copolymer was dissolved in 60 µl chloroform. Then the resulting solution was added to 10 mL of milli Q water. The resulting mixture was immersed into an ice bath and stirred for 30 min using a disperser (IKA, Type T 25 basic, Staufen, Germany) at rotation speed of 19000 rpm. This was followed by gentle stirring for four days at 4°C or for 48 h at room temperature in order to remove chloroform. The final concentration of the micelle solution was 0.2 mg/mL.

4.2.10 Fluorescence microscopy (FM) of worm-like aggregates

250 µL of solution with worm-like aggregates was taken in an Eppendorf tube, then 0.2 µL of 0.2 mM fluorescent dye (PKH26, Sigma) was added, the mixture was then gently mixed. 7 µL of this solution was placed on a glass slide. The spotted solution was then covered using round cover lip 18 mm. The worm-like aggregates were visualized using a fluorescence microscope. Brownian motion of worm-like aggregates was visualized at 570-600 nm

(excitation 543 nm), using a Leica TCS SP2 DM IRE2 confocal laser scanning microscope (CLSM) with a HCX PL APO 63x1.4 oil immersion objective (Leica Microsystems, Wetzlar, Germany). Images were recorded from single scans or time lapse series.

4.2.11 Transmission electron microscopy (TEM), and scanning electron microscopy (SEM)

The negatively stained samples were prepared by spreading 5 µL of the dispersion onto a Cu grid coated with a Formvar-film (PLANO, Wetzlar). After 1 min excess liquid was blotted off with filter paper and 5 µL of 1wt% aqueous uranyl acetate solution were placed onto the grid and drained off after 1 min. The dried specimens were examined with an EM 900 transmission electron microscope (Carl Zeiss Microscopy GmbH, Oberkochen, Germany). Micrographs were taken with a SSCCD SM-1k-120 camera (TRS, Moorenweis, Germany).

SEM images were prepared by coating a thin layer of a micelle solution (1 mg/mL) onto freshly cleaned silicon substrates. The water was let to evaporate at room temperature. The substrates was immersed for 2 s into milli Q water and dried again at ambient conditions. The sample was then coated with a 2-5 nm Pt layer by Cressington Sputter, and then characterized by Jeol JSM-6700F field emission scanning electron microscopy

4.3   Results and discussion

4.3.1   Synthesis and characterization of PGA-*g*-(PCL-*b*-PEO) and PCL-*b*-PEO

Figure 4.1 gives a summary of polymer backbones synthesis and grafting reactions carried out. PGA is synthesized enzymatically using DVA and glycerol as monomers. The resulting by product is vinyl alcohol which tautomerizes to acetaldehyde and thus evaporates at the reaction temperature.

PCL is introduced to PGA by a "grafting from" strategy using ring opening polymerization of ε-caprolactone as a monomer and tin octoate as a catalyst at different reaction times. The hydroxyl groups on the PGA backbone initiate this reaction. Three polymers are synthesized with different PCL molar masses. The results of the grafting polymerizations are summarized in Table4.1.

Table 4.1 M_n and M_w/M_n data of PGA-*g*-PCL synthesized at different reaction times.

Sample	Reaction Time (h)	$M_{n,PCL}$[a] (g/mol)	$M_{n,total}$[b] (g/mol)	M_w/M_n[c]
PGA$_{17}$-g-PCL$_{13}$	15	1500	28,600	1.3
PGA$_{17}$-g-PCL$_{15}$	20	1700	32,000	1.3
PGA$_{17}$-g-PCL$_{24}$	30	2700	48,800	1.5

[a] M_n of PCL attached to the PGA backbone calculated by ^{1}H NMR spectroscopy. [b] M_n of the graft copolymer is obtained by ^{1}H NMR spectroscopy. [c] Obtained by SEC. All subscripts in the sample column refer to the number of repeat monomeric units.

Actually, increasing the reaction time causes an increase of the molar mass of PCL side chains and polydispersity. The SEC traces of PGA and PGA-*g*-PCL of different molar masses are shown in Figure 4.3. The graft copolymers have higher molar masses (lower elution volumes) than the PGA backbone. Furthermore, no trace of free PCL chains can be detected which confirms the efficiency of the purification step.
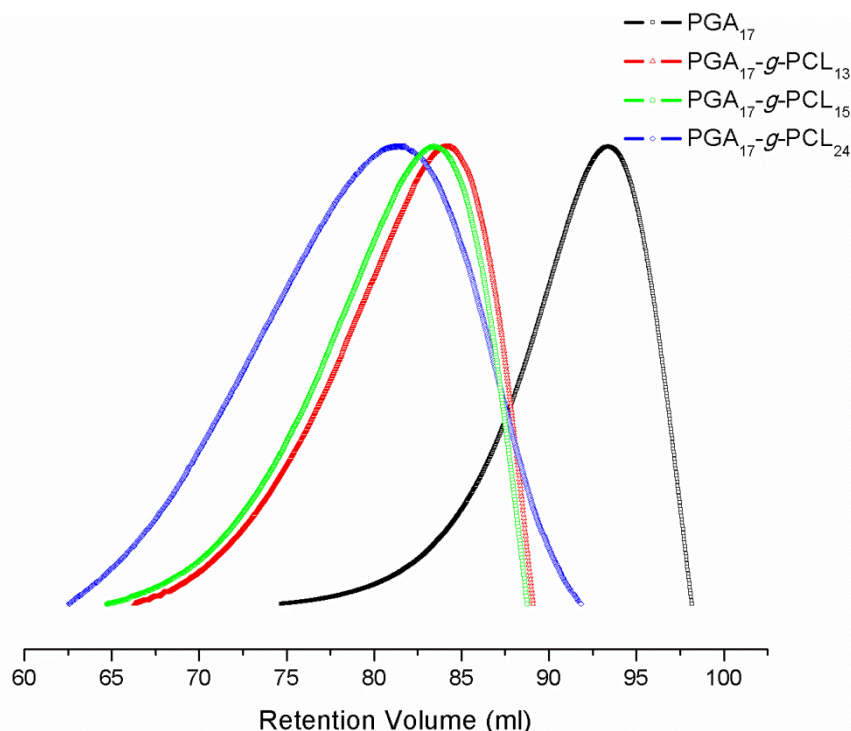
Figure 4.3 Comparison of the SEC traces of PGA and PGA$_{17}$-*g*-PCL$_{13}$, PGA$_{17}$-*g*-PCL$_{15}$, PGA$_{17}$-*g*-PCL$_{24}$ taken at room temperature in THF.

The ^{1}HNMR spectrum of PGA$_{17}$-*g*-PCL$_{15}$ is shown in Figure 4.4. Actually, the integral ratio between peak H` and peak D of the $^1$H NMR spectrum is 2 : 0.97 which indicates that the grafting is carried out nearly quantitative on all hydroxyl groups of the PGA backbone. Furthermore, the integral ratio between peak H` and peak E is used to calculate the length of the grafted PCL chain. As a catalyst tin octoate is used which has FDA approval as a food additive.[209]

mPEO-N$_3$ of molar mass of 2000 g/mol is introduced to the polymer backbone by the "grafting onto" strategy using CuAAC. This route is achieved by two steps C and D explained in Figure 4.1. Firstly, the hydroxyl groups at the end of the PCL side chains are connected to alkyne groups by esterification using 5-hexynoic acid. Secondly, this is followed by CuAAC with mPEO-N$_3$ at room temperature. Figure 4.4C reveals the complete disappearance of the signal H` after esterification reaction with 5-hexynoic acid which essentially means that all repeating units are linked with alkyne groups. This is followed by the coupling reaction under mild conditions. The results of this coupling are summarized in Table 4.2.
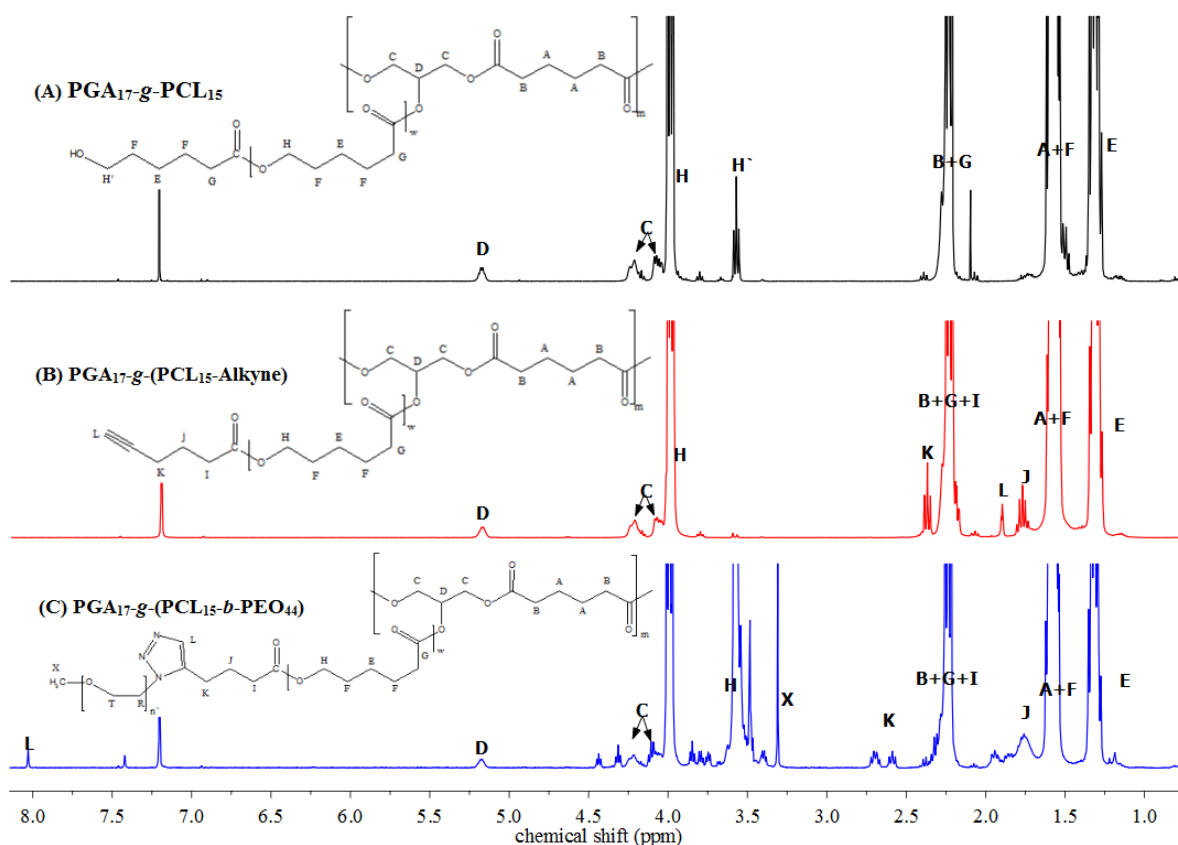

Figure 4.4 ^{1}H NMR spectra of (A) PGA$_{17}$-*g*-PCL$_{15}$, (B) PGA$_{17}$-*g*-(PCL$_{15}$-alkyne) and (C)PGA$_{17}$-*g*-(PCL$_{15}$-*b*-PEO$_{44}$) measured at room temperature in CDCl$_3$.

Table 4.2   The coupling ratio, M_n, $M_{n,\text{total}}$, M_w/M_n of the polymers.

Sample	Coupling ratio[a] (mol %)	$M_{n,\text{PCL}}$[b] (g/mol)	$M_{n,\text{total}}$[c] (g/mol)	M_w/M_n[d]
PGA$_{17}$-*g*-(PCL$_{15}$-*b*-PEO$_{44}$)	100	1700	65680	1.6
PGA$_{17}$-*g*-(PCL$_{24}$-*b*-PEO$_{44}$)	90	2700	79140	1.2
PCL$_{16}$-*b*-PEO$_{44}$	100	1800	3800	1.4
PCL$_{25}$-*b*-PEO$_{44}$	100	2900	4900	1.2

[a] Determined by ^{1}H NMR, [b, c] calculated using ^{1}H NMR spectroscopy. [d] Obtained by SEC. All subscripts in the sample column refer to the number of repeat monomeric units.

Typically, the ratio between peak Q and peak D in Figure 4.4 is used to determine the coupling ratio. A comparison between the FT-IR spectra of PGA$_{17}$-*g*-(PCL$_{24}$-alkyne) and PGA$_{17}$-*g*-(PCL$_{24}$-*b*-PEO$_{44}$) which is shown in Figure 4.5 reveals the complete disappearance of alkyne vibrations at 650 cm^{-1} and 3295 cm^{-1}.
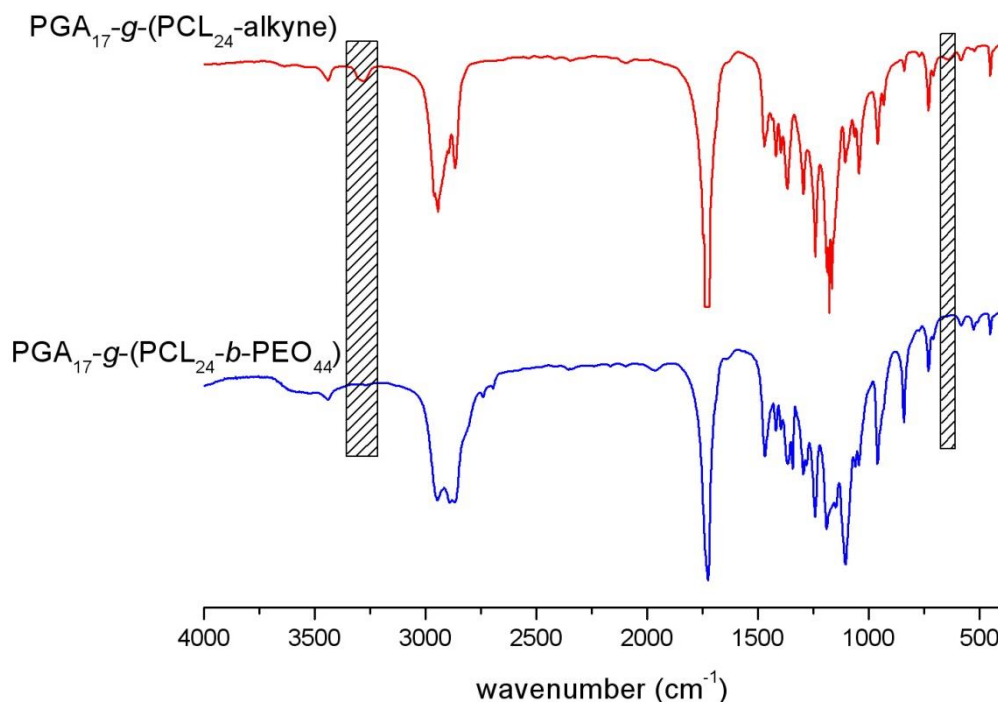

Figure 4.5 FT-IR spectra of PGA$_{17}$-*g*-(PCL$_{24}$-alkyne) and PGA$_{17}$-*g*-(PCL$_{24}$-*b*-PEO$_{44}$).Shaded areas represent alkyne peaks.

The FT-IR spectrum of PGA_{17}-g-$(PCL_{24}$-b-$PEO_{44})$ does not show an azide peak at 2100 cm^{-1} which indicates the absence of free $mPEO$-N_3 chains from the final product.
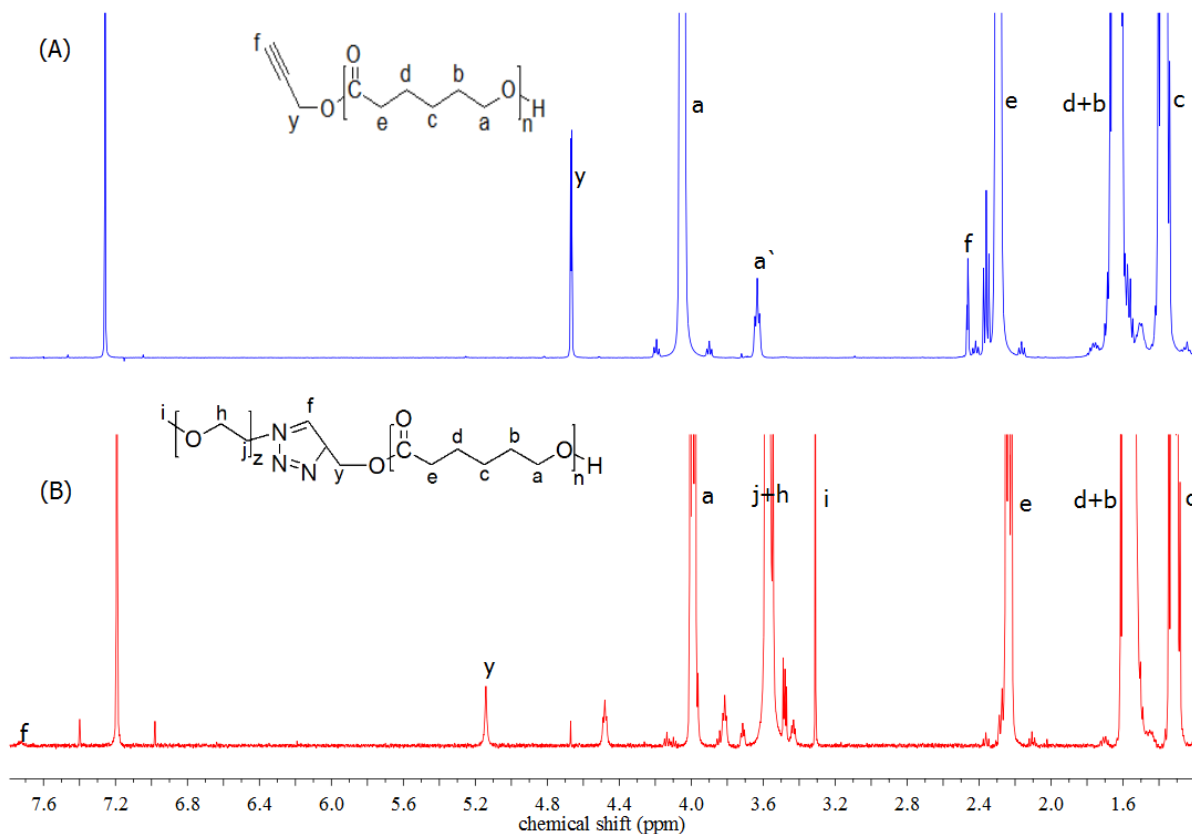
Figure 4.6 ^{1}H NMR of (A) alkyne-PCL_{25} and (B) PCL_{25}-b-PEO_{44} measured in $CDCl_3$ at 500MHz.

For comparison of the properties, a linear block copolymer of PCL-b-PEO with comparable molar masses to the respective grafted blocks at the PGA backbone is synthesized. The synthetic route for this block copolymer is shown in Figure 4.2. CuAAC is used to couple both blocks. The reaction is confirmed using ^{1}H NMR spectroscopy showing the complete disappearance of methine hydrogen resonance at δ = 2.47 ppm Figure 4.6. The comparison between the SEC traces of alkyne-PCL_{25} and PCL_{25}-b-PEO_{44} shows a shift towards the higher molar mass region after coupling reaction which is shown Figure 4.7

Figure 4.7 SEC curves of alkyne-PCL$_{25}$ and PCL$_{25}$-b-PEO$_{44}$ recorded using THF as eluent.

4.3.2 Dynamic Light Scattering (DLS)

The aggregation of polymers in water is characterized using DLS. Both PGA$_{17}$-*g*-(PCL$_{15}$-*b*-PEO$_{44}$) and PGA$_{17}$-g-(PCL$_{24}$-*b*-PEO$_{44}$) a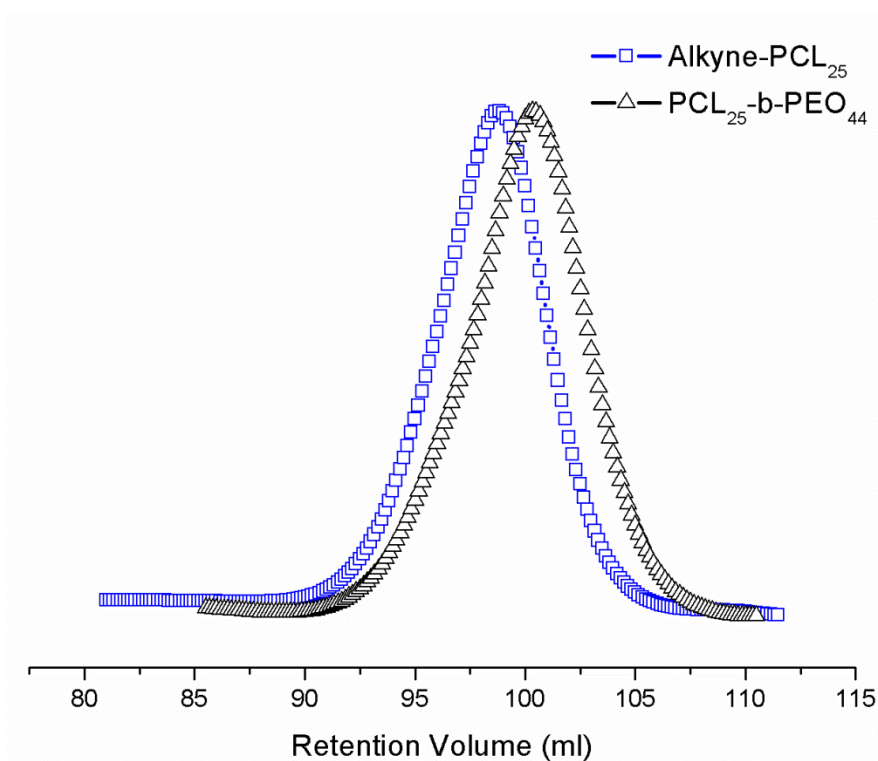re insoluble in water. However, micellar solutions of both polymers in water are achieved by dialyzing its acetone solution against water. The DLS results are summarized in the Table 4.3. Each radius represents the average of twelve radii measured at different angles. Typically, the size of micelles formed by simple diblock copolymer of PCL-*b*-PEO varies according to the preparation method.[210] In agreement with these results, Luo et al.[211] showed that PCL$_{23}$-*b*-PEO$_{45}$ can form micelles of diameter of 25±2 nm when the micelles are prepared by dialysis from DMF solution against water. PCL$_{16}$-*b*-PEO$_{44}$ has a shorter hydrophobic chain length hence it has a smaller micelle radius than PCL$_{25}$-*b*-PEO$_{44}$. Both graft copolymers show two types of aggregates. The small aggregates have similar dimensions as the micelles of the diblock copolymers and they can thus be assigned to micelles. The intensity of the large aggregates is equal or even smaller than the intensity of aggregates with smaller radius as shown in figure 4.8. As the intensity is proportional to the fifth-order of radius the population of aggregates with larger radius is very small compared to those with smaller radius.[212]
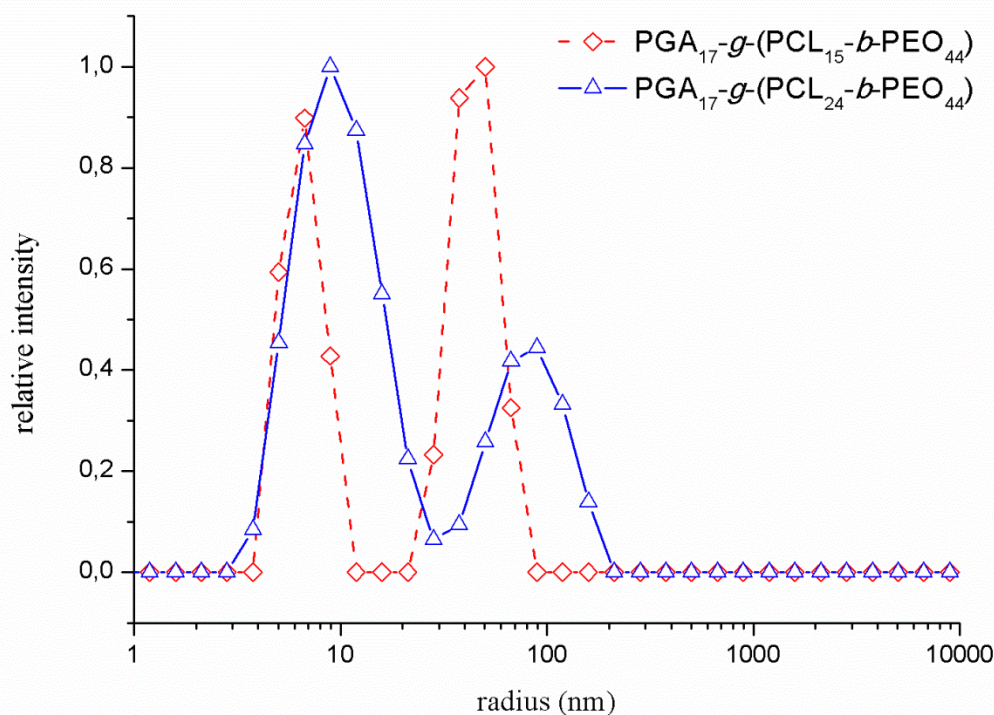
Figure 4.8 Hydrodynamic radius distribution of PGA$_{17}$-g-(PCL$_{15}$-b-PEO$_{44}$) and PGA$_{17}$-g-(PCL$_{24}$-b-PEO$_{44}$) in water at a concentration of 1 g/L, scattering angle of 40°, and temperature of 25 °C.

Table 4.3   Average of hydrodynamic radii measured in water at room temperature at twelve different angles by DLS.

Sample	First Radius (nm)	Second Radius (nm)
PCL$_{16}$-b-PEO$_{44}$	9.4±0.82	---
PCL$_{25}$-b-PEO$_{44}$	11.3±1.25	---
PGA$_{17}$-g-(PCL$_{15}$-b-PEO$_{44}$)	8.5±1	57±6
PGA$_{17}$-g-(PCL$_{24}$-b-PEO$_{44}$)	9.5±1.2	76.3±18

4.3.3   Micelle characterization by ^{1}H NMR spectroscopy

A comparison between the ^{1}H NMR spectra of PGA$_{17}$-g-(PCL$_{15}$-b-PEO$_{44}$) obtained in D$_2$O and in CDCl$_3$ is carried out. Actually, CDCl$_3$ is considered to be a good solvent for all blocks and the polymer backbone whereas D$_2$O is only a good solvent for PEO.

Figure 4.9 ^{1}H NMR spectra of PGA$_{17}$-g-(PCL$_{15}$-b-PEO$_{44}$) obtained in D$_2$O and in CDCl$_3$ at room temperature.

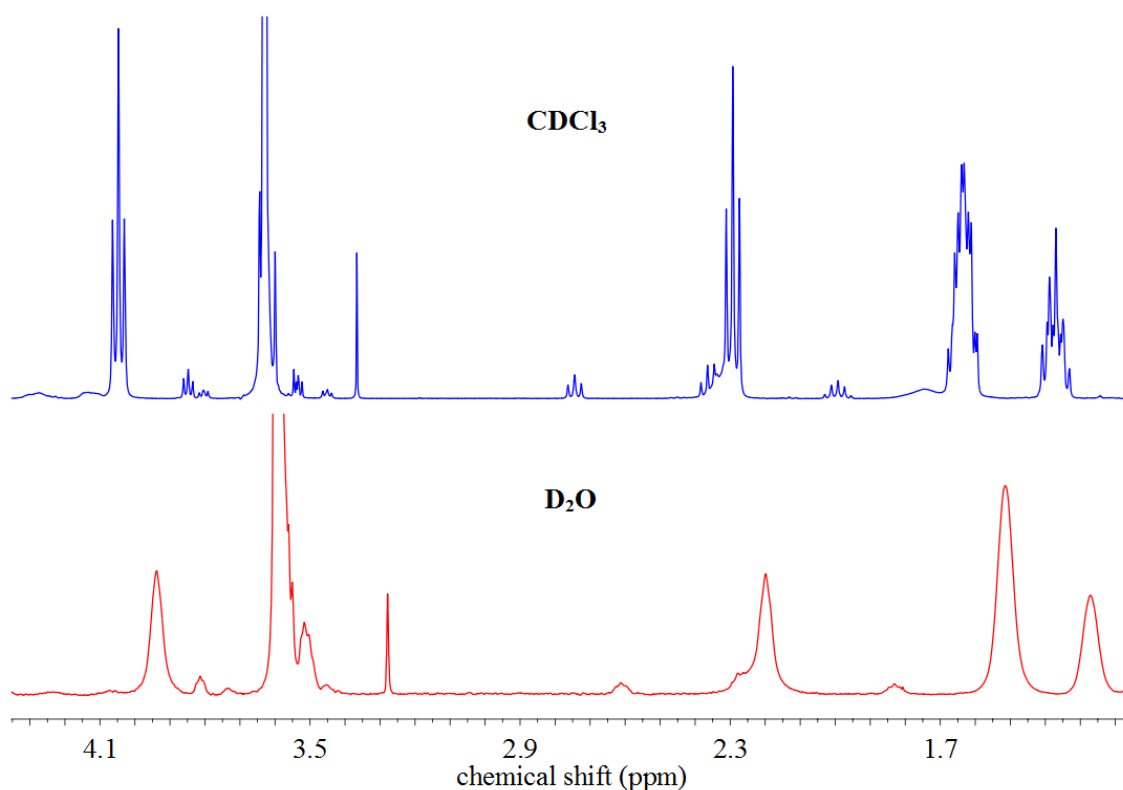Figure 4.9 shows the spectra in both solvents. The comparison between both spectra reveals that the peaks at 1.37, 1.63, 2.3, 2.75, 4.05 ppm, which belongs to the hydrophobic part of the polymer (PGA and PCL), have a lower resolution in D$_2$O in a comparison with the peaks in CDCl$_3$. Attenuation and disappearance of the splitting of signals in ^{1}H NMR spectra indicate a decrease of chain mobility.[213–215] A reduced mobility suggests that the hydrophobic parts of the graft copolymer form the core of micelles in water.

Figure 4.10 provides a comparison between the expanded ^{1}H NMR spectra of PGA$_{17}$-g-(PCL$_{15}$-b-PEO$_{44}$) and PCL$_{16}$-b-PEO$_{44}$ micelles in D$_2$O at different temperatures. The peaks in all spectra are related to the CH$_2$ groups of the hydrophobic PCL block and the PGA backbone. The spectra of both polymers show a significant upfield shift of the resonance signal with increasing temperature. The upfield shift is induced by changing of magnetic susceptibility of the protons upon raising temperature as a result of the decreasing polarity of water.[216] Additionally, both spectra reveal that an increasing solution temperature leads also to an increased resolution of the peaks. This is caused by an increase of the mobility of the hydrophobic cores in the micelles of both polymers.
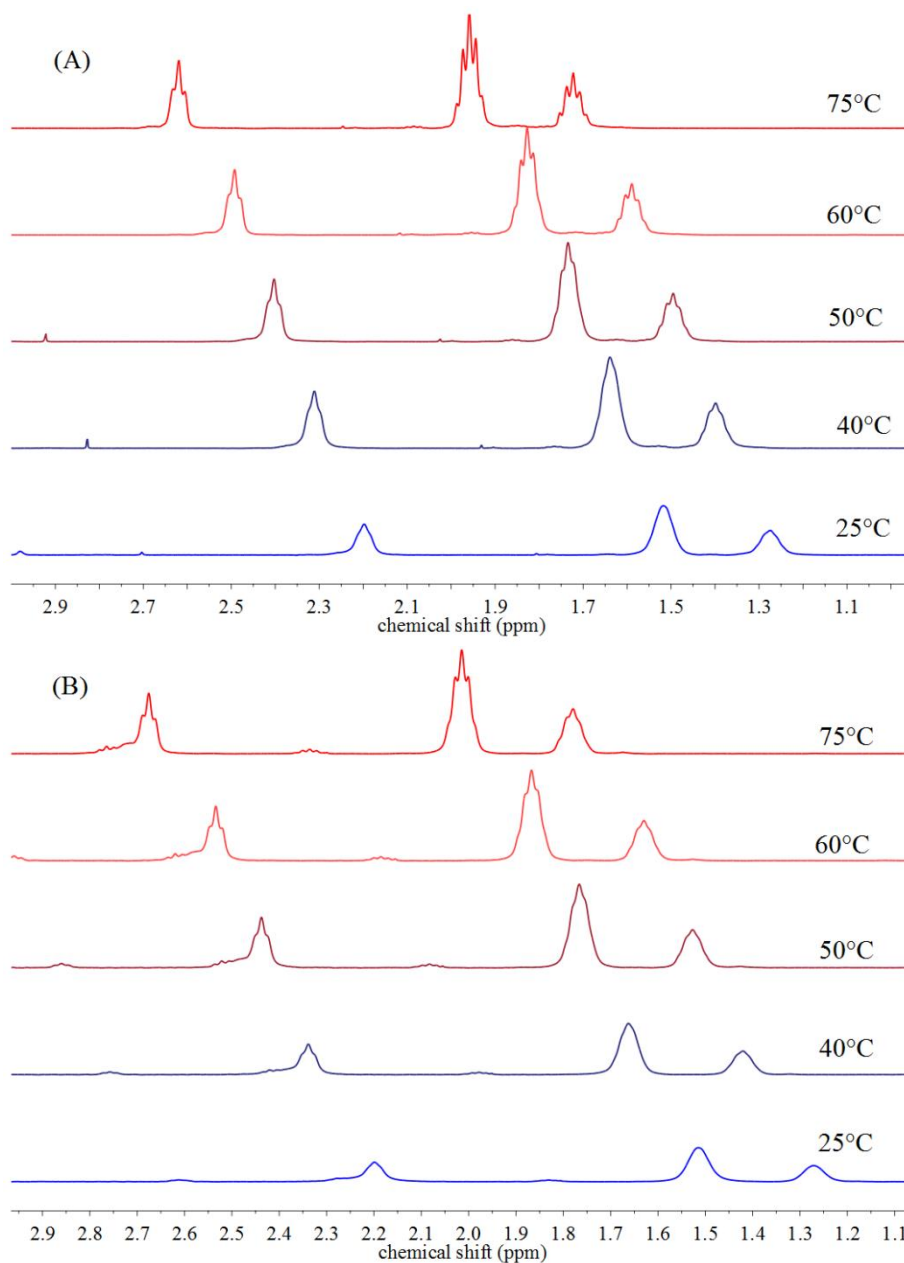
Figure 4.10 Expanded ^{1}H NMR spectra of (A) PCL$_{16}$-*b*-PEO$_{44}$, and (B) PGA$_{17}$-*g*-(PCL$_{15}$-*b*-PEO$_{44}$) obtained in D$_2$O at different temperatures.

Interestingly, the increased resolution by raising the temperature is higher for the PCL$_{16}$-b-PEO$_{44}$ compared to PGA$_{17}$-*g*-(PCL$_{15}$-*b*-PEO$_{44}$). This strongly suggests that micelles formed by amphiphilic graft copolymers have a higher stability against temperature increase of aqueous solutions compared to linear block copolymers of similar chemical composition of the grafted side chains. Obviously, the polymer backbone of the graft copolymers plays a key role in stabilizing the micelles.

4.3.4   Surface tension measurements

Figure 4.11 depicts the surface tension γ of aqueous solutions of PGA_{17}-*g*-$(PCL_{15}$-*b*-$PEO_{44})$ and PGA_{17}-*g*-$(PCL_{24}$-*b*-$PEO_{44})$ as a function of polymer concentration at 25°. This gives the critical micelle concentration (cmc) indicated by the intersection of the extrapolation of the two linear regimes where the curves show a sharp change in slope. The obtained values are 0.4 µg/mL for PGA_{17}-*g*-$(PCL_{15}$-*b*-$PEO_{44})$ and 1 µg/mL for PGA_{17}-*g*-$(PCL_{24}$-*b*-$PEO_{44})$. Both values are much smaller than the cmc values of PCL_{19}-b-PEO_{44}, $PHEMA_{200}$-*g*-$(PCL_{22}$-*b*-$PEO_{45})$, and $PHEMA_{70}$-*g*-$(PCL_{20}$-*b*-$PEO_{45})$ where (PHEMA is poly(2-hydroxyethyl methacrylate).[181]
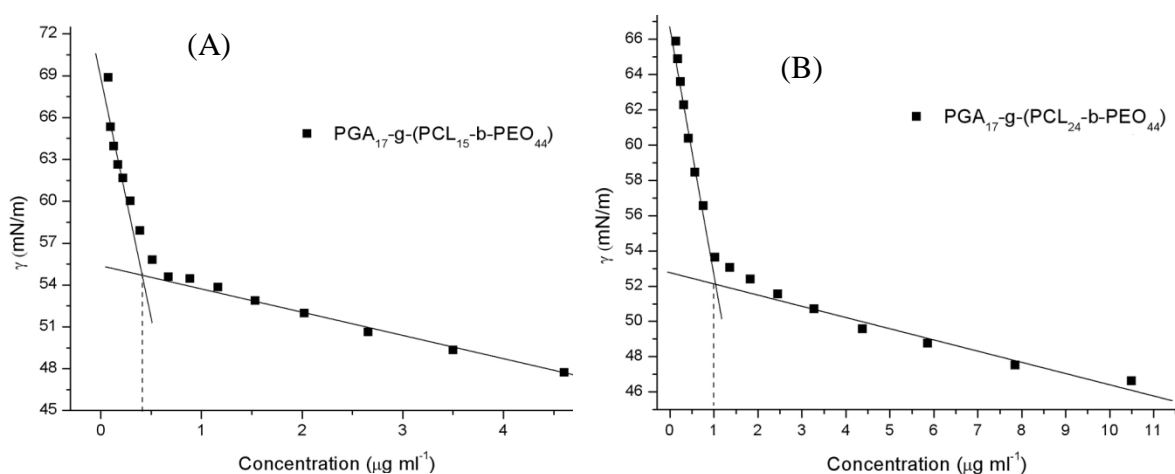
Figure 4.11 Surface tension of (A) PGA_{17}-*g*-$(PCL_{15}$-*b*-$PEO_{44})$ and (B) PGA_{17}-*g*-$(PCL_{24}$-*b*-$PEO_{44})$ as a function of polymer concentration at room temperature.

The cmc can be considered as indicator for micelle stability which is an important factor when polymers are used in the field of drug delivery. According to literature,[181] two factors are proposed for the higher stability of graft copolymer micelles compared to micelles of linear block copolymers of the same chemical structure as the grafted side chains. Firstly, the hydrophobic interactions can be strengthened in the case of graft copolymers according to the intermolecular interactions of PCL side chains. Secondly, PCL blocks from different graft polymer chains are able to entangle with each other.

4.3.5   Scanning electron microscopy (SEM)

Casted and dried spherical micelles formed by PGA_{17}-*g*-$(PCL_{15}$-*b*-$PEO_{44})$ in water prepared by dialysis are shown in the SEM image of Figure 4.12. The image reveals well-dispersed spherical micelles. They are relatively uniform in size with an average radius of 10 nm in

agreement with DLS data. Additionally, some aggregates of micelles are observed and some larger aggregates are also depicted in the inset of Figure 4.12 in agreement with DLS data.
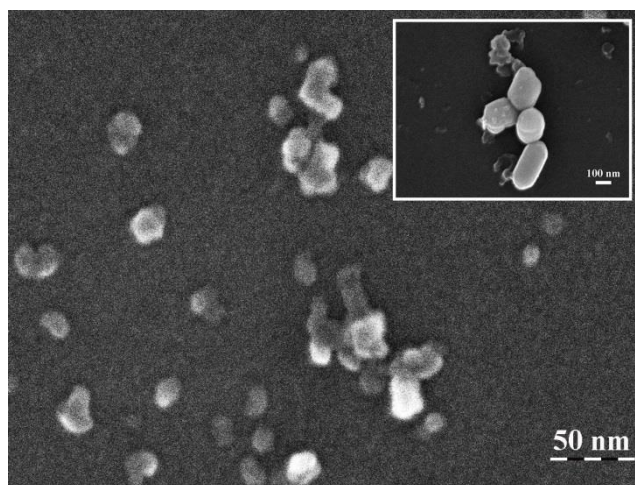
Figure 4.12 SEM image of PGA_{17}-g-(PCL_{15}-b-PEO_{44}) micelles. The inset shows the presence of some aggregates larger than micelles.

4.3.6   Preparation and characterization of worm-like aggregates

Figure 4.13 shows fluorescence microscopy images of PGA_{17}-g-(PCL_{24}-b-PEO_{44}) worm-like aggregates prepared by the cosolvent/evaporation method.[199]
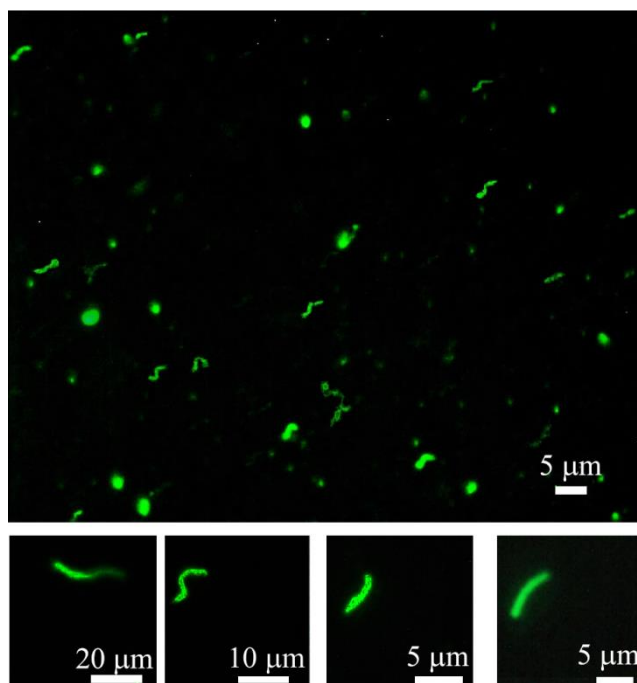
Figure 4.13 PGA_{17}-g-(PCL_{24}-b-PEO_{44}) worm-like aggregates formed in water visualized by fluorescence microscopy.

The hydrophobic fluorescence dye PKH26GL is loaded into the worm-like aggregates by direct addition to the polymer solution. The fluorescence image shows the existence of worm-like and apparently spherical aggregates. Most of the worm-like aggregates have a contour length in the range of 2-10 μm. A vertical view of the worm-like aggregates sample is taken by confocal laser scanning microscopy Figure 4.14. This reveals that some of the apparently spherical aggregates are in fact also worm-like aggregates but oriented perpendicular to the glass slide. The spherical aggregates could be attributed also to the worm aggregates that have contour length smaller than the resolution of fluorescence microscope and thus they apear as dots.
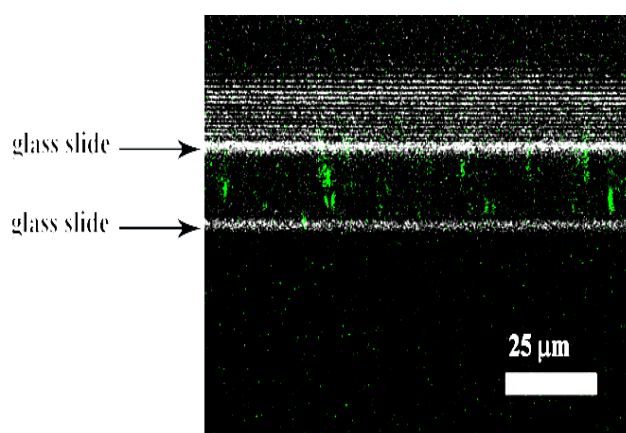
Figure 4.14 A vertical view of PGA$_{17}$-g-(PCL$_{24}$-b-PEO$_{44}$) worm-like aggregates sample taken by confocal fluorescence microscopy.

Typically, aqueous solutions of PEO containing linear block copolymers exhibit worm-like micelle self-assembly when the weight fraction of PEO is in range of 0.42 to 0.55.[192,217,218] The aqueous solution of PCL$_{24}$-b-PEO$_{44}$ is reported previously to form worm-like micelles.[198] This block copolymer has the same chemical composition as the grafted side chain of PGA$_{17}$-g-(PCL$_{24}$-b-PEO$_{44}$). However, the weight fraction of PEO in the graft polymer is only 38wt%. This suggests that this polymer will form polymersomes rather than worm-like micelle. Thus, further investigation using TEM and SEM is necessary in order to achieve a detailed understanding of the morphology of these worm-like aggregates.

Figures 4.15 (A) and (B) obtained by negative staining TEM show two examples of extended worm-like aggregates. They are formed by aggregated polymersomes with an average diameter of 25 nm. The dark circular structures are caused by an enrichment of the staining agent in PGA rich regions of the polymersomes since PGA is an amorphous polymer and has a lower packing density compared to PEO and PCL which are additionally able to crystalline.

Both TEM images show aggregates of polymersomes joined together in an elongated fashion caused by strong shear force during the formation. This is further illustrated in Figure 4.15 (C) The aggregates seem to have different length and different radii. Also Liu et al.[219] reported recently the occurrence of polymersomes by ternary graft copolymers and their aggregation.
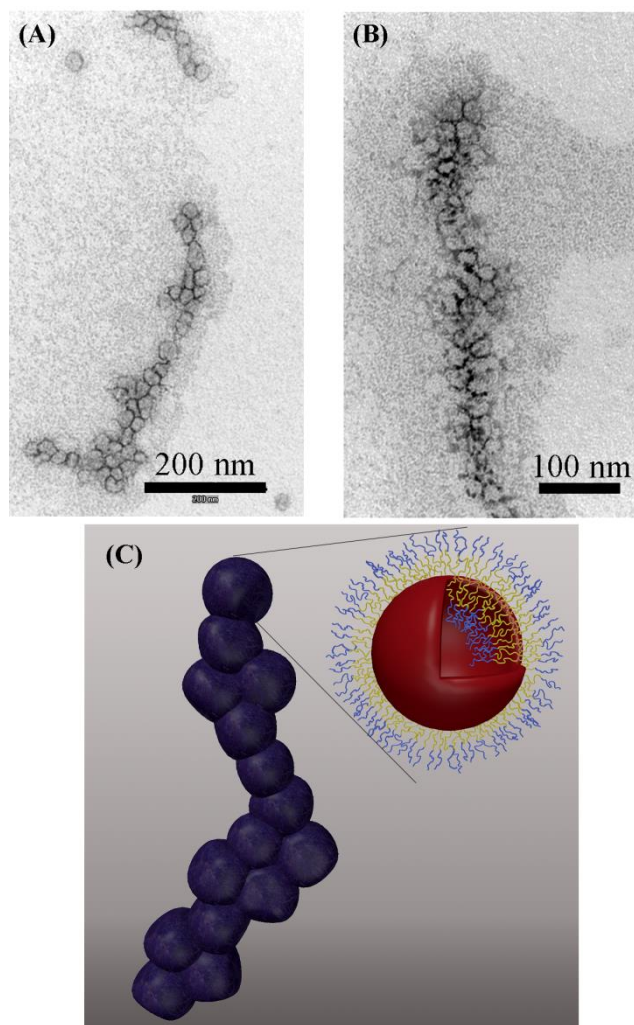
Figure 4.15 (A) and (B) Typical TEM images of worm-like aggregates of PGA_{17}-*g*- (PCL_{24}-*b*-PEO_{44}) prepared by the cosolvent/evaporation method. (C) Schematic drawing of a polymersome and the formation of worm-like aggregates.

Furthermore, tracking of Brownian motion of single worm-like aggregates with time using CLSM is shown in Figure 4.16. Actually, the snapshots reveal a rigid behavior of the worm-like aggregates. Thus, the worms are rigid over their entire contour. Complete or partial rigidity of worm-like micelles of PEO-*b*-PCL has been explained previously as a result of PCL crystallization within the micelle core.[192] In our case, the rigidity is obviously caused by the entanglement of PGA backbone chains as discussed below.
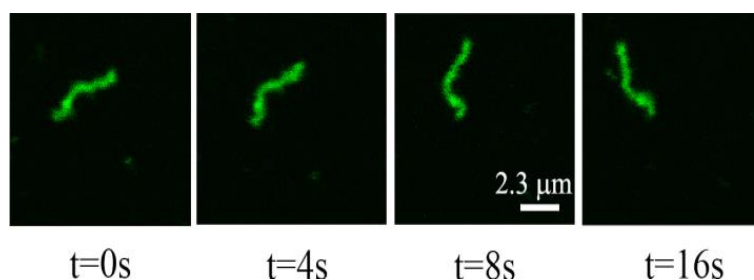
Figure 4.16 Snapshots represent the Brownian motion of a single worm-like aggregate of PGA$_{17}$-g-(PCL$_{24}$-b-PEO$_{44}$) in water with time using CLSM.

The overall procces to form these worm-like aggregates can be explained as follows. A concentrated solution of the polymer in chloroform is added to water with a volume ratio of 1000 : 6 to form two immiscible layers. Both layers are stirred using a disperser at a high revolution speed. During stirring the chloroform will begin to evaporate and the polymer chains will thus diffuse out of the chloroform phase into the water phase where they self-assemble as polymersomes. Actually, the temperature of the solution during the stirring increases to 40-50°C even in the presence of an ice bath. The resulting polymersomes collide with each other under vigorous stirring. In general, when two polymersomes which are usually formed by block copolymers collide with each other they should fuse to form one polymersome with larger radius. In the case of graft copolymers, the polymer backbone may prevent the fusion process. These considerations are summarized in Figure 4.17.

The worm-like aggregates show a long time stability. Contrary to the worm-like micelles formed by PCL-b-PEO which show a significant degradation,[199] no significant changes are noticed for the case of worm-like aggregatess formed by the graft copolymer even after weeks when the solution is kept at 4°C. This stability can be attributed to the reduced hydrolysis of PCL chains as a result of the absence of hydroxyl end group on both ends of the PCL block in our graft copolymers. Additionally, the process of worm prepreation is considered as an easy, clean and rapid process since the worms are formed spontaneously during the mixing without the need of any surfactant. Contrary to the method suggested by He et al.[220] to prepare cylindrical micelles from PCL-b-PEO, the final product in our process contains only water as a solvent an thus is also applicable in *vivo*. These worm-like aggregates have the additional advantage, that they can be emoployed for delivering both hydrophobic and hydrophilic drugs at the same time. Thus, the resulting worms can be considered as multi-drug carriers. Furthermore, Discher et al.[198] reported that filament particles have a significant longer circulation time comparing to their spherical counterparts. Thus, further *in vitro* and *in vivo*

invistigations are necessary to achieve an understanding of these new polymers for biomedical and pharmaceutical applications.
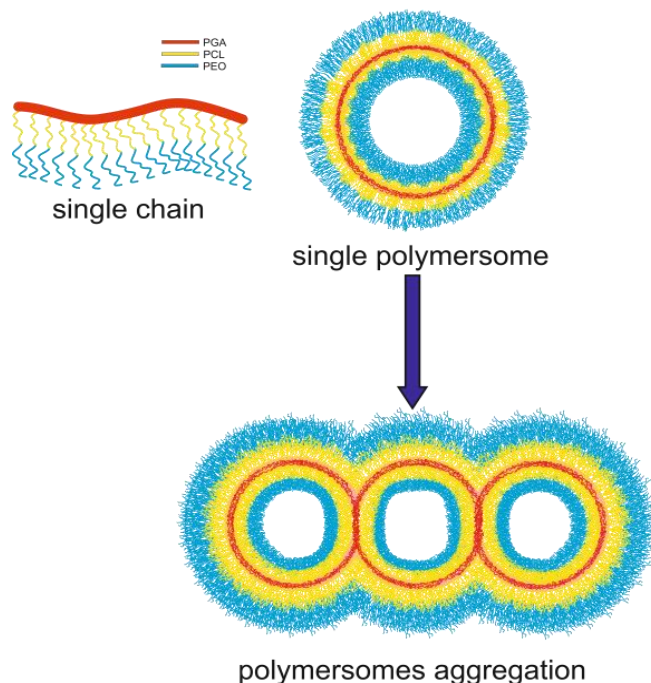
Figure 4.17 The structure of polymersomes formed by self-assembly of PGA_{17}-g-(PCL_{24}-b-PEO_{44}) in water and the worm-like aggregates formed by vigurous stirring during the polymersome formation.

4.4 Conclusions

Water soluble biodegradable and biocompatible graft copolymers are prepared using poly(glycerol adipate) (PGA) as a backbone. This backbone is synthesized by enzymatic polymerization using divinyl adipate and glycerol to yield aliphatic linear polyester with free pendent hydroxyl groups. PGA-*g*-(PCL-*b*-PEO) is prepared by combination of "grafting from" and "grafting onto" methods. The later polymer has a high hydrophobic ratio which increases drug loading capabilities. PGA-*g*-(PCL-*b*-PEO) is not water soluble but it forms micelles by dialyzing its acetone solution against water. Spherical micelles are formed with a hydrodynamic radius close to that formed by PCL-b-PEO with identical composition as the graft block copolymer chains. On the other hand, micelles of PGA-*g*-(PCL-*b*-PEO) show a higher stability at elevated temperatures compared to PCL-*b*-PEO of the same chemical composition. Interestingly, PGA_{17}-g-(PCL_{24}-*b*-PEO_{44}) can form polymersomes of an average diameter of 25 nm. These polymersomes form worm-like aggregates caused by collision as a result of shear forces during the preparation. The worm-like aggregates are visualized using

fluorescence and electron microscopy. They are shape persistent during the Brownian motion and have potential applications as effective multi-drug carriers.

Chapter 5

The Behavior of Poly(ε-caprolactone) and Poly(ethylene oxide)-b-Poly(ε-caprolactone) Grafted to a Poly(glycerol adipate) Backbone at the Air/Water Interface

5.1   Introduction

Materials with a thickness in the nanometer range are the basis for several enabling technogies.[221] The Langmuir trough is a suitable tool to form well-organized molecular monolayers with nanometer thickness at the air/water (A/W) interface. The Langmuir technique can also be used to study the crystallization of liquid crystals,[222–226] as well as semi-crystalline polymers at the A/W interface.[227,228] In general, the crystallization kinetics of semi-crystalline polymers confined in thin films differs significantly when compared to bulk samples. This is mainly attributed to interfacial interactions between thin films and substrates which affects directly the diffusion of polymer chains toward the growth front of growing lamellae and subsequently growth rate, melting temperature, and crystal morphology.[229–241] Furthermore, using a Langmuir through coupled with light microscopy (Brewster angle and epifluorescence microscopy) or gracing incidence X-ray measurements (GI-WAXS and GI-SAXS) allow to study details of chain packing and crystal morphology as a function of trough temperature, surface concentration (surface pressure) and compression rate.[242] Additionally, using ultrapure water minimizes the nucleation density for crystallization, as no surface defects exist.[243] The Langmuir trough can also be equipped with infrared reflection absorption spectroscopy (IRRAS) to follow polymer chain orientation on a molecular level.[244] Poly(ε-caprolactone) (PCL) is a biodegradable semi-crystalline polyester with many biomedical applications.[188] The bulk crystallization of PCL has been investigated extensively since crystallinity plays an important role for its mechanical properties and biodegradability.[239,245–250] The crystallization of PCL has also been studied in thin films and in monolayers at the A/W interface.[23,32,-33,253] In order to provide an anchor to the aqueous subphase for the relatively hydrophobic PCL during compression at the A/W interface, it is reasonable to attach a hydrophilic poly(ethylene oxide) block.[254,255] Some research has been published recently on the behavior of graft copolymers at the A/W interface, which contain side chains of only one block.[62,155,256] Here, we study the differences of the compression isotherms and the morphology development at the A/W interface between PCL and PCL-*b*-PEO compared to graft copolymers where PCL and PCL-*b*-PEO chains are attached to the backbone of

poly(glycerol adipate) (PGA). These graft copolymers of poly(glycerol adipate)-*g*-poly(ε-caprolactone) PGA-*g*-PCL and poly(glycerol adipate)-*g*-(poly(ε-caprolactone)-*b*-poly(ethylene oxide)) PGA-*g*-(PCL-*b*-PEO) have one grafted chain per PGA monomer unit. The behavior of the graft copolymers has been studied at the A/W interface by Langmuir trough measurements coupled with BAM. The morphology of respective Langmuir-Blodgett films is investigated by atomic force microscopy (AFM).

5.2   Experimental section

5.2.1   Materials

The polymers used in this report were synthesized according to the procedure described by Naolou et al.[257] The chemical structures of the utilized graft copolymers are shown in Figure 5.1. Table 5.1 summarizes the molar masses of the linear and graft polymers used.
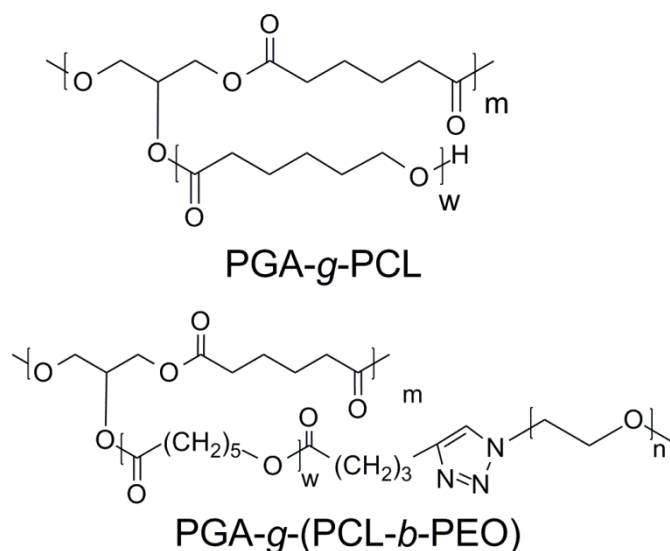
Figure 5.1 Chemical structures of PGA-*g*-PCL and PGA-*g*-(PCL-*b*-PEO).

5.2.2   Surface Pressure Measurements

The surface pressure π as a function of mean molecular area (*mmA*) was measured using a Langmuir trough (KSV, Helsinki, Finland). It was equipped with a Teflon trough and a micro roughened platinum Wilhelmy plate. The temperature of the water subphase was adjusted by circulating thermostated water. All experiments were carried out at 20 °C unless otherwise stated. All samples were dissolved in chloroform prior to the placement on the water surface. The experiments were carried out after 20 min of the placement of the polymer solution in order to let the chloroform evaporate and the polymer chains equilibrate. The polymer solutions were spread at different initial pressures, and different parts of the isotherm

were recorded in order to obtain the complete isotherms. The parts were then combined into one plot. They overlapped within the experimental error. The compression and expansion rates for all experiments were 750 mm^2 min^{-1}. The static elasticity (ε_s) was calculated according to Esker et al.[243] by:

$$\varepsilon_s = -A \left(\frac{\partial \pi}{\partial A} \right)_T$$

Table 5.1 Molar Masses and polydispersities (M_w/M_n) of the polymers

Sample name	$M_{n,PCL}$[a]	$M_{n,total}$[b]	M_w/M_n[c]
	(g/mol)	(g/mol)	
PCL$_{16}$[d]	1,800	1,700	1.2
PCL$_{25}$	2,800	2,800	1.3
PGA$_{17}$-g-PCL$_{15}$	1,700[c]	32,000	1.3
PGA$_{17}$-g-PCL$_{24}$	2,700[c]	48,800	1.5
PCL$_{16}$-b-PEO$_{44}$	1,800	3,800	1.4
PCL$_{25}$-b-PEO$_{44}$	2,800	4,900	1.2
PGA$_{17}$-g-(PCL$_{15}$-b-PEO$_{44}$)	1,700	65,700	1.6
PGA$_{17}$-g-(PCL$_{24}$-b-PEO$_{44}$)	2,700	79,100	1.2

[a]   The molar masses of PCL were calculated by ^{1}H NMR spectroscopy.

[b]   The total molar mass was calculated using the integrals of the different peaks in ^{1}H NMR spectroscopy of each polymer whereas the molar mass of the backbone (PGA) was obtained by SEC using THF as eluent.

[c]   Polydispersities were determined by SEC using THF at room temperature and polystyrene standards.

[d]   The subscripts represent the degrees of polymerization.

5.2.3   Brewster Angle Microscopy (BAM)

Direct observation of the film formed by different polymers at A/W interface was carried out using a MiniBAM instrument delivering images from a surface of around 7×5 mm with a lateral resolution of approximately 20 µm (Nanofilm Technologie GmbH, Germany).

5.2.4   Deposition of Langmuir–Blodgett (LB) Films

The deposition of PGA-*g*-PCL films formed at the A/W interface was carried out on hydrophobically modified silicon wafer whereas the deposition of PGA-*g*-(PCL-*b*-PEO) was achieved on hydrophilic silicon wafer. The wafer surfaces were modified and cleaned in both cases according to the procedure described by Peetla et al.[258] After treatment, silicon wafers were then cut into small pieces of 1×1.5 cm and immersed into the water subphase of the Langmuir trough. Polymer solutions were then spread onto the water surface. After 20 min of equilibration, the surface was compressed using a compression rate of 750 mm^2 min^{-1} until the desired transfer surface pressure was achieved. After another waiting period of 20 min, the films were then transferred at constant surface pressure onto the silicon substrate by vertical uptake through the films using a constant rate of 1 mm/min. Finally, the LB film was allowed to dry in a desiccator at room temperature for 24 h.

5.3   Results and discussion

5.3.1   The behavior of linear and grafted PCL at the A/W interface

The PGA backbone as shown in Figure 5.1 can be considered as a hydrophilic polymer due to the pendant OH-group in every repeat unit. Nevertheless, it is not water soluble but it swells to a large degree in water. The OH-groups can be employed for ring opening polymerization of ε-caprolactone which results in PGA-*g*-PCL. Of course, after the conversion of the OH-groups the polymer backbone becomes hydrophobic. Furthermore, using 'click' chemistry it is possible to prepare graft block copolymers of the type PGA-*g*-(PCL-*b*-PEO).[257] Figure 5.2 shows the compression isotherms for two PCL homopolymer samples with 16 and 25 monomer units, respectively. The inset shows the corresponding static elasticity values, for which the mmA value was divided by the degree of polymerization to obtain the area per monomer unit.
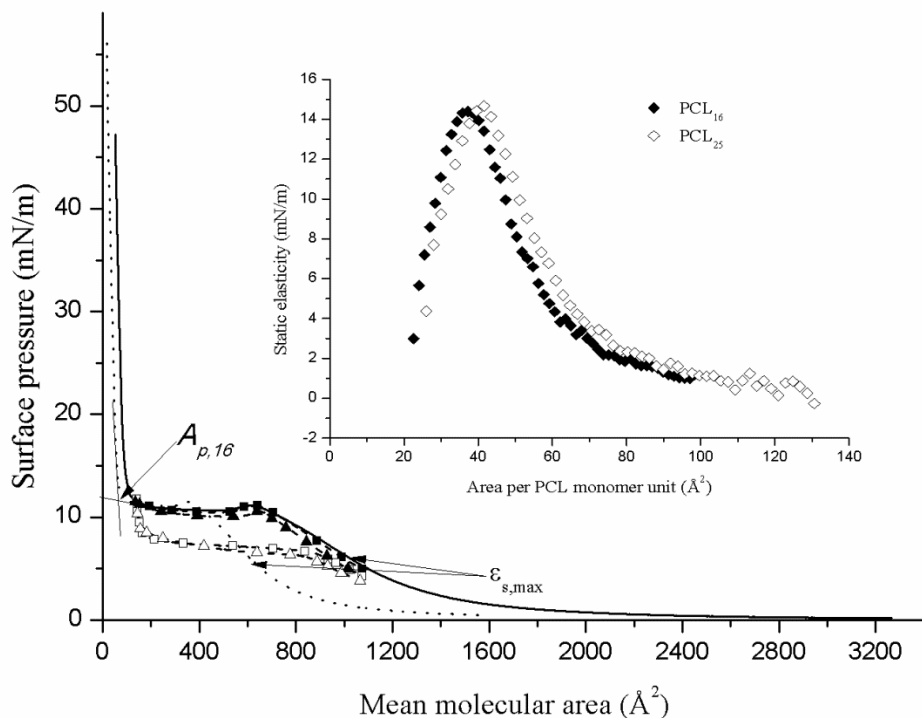
Figure 5.2 π-mmA isotherm of PCL$_{16}$ (dotted line) and PCL$_{25}$ (full line) measured at 20 °C. The dashed lines represent the compression-expansion hysteresis cycles of PCL$_{25}$ where (■) is first compression, (□) first expansion, (▲) second compression and (Δ) second expansion. The inset shows the static elasticity as a function of the area per monomer unit defined as mean molecular area divided by the degree of polymerization.

Each isotherm shows first a gentle increase of the surface pressure over an extended mmA range upon compression. Upon further compression the slope of isotherms becomes steeper caused by increased interactions between PCL chains. The inflection point of the first increase in the isotherms defines also the values for the highest static elasticity ε$_{s,max}$ at approximately 37 Å^2/ monomer unit for both PCL samples as shown in the inset of Figure 5.2. According to the parameters of the orthorhombic unit cell of PCL (a= 0.748 ± 0.002 nm, b= 0.498 ± 0.002 nm, c= 1.726 ± 0.003 nm) which contains two polymer chains each having two monomer units,[259,260] the surface area occupied by one monomer unit lying flat on the water surface is approximately $A_m = \frac{c}{2} \times \left(\frac{\frac{a}{2}+b}{2}\right) \approx 38$ Å^2 which is nearly the area at which maximum elasticity ε$_{s,max}$ occurs. The steep decrease of ε$_s$ at surface areas per monomer unit smaller than 37 Å^2 is interpreted as desorption of ester groups from the water surface.[243] Upon further compression of the polymer monolayer in both isotherms an inflection point occurs

76

and the slope becomes smaller. However, a slight decrease of surface pressures with compression occurs prior to the plateau region which is related to the fact that 3D crystals grow faster than the 2D polymer film is compressed.[261] A similar behavior has been observed previously in the case of liquid crystals,[222] amphiphilic amino acids,[262] and long fatty acids such as palmitic (C_{16}), stearic (C_{18}) and arachidic acid (C_{20}).[150,263–266] The reversibility of the PCL_{25} isotherm is studied by measuring compression-expansion cycles. The corresponding curves are shown in Figure 5.2. Complete reversibility over the total isotherm cannot be studied since the trough area is limited. At the beginning of expansion a sudden drop of surface pressure from ~12 mN/m to $\pi \sim$ 8 mN/m occurs. It is followed by a plateau region upon further expansion as a results of 'crystal melting', i.e. PCL monomer units leave the crystal and reabsorb to the A/W interface.[243] The surface pressure decreases again slightly before the first compression curve is reached again, and also the second compression isotherm shows a small shift towards smaller *mmA* values, which indicates that the melting process of PCL crystals is not completely reversible and some of the polymer chains are still packed within the crystal structure.[252] The intersections of the tangents of the plateau and the steep increase of the surface pressure at lower mmA values for the PCL_{16} and PCL_{25} isotherms are at $A_{p,16} = 60$ Å^2 and $A_{p,25} = 90$ Å^2, respectively. Dividing each of these numbers by the corresponding number of monomer units per chain gives an area of ~ 3.7 Å^2/monomer unit for both polymers. This means that for both polymers the end of the plateau occurs at the same surface area per monomer unit. This indicates that both polymer layers have the same average thickness on the water surface at this point. Due to the semicrystalline structure it can be expected that crystalline and amorphous regions will exist simultaneously on the water surface. For further calculations, the cross-sectional area of a PCL segment is estimated from the corresponding crystal dimension and is approximately $\frac{a \times b}{2} = 18.6$ Å^2. This indicates that in average, including crystalline and amorphous regions, 18.6/3.7=5 monomer units are stacked on top of each other. This height is the same for both PCL homopolymers, PCL_{16} and PCL_{25}.
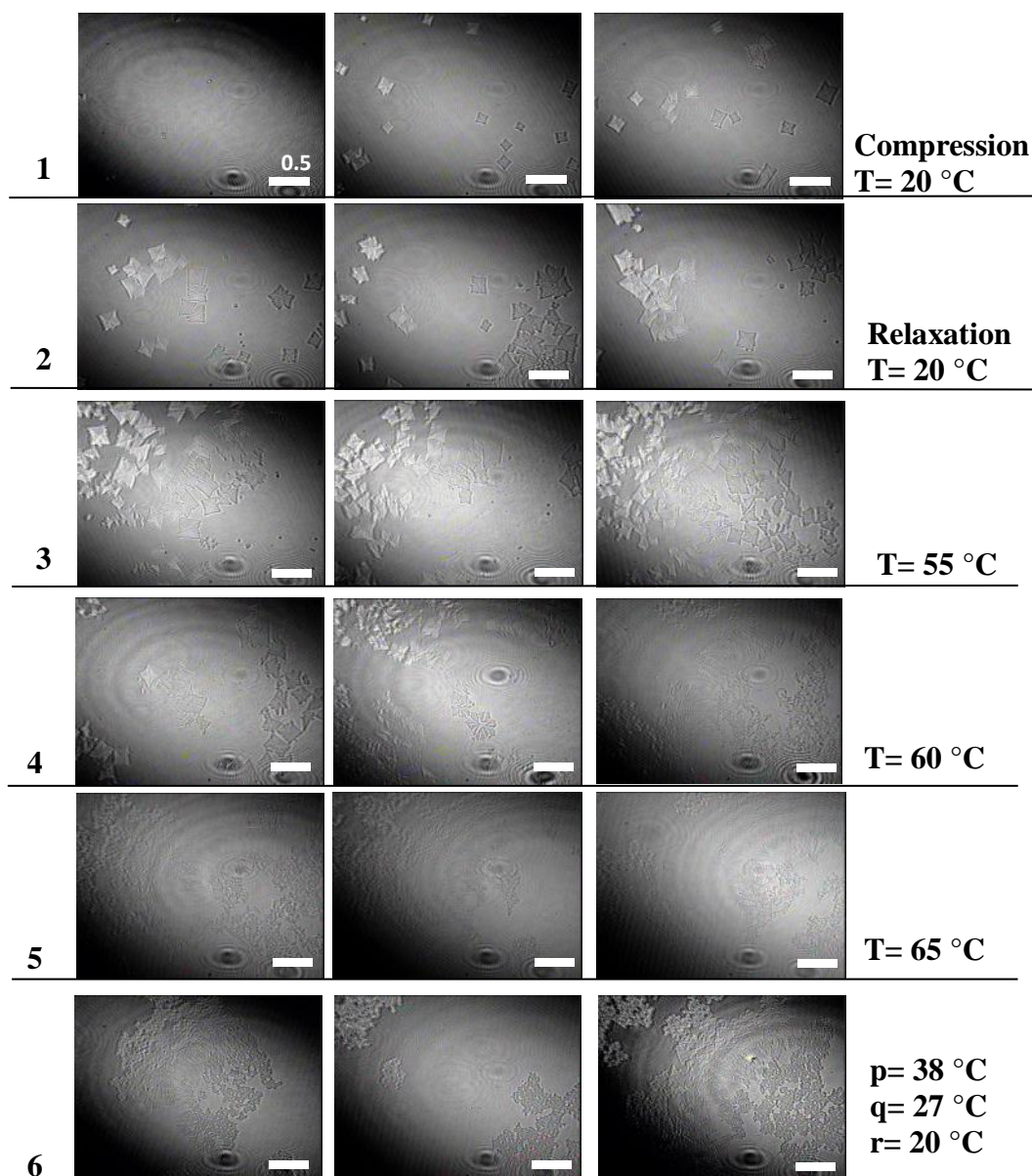
Figure 5.3 BAM images of PCL$_{25}$ crystals obtained: 1) during compression at 20°C at *mmA* of (a) 544 Å^2 (b) 303 Å^2 and (c) 227 Å^2. 2) Relaxation at 20°C with constant area of 214 Å^2, 3)-5) Relaxation at increased temperatures (55°C, 60°C, 65°C) and 6) during cooling back to 20 °C, all at constant area of 214 Å^2. Further details are given the text.

BAM images of PCL$_{25}$ taken during compression at 20 °C show the appearance of crystals (Figure 5.3 a-c). The compression stopped at *mmA* = 214 Å^2 and the monolayer is kept for another ~ 25 min at constant mmA. The crystals size becomes larger during this time

as shown in (Figure 5.3 c-e). The subphase temperature is then raised within 30 min to 55 °C which is close to the melting temperature of PCL_{25} in bulk ($T_{m,PCL25}$=52.2 °C).[267] No significant changes of the morphology of PCL crystals can be observed (Figure 5.3 g, and h). Only slight defects at the crystals edges can be seen in Figure 5.3 i. Then, the subphase temperature is raised further to 60 °C for another 30 min. Figure 5.3 k reveals the beginning of the melting process indicated by the disintegration of the crystals into small pieces. Surprisingly, even after the apparent disappearance of the crystals two phases are observed in the BAM images taken after 25 min of raising the subphase temperature to 60 °C Figure 5.3 l. This might indicate the formation of a mesophase above the melting temperature of PCL. This behavior is obviously different to the disappearance of crystals upon expansion where the chains (ester groups) obviously reabsorb at the A/W interface. When the temperature is raised to T=65 °C for 30 min, no significant changes were observed and the mesophase remained (Figure 5.3 m-o). Higher temperatures cannot be employed since the movement on the water surface becomes very fast and it is impossible to acquire BAM images. A further gradual decrease of the subphase temperature to 20 °C produces crystals with a different morphology (Figure 5.3 p-r) compared with the crystals formed during the first compression.

Figure 5.4 presents the compression isotherms of PGA_{17}-*g*-PCL_{14} and PGA_{17}-*g*-PCL_{24}. The area per PCL monomer unit was calculated according to the equation

$$A = mmA \, / \, \frac{(M_{n,total} - M_{n,PGA})}{M_{n,caprolactone}}$$

Actually, both isotherms are similar to the isotherms of linear PCL which is also valid for the static elasticity diagrams. The maximum of the static elasticity of $\varepsilon_{s,max}$ is at *mmA* of ~ 37 Å^2 and, therefore, similar to the value of linear PCL chains. However, the isotherms of both graft copolymers do not show the slight drop in surface pressure of the isotherms prior to reaching the plateau region. As it was mentioned above, such a drop in the isotherms indicates that the transfer of polymer chains from the monolayer to a crystal lamella is faster than the compression of the monolayer. Thus, the isotherms of the graft copolymers prove that the crystallization rates in graft copolymers are slower compared to linear PCL. This seems to be reasonable since the amorphous polymer backbone of the graft copolymers effectively hinders the organization of the PCL graft chains into lamellae.
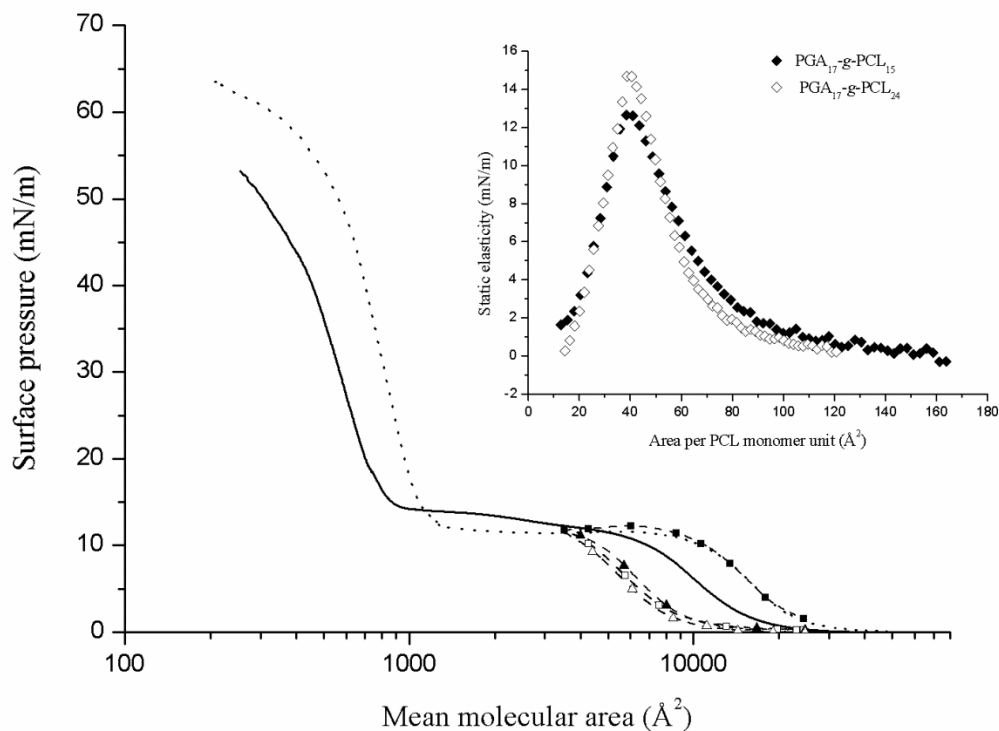
Figure 5.4 π-*mmA* isotherm of PGA_{17}-*g*-PCL_{15} (full line) and PGA_{17}-*g*-PCL_{24} (dotted line) measured at 20°C. The dashed lines represent the compression-expansion hysteresis cycles of PGA_{17}-*g*-PCL_{24} where (■) is first compression, (□) first expansion, (▲) second compression and (Δ) second expansion. The inset shows the static elasticity as a function of area per PCL monomer unit.

BAM images of the PGA_{17}-*g*-PCL_{24} monolayer during compression indicate also another difference compared to the crystal morphology of linear PCL (Figure 5.5 a-c). The images show that PGA_{17}-*g*-PCL_{24} chains form crystals with smaller size compared to linear PCL_{25}. Actually, similar differences between crystal sizes of linear and graft polymers in bulk have been reported before and are interpreted as a result of increasing nucleation density of graft polymers due to the decrease of PCL chain mobility caused by grafting.[40,268] The increase of the nucleation rate in the case of graft copolymers could also be attributed to the fact that the grafted chains are forced to be parallel to each other on the water surface which increases the probability of the formation of stable crystal nuclei.
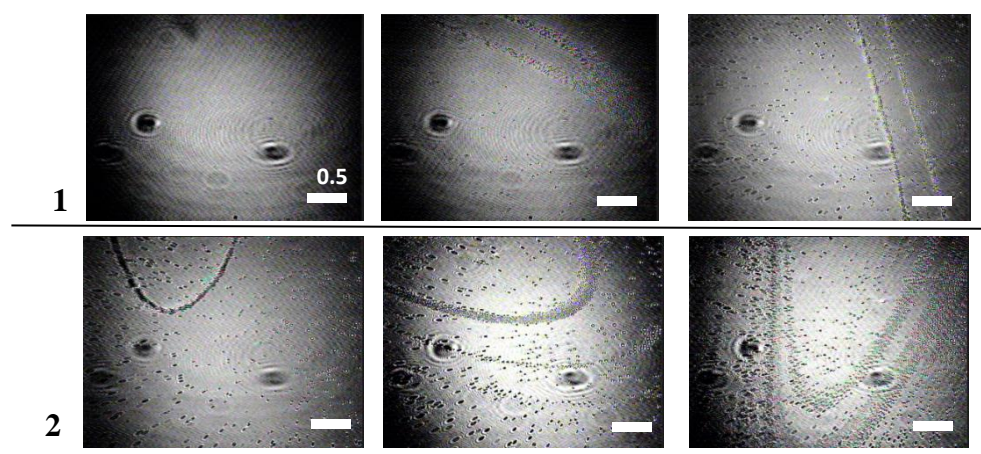
Figure 5.5 BAM images for PGA$_{17}$-*g*-PCL$_{24}$ obtained during the hysteresis experiment performed at 20°C. The images were obtained at surface areas of: 1- Compression: (a) 7140 Å^2, (b) 6590 Å^2, (c) 5500 Å^2. 2- Expansion: (d) 6580 Å^2, (e) 9700 Å^2, (f) 16600 Å^2.

Another interesting difference between linear and grafted PCL is revealed in the hysteresis isotherms of PGA$_{17}$-*g*-PCL$_{24}$ which are also shown in Figure 5.4. A drop of the surface pressure from ~11 mN/m to ~1 mN/m is seen in the hysteresis isotherm of PGA$_{17}$-*g*-PCL$_{24}$ upon expansion followed by a gradual decrease to 0 mN/m. Actually, the absence of a plateau region (significantly above π=0 mN/m) in the expansion isotherm, indicates that the structure formed by graft copolymers is more stable than those formed by PCL resulting in a slower re-adsorption of PCL chains at the A/W interface. Furthermore, the second compression does not follow the first compression isotherm, but the first expansion isotherm. This supports the above mentioned assumption that the 3D structures formed by the graft copolymer do not melt during the expansion process. The second expansion isotherm is similar to the first expansion. A waiting period of about 1 h between the first expansion and second compression is also performed. However, no change of the corresponding isotherm is noticed. The stability of crystals during expansion is also confirmed by BAM images in (Figure 5.5 d-f).

5.3.2   The behavior of linear and grafted PCL-*b*-PEO at the A/W interface

Figure 5.6 shows the π-*mmA* isotherms of PCL_{16}-*b*-PEO_{44} and PCL_{25}-*b*-PEO_{44}, PGA_{17}-*g*-(PCL_{15}-*b*-PEO_{44}), and PGA_{17}-*g*-(PCL_{24}-*b*-PEO_{44}) measured at 20 °C. All isotherms show distinct features at a surface pressure of ~ 10 mN/m. Typically, amphiphilic block copolymers having PEO as water soluble block show a phase transition from pancake to brush conformation at surface pressures between 9 and 13 mN/m depending on PEO block length.[62,255,258,269,270] At this surface pressure the PEO chains leave the water surface and submerge into the water subphase. In the same surface pressure range the crystallization of PCL blocks occurs at the A/W interface.[254,255] This is further confirmed by the BAM image of PCL_{25}-*b*-PEO_{44} shown in the inset of Figure 5.6 A. The image reveals the presence of filament crystals at the A/W interface. Actually, this result is consistent with the crystal morphology reported previously for LB films formed by PCL-*b*-PEO.[255]

At higher surface pressures all four isotherms indicate a collapse of the monolayer. Only the linear block copolymer with the smallest PCL block (PCL_{16}-*b*-PEO_{44}) shows a nearly perfect multilayer formation, i.e. the sliding of the polymer blocks on top of each other without any resistance (i.e. at nearly constant surface pressure).[261] The other polymers show a substantial increase of surface pressure upon compression in the roll-over region which is most significant for PCL_{25}-*b*-PEO_{44}.[40] The isotherms of PCL_{16}-*b*-PEO_{44}, PGA_{17}-*g*-(PCL_{15}-*b*-PEO_{44}), and PGA_{17}-*g*-(PCL_{24}-*b*-PEO_{44}) show the plateau region at a surface pressure of ~ 30 mN/m. Such type of extended plateau at the end of isotherms has been assigned to the collapse region which occurred either by "giant folds" or "multiple folds" or according to the multilayer mechanism.[149–151]
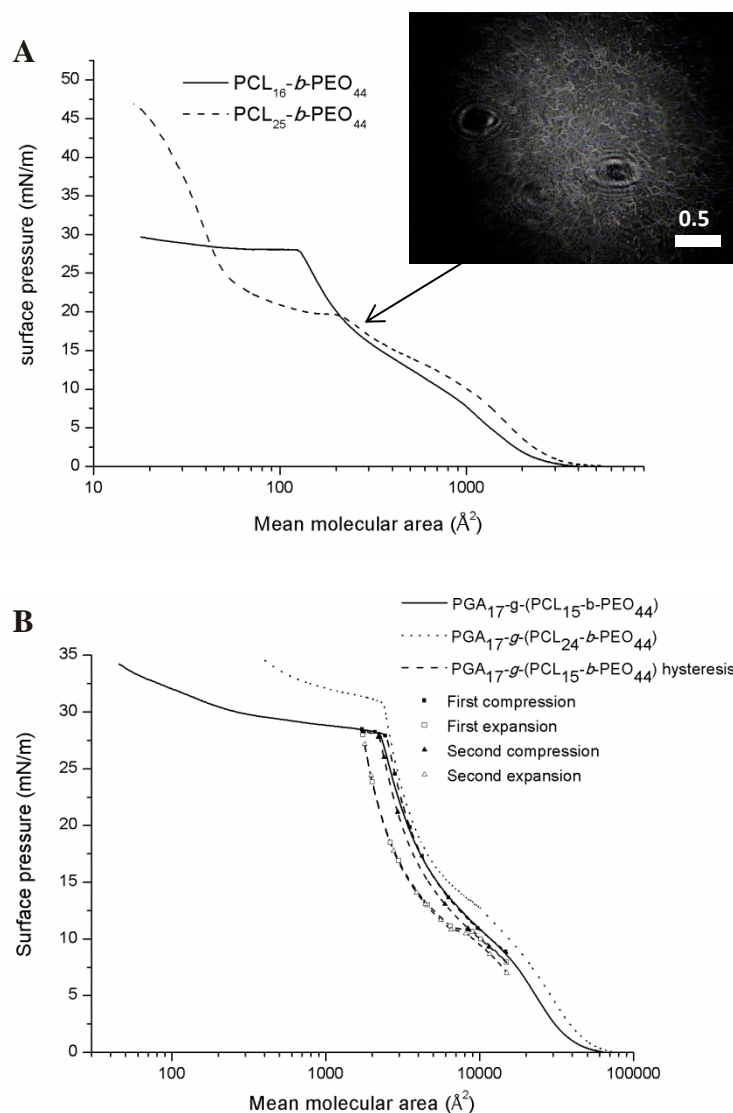
Figure 5.6 The π-*mmA* isotherms of (A) PCL$_{16}$-*b*-PEO$_{44}$ and PCL$_{25}$-*b*-PEO$_{44}$ linear block copolymers. The inset shows a BAM image of PCL$_{25}$-*b*-PEO$_{44}$ taken at surface pressure of $\pi \sim 16.5$ mN/m (B) PGA$_{17}$-*g*-(PCL$_{15}$-*b*-PEO$_{44}$), and PGA$_{17}$-*g*-(PCL$_{24}$-*b*-PEO$_{44}$) isotherms and the PGA$_{17}$-*g*-(PCL$_{24}$-*b*-PEO$_{44}$) hysteresis measurements.

The hysteresis isotherm of PGA$_{17}$-*g*-(PCL$_{15}$-*b*-PEO$_{44}$) in Figure 5.6 B shows a short pseudo plateau during monolayer expansion at the surface pressure of ~ 11 mN/m which can be assigned to the melting of PCL crystals at A/W interface (i.e. the readsorption of PCL monomer units at the A/W interface).[255] Similar to linear PCL, the shift of the isotherm during the second compression towards smaller mean molecular area values indicates that the

melting process does not include all PCL chains and thus some PCL chains are still packed in the 3D structure of the PCL crystals.
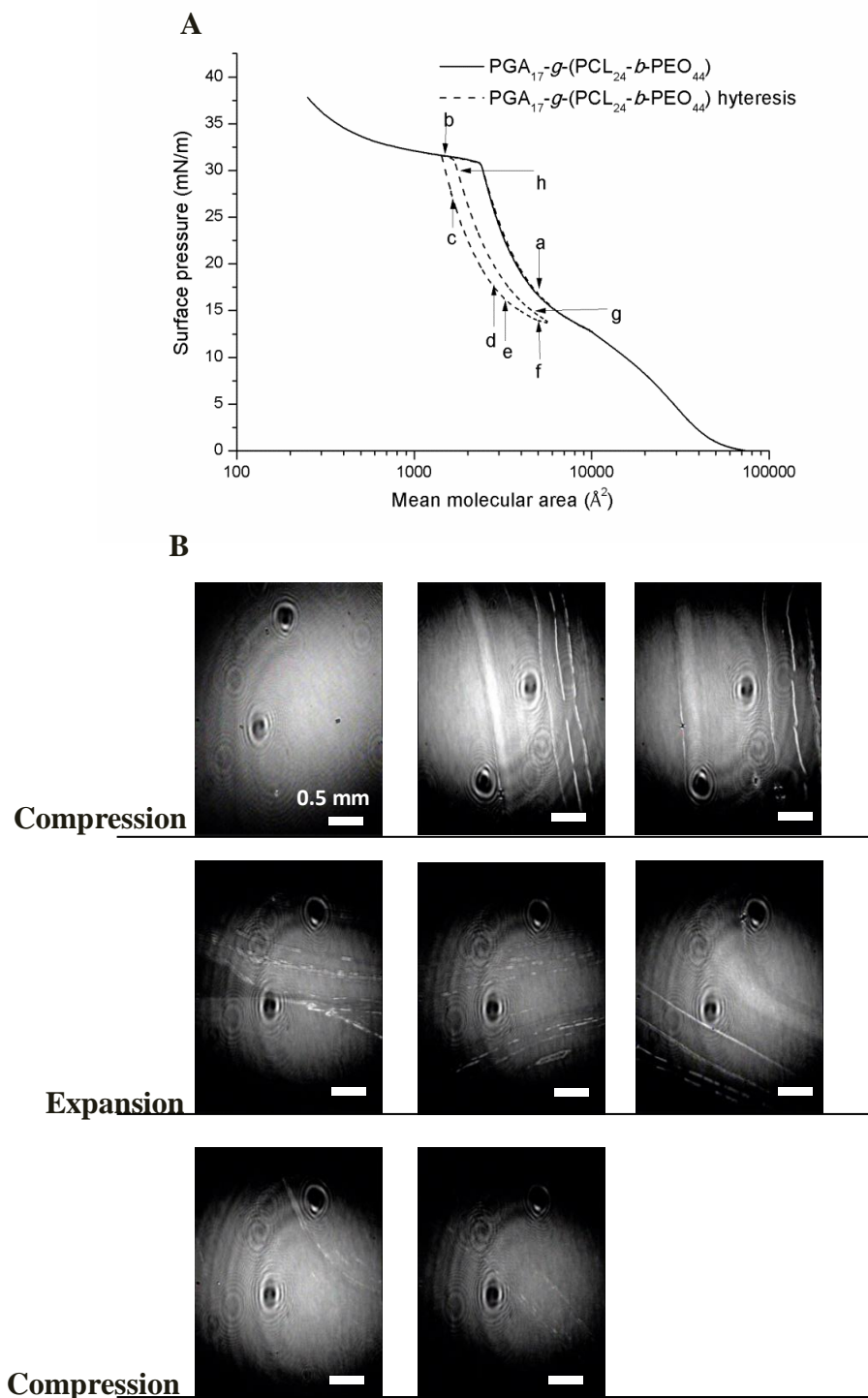
Figure 5.7 (A) The π-A isotherm and hysteresis isotherm of PGA$_{17}$-g-(PCL$_{24}$-b-PEO$_{44}$). (B) BAM images of PGA$_{17}$-g-(PCL$_{24}$-b-PEO$_{44}$) taken during compression-expansion-compression cycles. For details see text.

BAM images are also taken during the hysteresis experiment of PGA_{17}-g-(PCL_{24}-b-PEO_{44}) in order to confirm and clarify the collapse mechanism of the monolayer (see Figure 5.7). The hysteresis experiment is carried out in the region between collapse and before melting of PCL crystals (the pseudo plateau seen during expansion). BAM images b and c in Figure 5.7 B reveal the presence of parallel fracture lines which appear within the polymer monolayer. This suggests that collapse occurred according to the multilayer formation mechanism.

Clear cracks within the polymer films appear during the expansion process which causes the appearance of isolated condensed domains (Figure 5.7 B d-f). The BAM images reveal also that the folds formed during the collapse process do not totally disappear during expansion. On the other hand, the second compression shows a significant shift of the corresponding isotherm towards smaller *mmA* values which confirms that the multilayers formed during collapse do not disappear totally during expansion. Furthermore, the second compression isotherm returns to the same point (*b* in Figure 5.7A) as in the first compression indicating that no chains are desorbed from the A/W interface during collapse. It is worth mentioning here that the monolayer is not left to relax between the hysteresis circles, and thus the conclusions stated here are attributed to our experimental conditions.

5.3.3   Langmuir Blodgett films

Figure 5.8 depicts an AFM image and corresponding height profiles of an LB film of PGA_{17}-g-PCL_{24} taken at *mmA*= 7000 Å^2. The image reveals the presence of disk-like crystals of different diameter. The corresponding height profiles show that these crystals have a homogeneous thickness of ~ 7.7 nm which matches the reported lamellar thickness formed by linear PCL at the A/W interface and also the flat-on lamella formed after spin coating of PCL solutions.[239,252] This height corresponds to a staple of 8-9 monomer units (calculated from the orthorhombic unit cell parameters of PCL to be c/2=1.726/2=0.863 nm per monomer unit). Additionally, this image reveals also the presence of filament crystals on the surface of the disk crystals with a thickness equal to multiples of approximately 7 nm. Such filaments can be formed as distortions within the disk-like crystals during the deposition process onto silicon substrates.
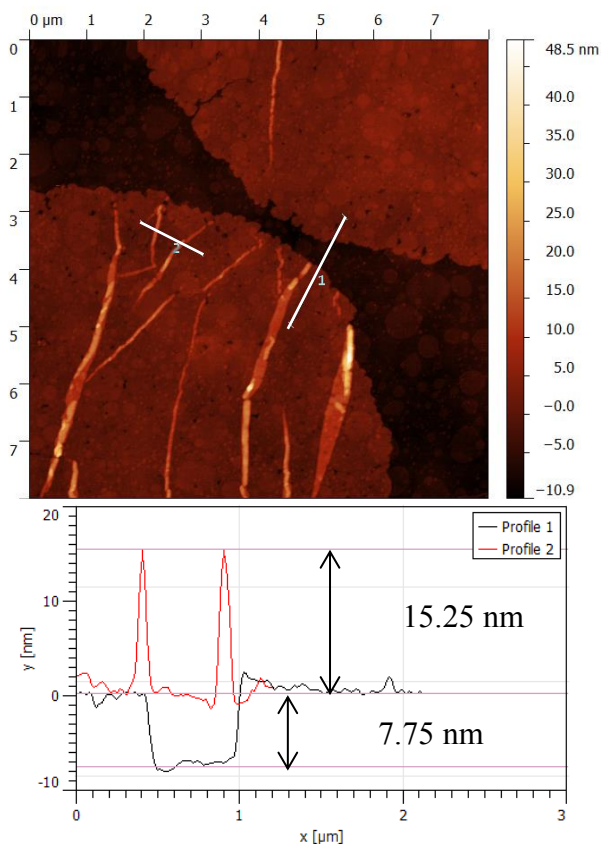
Figure 5.8 AFM height images of LB film of PGA_{17}-g-PCL_{24} transferred at 7000 $Å^2$ and the corresponding height profile.

The monolayer of PGA_{17}-g-(PCL_{24}-b-PEO_{44}) was transferred onto the silica substrate at a surface pressure of 16 mN/m. The topographic AFM images reveal the presence of branched crystals (Figure 5.9 a and b). Small platelets are joined by filament crystals. The height profiles (Figure 5.9 c) indicate that the branched crystals have a height of ~ 7.8 nm which is again close to the thickness of PCL crystals at A/W interface.[252] Furthermore, the height profile shows that the platelets have a thickness of ~ 15 nm which is roughly equal to the double of the thickness of PCL crystals.
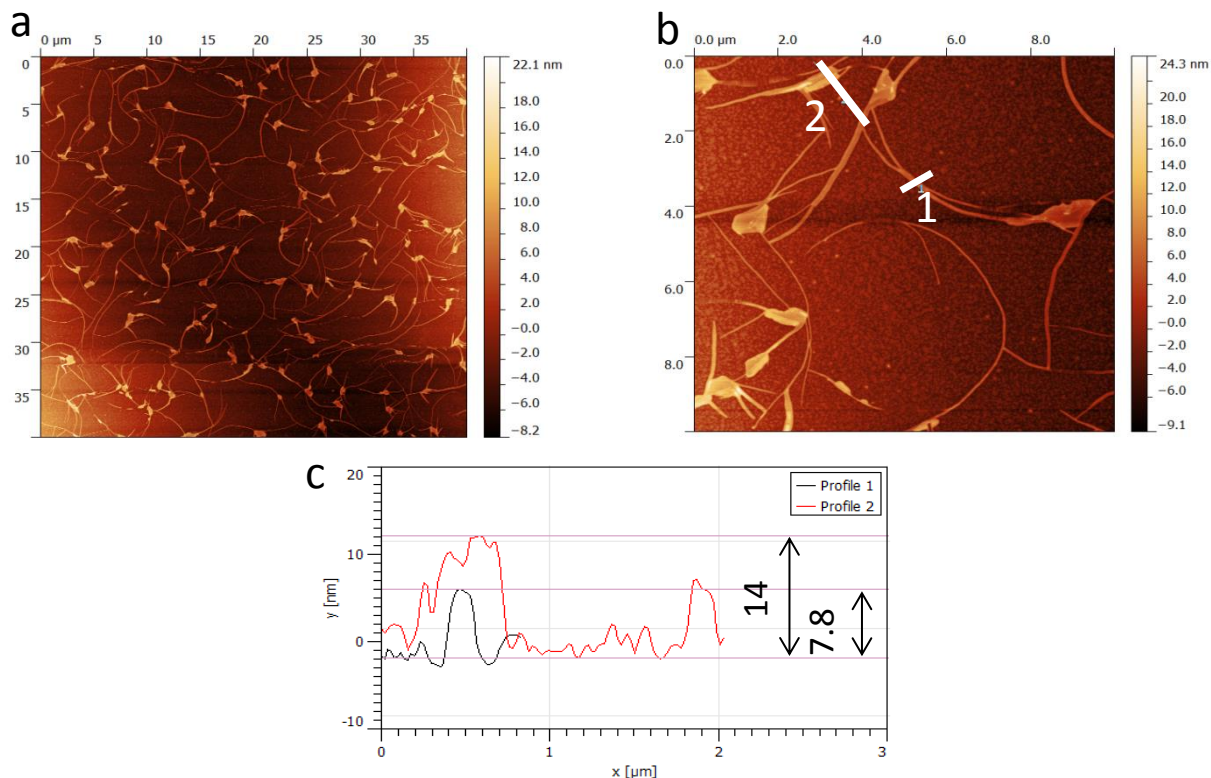
Figure 5.9 (a) and (b) AFM height image of LB films of PGA_{17}-g-$(PCL_{24}$-b-$PEO_{44})$, transferred at $\pi = 16$ mN/m. (c) Height profiles taken along the lines 1, and 2 in image (b).

5.4 Conclusions

PCL grafted onto a PGA backbone has compared to linear PCL an increased nucleation rate, decreased crystallization rate, and produces entities with significantly smaller size at the A/W interface. Additionally, the crystals formed by PGA_{17}-g-PCL_{24} do not melt upon expansion on the Langmuir trough at temperatures well above the melting temperature of bulk PCL in contrast to crystals of linear PCL at the A/W interface. The AFM height image of LB films of PGA_{17}-g-PCL_{24} depicts the presence of disk-like crystals having a lamella thickness of ~7.6 nm which matches the previously reported lamella thickness of linear PCL formed at the A/W interface. BAM images reveal that the crystals formed by linear PCL_{25} form mesophase upon raising the subphase temperature above the bulk melting point of PCL_{25} at constant mean molecular area. The crystals formed after cooling the subphase to room temperature have a different morphology than those formed at the beginning. Linear and grafted PCL-b-PEO copolymers show one transition within their isotherms before collapse. This transition which appears at the surface pressure of ~10 mN/m is assigned to the dissolution of PEO chains into water subphase and to the crystallization of PCL segments at

A/W interface. Hysteresis isotherms of PGA_{17}-g-$(PCL_{24}$-b-$PEO_{44})$ show a short plateau region during expansion due to the melting (readsorption) of PCL crystals at A/W interface. Furthermore, the isotherms of all polymers, except PCL_{25}-b-PEO_{44}, show long plateau regions at a surface pressure of ~30 mN/m. They are assigned to the collapse of the polymer monolayer by a multilayer formation mechanism. This interpretation is further confirmed by BAM images of PGA_{17}-g-$(PCL_{24}$-b-$PEO_{44})$ within this region. Finally, the AFM image of PGA_{17}-g-$(PCL_{24}$-b-$PEO_{44})$ of LB films shows branched crystals formed by platelets and connected by filament crystals.

Chapter 6
Summary

The interest in the synthesis and characterization of graft copolymers has increased recently due to their possible applications in many important fields. It has been reported that the graft copolymers display superior properties in the field of nano-drug carriers when compared with their linear counterparts. Biodegradability and biocompatibility properties of polymers that are designed for biomedical applications should be considered.

The aim of the presented work was to synthesing and characterize series of novel graft copolymers that are suitable for pharmaceutical applications. Many synthetic approaches were applied here to achieve this target. Aliphatic polyesters with free pendent functional groups were used always as polymer backbone to synthesize the graft copolymers.

The first part of this thesis discussed the preparation of linear aliphatic polyesters with free pendent azide groups by enzymatic polycondensation in the presence of lipase from *Candida antarctica* type B (CAL-B). The grafting reaction to the N_3-functional polyester was carried out quantitatively at room temperature using copper-catalyzed azide-alkyne cycloaddition (CuAAC, "click" reaction) with monoalkyne-functional poly(ethylene oxide) (alkyne-PEO, M_n = 750 g/mol). Furthermore, both enzymatic polycondensation and "click" reaction were carried out successfully in sequential one-pot reaction. The graft copolymer was surface-active and self-assembled in water. The graft copolymer had a critical aggregation concentration (cac) of 3×10^{-2} µM in water determined by surface tension measurements. Above cac, the graft copolymer formed single chains and aggregates having a hydrodynamic radius of ~75 nm. Furthermore, the surface activity of the polymers at the air-water interface was studied by Langmuir trough measurements. The Langmuir isotherm of the graft polymer showed a pseudoplateau resulting from desorption of PEO chains into the subphase upon compression.

The second part of the thesis disscused synthesis of graft copolymers, similar to those synthesized in the first chapter, by utilization of poly(glycerol adipate) (PGA) as polymer backbone. PGA was synthesized by enzymatic polymerization using glycerol and either divinyl adipate or dimethyl adipate. The PGA was linear when the enzymatic reaction was carried out at 40°C while branching occurred at higher temperatures. The hydroxyl pendent groups were quantitatively esterified with 5-hexynoic acid to yield PGA with alkyne functional pendent functional groups. Afterwards, poly(ethylene oxide) monomethylether

azide mPEO-N$_3$ chains were quantitatively attached onto PGA using "click" reaction under very mild condition. The linear PGA backbone was modified also by esterification with fatty acids of different lengths yielding comb-like polymers. The melting temperature and specific enthalpy of fusion increase with increasing degree of substitution and/or by increasing length of the saturated fatty acids used to modify the PGA backbone. Furthermore, the comb-like polymers have a higher thermal stability compared to the original PGA backbone. The shape of nanoparticles prepared by an optimized interfacial deposition method depend on the type of fatty acid used and on the degree of substitution. The nanoparticles are phase separated as a result of the incompatibility between the polymer backbone and the teeth of the comb-like polymers. These nanoparticles offer promising possibilities as delivery systems for lipophilic, amphiphilic and water soluble drugs.

In the third part, poly(glycerol adipate)-*graft*-(poly(3-caprolactone)-block-poly(ethylene oxide)) (PGA-g-(PCL-b-PEO)) was synthesized by ring opening polymerization of ε-caprolactone initiated by the hydroxyl groups of PGA. This was followed by grafting of mPEO-N$_3$ onto the PCL by CuAAC,"click" reaction. All polymers form micelles of radii in the range of 10 nm after dissolving in acetone and dialysis against water. Micelles formed by PGA-*g*-(PCL-*b*-PEO) show smaller critical micelle concentration (cmc) and higher stability against temperature increase compared to micelles formed by PCL-*b*-PEO with an identical chemical composition to the grafted segments. Additionally, PGA$_{17}$-*g*-(PCL$_{24}$-*b*-PEO$_{44}$) forms worm-like aggregates prepared by the cosolvent/evaporation method. The resulting worm-like aggregates were visualized by transmission electron and confocal laser scanning microscopy and showed shape persistent behavior over their entire contour length. It is suggested that these worm-like aggregates are formed by partially fused polymersomes under the influence of shear flow. They have the potential for simultaneous delivery of hydrophobic and hydrophilic drugs.

Finally, The behavior of crystallizable poly(ε-caprolactone) (PCL) and poly(ε-caprolactone)-*b*-poly(ethylene oxide) (PCL-*b*-PEO) is studied at the air/water interface prior and after grafting to an amorphous poly(glycerol adipate) (PGA) backbone (PGA-*g*-PCL, PGA-*g*-(PCL-*b*-PEO). Langmuir isotherms are measured and the structure formation in the monolayer films on the water surface is followed by Brewster angle microscopy (BAM) and in Langmuir-Blodgett films after transfer to silicon substrates by atomic force microscopy (AFM). It is observed that PGA-*g*-PCL forms significantly smaller crystals and has smaller crystallization rate compared to PCL homopolymers of identical molar masses as the grafted chains. In contrast to crystals formed by linear PCL, the crystals formed by grafted PCL in

PGA-*g*-PCL do not melt (readsorb at the water surface) upon expansion on the Langmuir trough. Additionally, raising the subphase temperature at constant surface area significantly above the melting point of linear PCL results in the formation of a mesophase instead of the disappearance of crystals. AFM images of Langmuir-Blodgett films reveal that PCL chains in PGA-*g*-PCL and PGA-*g*-(PCL-*b*-PEO) form lamellar crystals with a disk-shape and interconnected platelets, respectively.

Some of the chapters of this thesis are based on the following publications:

- Chapter 2 based on

Naolou, T.; Busse, K.; Kressler, J. Synthesis of well-defined graft copolymers by combination of enzymatic polycondensation and "click" chemistry. *Biomacromolecules* **2010**, *11*, 3660–3667.

- Chapter 3 based on

Naolou, T.; Weiss, V. M.; Conrad, D.; Busse, K.; Mäder, K.; Kressler, J. Fatty acid modified poly(glycerol adipate) - polymeric analogues of glycerides, In *Tailored Polymer Architectures for Pharmaceutical and Biomedical Applications*; Scholz, C.; Kressler, J., Eds.; American Chemical Society: Washington, DC, 2013; Vol. 1135, pp. 39–52.

- Chapter 4 based on

Naolou, T.; Meister, A.; Schöps, R.; Pietzsch, M.; Kressler, J. Synthesis and characterization of graft copolymers able to form polymersomes and worm-like aggregates. *Soft Matter* **2013**, *9*, 10364.

References

(1)   Painter, P. C.; Michael M. Coleman *Essentials of Polymer Science and Engineering*; DEStech Publications, Inc, 2008; p. 542.

(2)   *Chemical Sciences in the 20th Century*; Reinhardt, C., Ed.; Wiley-VCH Verlag GmbH: Weinheim, Germany, 2001.

(3)   David I. Bower *An Introduction to Polymer Physics*; Cambridge University Press, 2002; p. 468.

(4)   Szwarc, M.; Levy, M.; Milkovich, R. *J. Am. Chem. Soc.* **1956**, *78*, 2656–2657.

(5)   Higashimura, T.; Kishiro, O. *Polym. J.* **1977**, *9*, 87–93.

(6)   Miyamoto, M.; Sawamoto, M.; Higashimura, T. *Macromolecules* **1984**, *17*, 265–268.

(7)   Aoshima, S.; Kanaoka, S. *Chem. Rev.* **2009**, *109*, 5245–5287.

(8)   Kobayashi, S.; Uyama, H. In *Biopolymers Online*; Wiley-VCH Verlag GmbH & Co. KGaA, 2005.

(9)   Braunecker, W. A.; Matyjaszewski, K. *Prog. Polym. Sci.* **2007**, *32*, 93–146.

(10)   Chiefari, J.; Chong, Y. K. (Bill); Ercole, F.; Krstina, J.; Jeffery, J.; Le, T. P. T.; Mayadunne, R. T. A.; Meijs, G. F.; Moad, C. L.; Moad, G.; Rizzardo, E.; Thang, S. H. *Macromolecules* **1998**, *31*, 5559–5562.

(11)   Matyjaszewski, K.; Xia, J. *Chem. Rev.* **2001**, *101*, 2921–2990.

(12)   Wang, J.-S.; Matyjaszewski, K. *J. Am. Chem. Soc.* **1995**, *117*, 5614–5615.

(13)   Solomon, D. H. *J. Polym. Sci. Part A Polym. Chem.* **2005**, *43*, 5748–5764.

(14)   Wilco P. J. Appel; Marko M. L. Nieuwenhuizen; Meijer, E. W. *Supramolecular Polymer Chemistry*; Harada, A., Ed.; Akira Hara.; Wiley-VCH Verlag GmbH & Co. KGaA: Weinheim, Germany, 2011; p. 390.

(15)   *Complex Macromolecular Architectures*; Hadjichristidis, N.; Hirao, A.; Tezuka, Y.; Du Prez, F., Eds.; John Wiley & Sons (Asia) Pte Ltd: Singapore, 2011.

(16)   Axel H. E. Müller; Matyjaszewski, K. In *Controlled and Living Polymerizations: From Mechanisms to Applications*; Axel H. E. Müller; Matyjaszewski, K., Eds.; Wiley-VCH Verlag GmbH & Co. KGaA, 2010.

(17)   Feng, C.; Li, Y.; Yang, D.; Hu, J.; Zhang, X.; Huang, X. *Chem. Soc. Rev.* **2011**, *40*, 1282–1295.

(18)   Cai, C.; Lin, J.; Chen, T.; Tian, X. *Langmuir* **2010**, *26*, 2791–2797.

(19)   Qi, L.; Cölfen, H.; Antonietti, M. *Nano Lett.* **2001**, *1*, 61–65.

(20)   Sato, Y.; Kobayashi, Y.; Kamiya, T.; Watanabe, H.; Akaike, T.; Yoshikawa, K.; Maruyama, A. *Biomaterials* **2005**, *26*, 703–711.

(21) Pakula, T.; Zhang, Y.; Matyjaszewski, K.; Lee, H.; Boerner, H.; Qin, S.; Berry, G. C. *Polymer.* **2006**, *47*, 7198–7206.

(22) Rzayev, J. *Macromolecules* **2009**, *42*, 2135–2141.

(23) Shi, H.; Zhao, Y.; Dong, X.; Zhou, Y.; Wang, D. *Chem. Soc. Rev.* **2012**.

(24) Majnusz, J.; Catala, J.; Lenz, R. *Eur. Polym. J.* **1983**, *19*, 1043–1046.

(25) Watanabe, J.; Harkness, B. R.; Sone, M.; Ichimura, H. *Macromolecules* **1994**, *27*, 507–512.

(26) Rehberg, C. E.; Fisher, C. H. *J. Am. Chem. Soc.* **1944**, *66*, 1203–1207.

(27) Jordan, E. F.; Feldeisen, D. W.; Wrigley, A. N. *J. Polym. Sci. Part A Polym. Chem.* **1971**, *9*, 1835–1851.

(28) Feng, L.-B.; Zhou, S.-X.; You, B.; Wu, L.-M. *J. Appl. Polym. Sci.* **2007**, *103*, 1458–1465.

(29) Bo, G.; Wesslén, B.; Wessléen, K. B. *J. Polym. Sci. Part A Polym. Chem.* **1992**, *30*, 1799–1808.

(30) Horgan, A.; Saunders, B.; Vincent, B.; Heenan, R. K. *J. Colloid Interface Sci.* **2003**, *262*, 548–559.

(31) Gao, H.; Matyjaszewski, K. *J. Am. Chem. Soc.* **2007**, *129*, 6633–6639.

(32) Yu, Y.; Zou, J.; Yu, L.; Ji, W.; Li, Y.; Law, W.; Cheng, C. *Macromolecules* **2011**, *44*, 4793–4800.

(33) Schubert, U. S.; Hofmeier, H. *Macromol. Rapid Commun.* **2002**, *23*, 561–566.

(34) Ikkala, O.; ten Brinke, G. *Science* **2002**, *295*, 2407–2409.

(35) Takahashi, T.; Kimura, T.; Sakurai, K. *Polymer.* **1999**, *40*, 5939–5945.

(36) Aoi, K.; Aoi, H.; Okada, M. *Macromol. Chem. Phys.* **2002**, *203*, 1018–1028.

(37) Zhang, B.; Fischer, K.; Schmidt, M. *Macromol. Chem. Phys.* **2005**, *206*, 157–162.

(38) Lian, X.; Wu, D.; Song, X.; Zhao, H. *Macromolecules* **2010**, *43*, 7434–7445.

(39) Villarroya, S.; Dudek, K.; Zhou, J.; Irvine, D. J.; Howdle, S. M. *J. Mater. Chem.* **2008**, *18*, 989–997.

(40) Yuan, W.; Yuan, J.; Zhang, F.; Xie, X.; Pan, C. *Macromolecules* **2007**, *40*, 9094–9102.

(41) Tokiwa, Y.; Calabia, B. P. *J. Polym. Environ.* **2007**, *15*, 259–267.

(42) Sartorius, I. *Biopolym. Online* **2005**.

(43) Albertsson, A.; Varma, I. In *Degradable Aliphatic Polyesters*; Springer Berlin Heidelberg, 2002; Vol. 157, pp. 1–40.

(44) Ohya, Y.; Takahashi, A.; Nagahama, K. In *Polymers in Nanomedicine*; Kunugi, S.; Yamaoka, T., Eds.; Springer Berlin Heidelberg, 2011; pp. 65–114.

(45) Weiss, V. M.; Naolou, T.; Groth, T.; Kressler, J.; Mäder, K. *J. Appl. Biomater. Funct. Mater.* **2012**, *10*, 163–169.

(46) Weiss, V. M.; Naolou, T.; Amado, E.; Busse, K.; Mäder, K.; Kressler, J. *Macromol. Rapid Commun.* **2011**, 1–6.

(47) Weiss, V. M.; Naolou, T.; Hause, G.; Kuntsche, J.; Kressler, J.; Mäder, K. *J. Control. Release* **2012**, *158*, 156–164.

(48) Riva, R.; Schmeits, S.; Stoffelbach, F.; Jérôme, C.; Jérôme, R.; Lecomte, P. *Chem. Commun.* **2005**, *40*, 5334–5336.

(49) Chen, Y.; Wilbon, P. a.; Chen, Y. P.; Zhou, J.; Nagarkatti, M.; Wang, C.; Chu, F.; Decho, A. W.; Tang, C. *RSC Adv.* **2012**, *2*, 10275–10282.

(50) Pechar, M.; Ulbrich, K.; Šubr, V.; Seymour, L. W.; Schacht, E. H. *Bioconjug. Chem.* **2000**, *11*, 131–139.

(51) Kim, S. H.; Tan, J. P. K.; Nederberg, F.; Fukushima, K.; Colson, J.; Yang, C.; Nelson, A.; Yang, Y.-Y.; Hedrick, J. L. *Biomaterials* **2010**, *31*, 8063–71.

(52) Kataoka, K.; Matsumoto, T.; Yokoyama, M.; Okano, T.; Sakurai, Y.; Fukushima, S.; Okamoto, K.; Kwon, G. S. *J. Control. Release* **2000**, *64*, 143–153.

(53) Li, G.; Song, S.; Guo, L.; Ma, S. *J. Polym. Sci. Part A Polym. Chem.* **2008**, *46*, 5028–5035.

(54) Xiong, X.-B.; Mahmud, A.; Uludağ, H.; Lavasanifar, A. *Pharm. Res.* **2008**, *25*, 2555–2566.

(55) Hu, X.; Liu, S.; Chen, X.; Mo, G.; Xie, Z.; Jing, X. *Biomacromolecules* **2008**, *9*, 553–560.

(56) Grafahrend, D.; Calvet, J. L.; Klinkhammer, K.; Salber, J.; Dalton, P. D.; Möller, M.; Klee, D. *Biotechnol. Bioeng.* **2008**, *101*, 609–621.

(57) Chang, L.; Deng, L.; Wang, W.; Lv, Z.; Hu, F.; Dong, A.; Zhang, J. *Biomacromolecules* **2012**, *13*, 3301–10.

(58) Ponsart, S.; Coudane, J.; Vert, M. *Biomacromolecules* **2000**, *1*, 275–81.

(59) Lecomte, P.; Riva, R.; Schmeits, S.; Rieger, J.; Van Butsele, K.; Jérôme, C.; Jérôme, R. *Macromol. Symp.* **2006**, *240*, 157–165.

(60) Habnouni, S. El; Darcos, V.; Coudane, J. *Macromol. Rapid Commun.* **2009**, *30*, 165–169.

(61) Parrish, B.; Breitenkamp, R. B.; Emrick, T. *J. Am. Chem. Soc.* **2005**, *127*, 7404–10.

(62) Naolou, T.; Busse, K.; Kressler, J. *Biomacromolecules* **2010**, *11*, 3660–3667.

(63) Lu, Y.; Yin, L.; Zhang, Y.; Zhonghai, Z.; Xu, Y.; Tong, R.; Cheng, J. *ACS Macro Lett.* **2012**, *1*, 441–444.

(64) Billiet, L.; Fournier, D.; Du Prez, F. *J. Polym. Sci. Part A Polym. Chem.* **2008**, *46*, 6552–6564.

(65) Takasu, A.; Shibata, Y.; Narukawa, Y.; Hirabayashi, T. *Macromolecules* **2007**, *40*, 151–153.

(66) Alexander Steinbüchel *Biopolymers: General Aspects and Special Applications*; Wiley-VCH, 2003; p. 186.

(67) Löfgren, A.; Albertsson, A.; Dubois, P.; Jérôme, R. *J. Macromol. Sci., Polym. Rev.* **1995**, *35*, 379–418.

(68) Loos, K. *Biocatalysis in Polymer Chemistry*; Loos, K., Ed.; Wiley-VCH Verlag GmbH & Co. KGaA: Weinheim, Germany, 2010.

(69) Lou, X.; Detrembleur, C.; Jérôme, R. *Macromolecules* **2002**, *35*, 1190–1195.

(70) Seyednejad, H.; Vermonden, T.; Fedorovich, N. E.; van Eijk, R.; van Steenbergen, M. J.; Dhert, W. J. a; van Nostrum, C. F.; Hennink, W. E. *Biomacromolecules* **2009**, *10*, 3048–3054.

(71) Gerhardt, W. W.; Noga, D. E.; Hardcastle, K. I.; García, A. J.; Collard, D. M.; Weck, M. *Biomacromolecules* **2006**, *7*, 1735–42.

(72) Zhang, Z.; Yin, L.; Xu, Y.; Tong, R.; Lu, Y.; Ren, J.; Cheng, J. *Biomacromolecules* **2012**, *13*, 3456–3462.

(73) Thillaye du Boullay, O.; Bonduelle, C.; Martin-Vaca, B.; Bourissou, D. *Chem. Commun.* **2008**, 1786–1788.

(74) Pounder, R. J.; Dove, A. P. *Biomacromolecules* **2010**, *11*, 1930–1939.

(75) Dai, W.; Zhu, J.; Shangguan, A.; Lang, M. *Eur. Polym. J.* **2009**, *45*, 1659–1667.

(76) Tian, D.; Dubois, P.; Grandfils, C.; Jérôme, R. *Macromolecules* **1997**, *30*, 406–409.

(77) Kobayashi, S. *Macromol. Rapid Commun.* **2009**, *30*, 237–266.

(78) Halling, P.; Kvittingen, L. *Trends Biotechnol.* **1999**, *17*, 343–344.

(79) Zaks, A.; Klibanov, A. *Science.* **1984**, *224*, 1249–1251.

(80) Gross, R. a; Ganesh, M.; Lu, W. *Trends Biotechnol.* **2010**, *28*, 435–443.

(81) Yu, Y.; Wu, D.; Liu, C.; Zhao, Z.; Yang, Y.; Li, Q. *Process Biochem.* **2012**, *47*, 1027–1036.

(82) Uyama, H.; Kobayashi, S. In *Enzymatic Synthesis of Polyesters via Polycondensation*; Kobayashi, S.; Ritter, H.; Kaplan, D., Eds.; Springer-Verlag: Berlin/Heidelberg, 2006; Vol. 194, p. 133.

(83)   Puskas, J. E.; Seo, K. S.; Sen, M. Y. *Eur. Polym. J.* **2011**, *47*, 524–534.

(84)   Mateo, C.; Palomo, J. M.; Fernandez-Lorente, G.; Guisan, J. M.; Fernandez-Lafuente, R. *Enzyme Microb. Technol.* **2007**, *40*, 1451–1463.

(85)   Uyama, H.; Kobayashi, S. *Chem. Lett.* **1993**, 1149–1150.

(86)   Yeniad, B.; Naik, H.; Heise, A. *Adv. Biochem. Eng. Biotechnol.* **2011**, *125*, 69–95.

(87)   De Geus, M.; Peeters, J.; Wolffs, M.; Hermans, T.; Palmans, A. R. A.; Koning, C. E.; Heise, A. *Macromolecules* **2005**, *38*, 4220–4225.

(88)   Uppenberg, J.; Hansen, M. T.; Patkar, S.; Jones, T. A. *Structure* **1994**, *2*, 293–308.

(89)   Kobayashi, S. *Proc. Japan Acad. Ser. B* **2010**, *86*, 338–365.

(90)   Veld, M.; Palmans, A. In *Enzymatic Polymerisation*; Palmans, A. R. A.; Heise, A., Eds.; Springer-Verlag Berlin Heidelberg, 2011; pp. 55–78.

(91)   Patil, D. R.; Rethwisch, D. G.; Dordick, J. S. *Biotechnol. Bioeng.* **1991**, *37*, 639–646.

(92)   Kumar, A.; Kulshrestha, A. S.; Gao, W.; Gross, R. A. *Macromolecules* **2003**, *36*, 8219–8221.

(93)   Kato, M.; Toshima, K.; Matsumura, S. *Biomacromolecules* **2009**, *10*, 366–373.

(94)   Kulshrestha, A. S.; Sahoo, B.; Gao, W.; Fu, H.; Gross, R. A. *Macromolecules* **2005**, *38*, 3205–3213.

(95)   Kolb, H. C.; Finn, M. G.; Sharpless, K. B. *Angew. Chem. Int. Ed. Engl.* **2001**, *40*, 2004–2021.

(96)   Becer, C. R.; Hoogenboom, R.; Schubert, U. S. *Angew. Chem. Int. Ed. Engl.* **2009**, *48*, 4900–8.

(97)   Binder, W. H.; Sachsenhofer, R. *Macromol. Rapid Commun.* **2008**, *29*, 952–981.

(98)   Bock, V. D.; Hiemstra, H.; van Maarseveen, J. H. *European J. Org. Chem.* **2006**, *2006*, 51–68.

(99)   Tornøe, C. W.; Christensen, C.; Meldal, M. *J. Org. Chem.* **2002**, *67*, 3057–3064.

(100) Golas, P. L.; Tsarevsky, N. V.; Sumerlin, B. S.; Matyjaszewski, K. *Macromolecules* **2006**, *39*, 6451–6457.

(101) Hadjichristidis, N.; Hirao, A.; Tezuka, Y.; Prez, F. Du In *Complex Macromolecular Architectures*; Hadjichristidis, N.; Hirao, A.; Tezuka, Y.; Du Prez, F., Eds.; John Wiley & Sons (Asia) Pte Ltd: Singapore, 2011; pp. 230–265.

(102) Laughlin, S. T.; Baskin, J. M.; Amacher, S. L.; Bertozzi, C. R. *Science.* **2008**, *320*, 664–667.

(103) Durmaz, H.; Colakoglu, B.; Tunca, U.; Hizal, G. *J. Polym. Sci. Part A Polym. Chem.* **2006**, *44*, 1667–1675.

(104) Sinnwell, S.; Lammens, M.; Stenzel, M. H.; Du Prez, F. E.; Barner-Kowollik, C. *J. Polym. Sci. Part A Polym. Chem.* **2009**, *47*, 2207–2213.

(105) Inglis, A. J.; Sinnwell, S.; Stenzel, M. H.; Barner-Kowollik, C. *Angew. Chemie* **2009**, *121*, 2447–2450.

(106) Campos, L. M.; Killops, K. L.; Sakai, R.; Paulusse, J. M. J.; Damiron, D.; Drockenmuller, E.; Messmore, B. W.; Hawker, C. J. *Macromolecules* **2008**, *41*, 7063–7070.

(107) Qiu, L. Y.; Bae, Y. H. *Pharm. Res.* **2006**, *23*, 1–30.

(108) Du, J.-Z.; Tang, L.-Y.; Song, W.-J.; Shi, Y.; Wang, J. *Biomacromolecules* **2009**, *10*, 2169–2174.

(109) Zhang, W.; Li, Y.; Liu, L.; Sun, Q.; Shuai, X.; Zhu, W.; Chen, Y. *Biomacromolecules* **2010**, *11*, 1331–1338.

(110) Kim, K.-H.; Lee, J.-C.; Lee, J. *Macromol. Biosci.* **2008**, *8*, 339–346.

(111) Knop, K.; Hoogenboom, R.; Fischer, D.; Schubert, U. S. *Angew. Chemie Int. Ed.* **2010**, *49*, 6288–6308.

(112) Shi, D. *Introduction to biomaterials*; 1st ed.; World Scientific: Hackensack, NJ, 2006; p. 187.

(113) Saulnier, B.; Ponsart, S.; Coudane, J.; Garreau, H.; Vert, M. *Macromol. Biosci.* **2004**, *4*, 232–237.

(114) Ponsart, S.; Coudane, J.; Vert, M. *Biomacromolecules* **2000**, *1*, 275–281.

(115) Huang, M.-H.; Coudane, J.; Li, S.; Vert, M. *J. Polym. Sci. Part A Polym. Chem.* **2005**, *43*, 4196–4205.

(116) Riva, R.; Schmeits, S.; Jérôme, C.; Jérôme, R.; Lecomte, P. *Macromolecules* **2007**, *40*, 796–803.

(117) Cooper, B. M.; Chan-Seng, D.; Samanta, D.; Zhang, X.; Parelkar, S.; Emrick, T. *Chem. Commun.* **2009**, 815–817.

(118) Cooper, B. M.; Emrick, T. *J. Polym. Sci. Part A Polym. Chem.* **2009**, *47*, 7054–7065.

(119) Grignard, B.; Schmeits, S.; Riva, R.; Detrembleur, C.; Lecomte, P.; Jérôme, C. *Green Chem.* **2009**, *11*, 1525.

(120) Lecomte, P.; Riva, R.; Jérôme, C.; Jérôme, R. *Macromol. Rapid Commun.* **2008**, *29*, 982–997.

(121) Xu, N.; Wang, R.; Du, F.; Li, Z. *J. Polym. Sci. Part A Polym. Chem.* **2009**, *47*, 3583–3594.

(122) Kallinteri, P.; Higgins, S.; Hutcheon, G. A.; St Pourçain, C. B.; Garnett, M. C. *Biomacromolecules* **2005**, *6*, 1885–1894.

(123) Kobayashi, S.; Uyama, H.; Kimura, S. *Chem. Rev.* **2001**, *101*, 3793–3818.

(124) Kline, B. J.; Beckman, E. J.; Russell, A. J. *J. Am. Chem. Soc.* **1998**, *120*, 9475–9480.

(125) Tornøe, C. W.; Christensen, C.; Meldal, M. *J. Org. Chem.* **2002**, *67*, 3057–3064.

(126) Rostovtsev, V. V.; Green, L. G.; Fokin, V. V.; Sharpless, K. B. *Angew. Chem. Int. Ed* **2002**, 2596–2599.

(127) Li, C.; Finn, M. G. *J. Polym. Sci. Part A Polym. Chem.* **2006**, *44*, 5513–5518.

(128) Huisgen, R. *Pure Appl. Chem.* **1989**, *61*, 613–628.

(129) Griffith, L. G.; Naughton, G. *Science (80-.).* **2002**, *295*, 1009–1014.

(130) Lugo-Mas, P.; Taylor, W.; Schweitzer, D.; Theisen, R. M.; Xu, L.; Shearer, J.; Swartz, R. D.; Gleaves, M. C.; Dipasquale, A.; Kaminsky, W.; Kovacs, J. A. *Inorg. Chem.* **2008**, *47*, 11228–11236.

(131) Gao, H.; Min, K.; Matyjaszewski, K. *Macromol. Chem. Phys.* **2007**, *208*, 1370–1378.

(132) Uyama, H.; Kobayashi, S. *Chem. Lett.* **1994**, 1687–1690.

(133) Peeters, J. W.; van Leeuwen, O.; Palmans, A. R. A.; Meijer, E. W. *Macromolecules* **2005**, *38*, 5587–5592.

(134) Mahapatro, A.; Kalra, B.; Kumar, A.; Gross, R. a *Biomacromolecules* **2003**, *4*, 544–551.

(135) Kumar, A.; Gross, R. A. *Biomacromolecules* **2000**, *1*, 133–138.

(136) Uyama, H.; Yaguchi, S.; Kobayashi, S. *J. Polym. Sci. Part A Polym. Chem.* **1999**, *37*, 2737–2745.

(137) Ladmiral, V.; Legge, T. M.; Zhao, Y.; Perrier, S. *Macromolecules* **2008**, *41*, 6728–6732.

(138) Heusgen, R. *J. Org. Chem.* **1968**, *33*, 2291–2297.

(139) Amantini, D.; Fringuelli, F.; Piermatti, O.; Pizzo, F.; Zunino, E.; Vaccaro, L. *J. Org. Chem.* **2005**, *70*, 6526–9.

(140) Allgaier, J.; Poppe, A.; Willner, L.; Richter, D. *Macromolecules* **1997**, *30*, 1582–1586.

(141) Odian, G. *Principles of Polymerization*; John Wiley & Sons, Inc.: Hoboken, NJ, USA, 2004.

(142) Tsarevsky, N. V.; Bencherif, S. A.; Matyjaszewski, K. *Macromolecules* **2007**, *40*, 4439–4445.

(143) Lundberg, P.; Hawker, C. J.; Hult, A.; Malkoch, M. *Macromol. Rapid Commun.* **2008**, *29*, 998–1015.

(144) Sharma, R.; Chisti, Y.; Banerjee, U. C. *Biotechnol. Adv.* **2001**, *19*, 627–662.

(145) Zhou, J.; Villarroya, S.; Wang, W.; Wyatt, M. F.; Duxbury, C. J.; Thurecht, K. J.; Howdle, S. M. *Macromolecules* **2006**, *39*, 5352–5358.

(146) Villarroya, S.; Zhou, J.; Thurecht, K. J.; Howdle, S. M. *Macromolecules* **2006**, *39*, 9080–9086.

(147) *Handbook of Industrial Water Soluble Polymers*; Williams, P. A., Ed.; 1st ed.; Blackwell Publishing Ltd: Oxford, UK, 2007; p. 211.

(148) Gohy, J. In *Block Copolymers II*; 2005; pp. 65–136.

(149) Ybert, C.; Lu, W.; Möller, G.; Knobler, C. M. *J. Phys. Chem. B* **2002**, *106*, 2004–2008.

(150) McFate, C.; Ward, D.; Olmsted, J. *Langmuir* **1993**, *9*, 1036–1039.

(151) Ries, H. E.; Swift, H. *Langmuir* **1987**, *3*, 853–855.

(152) Busse, K.; Peetla, C.; Kressler, J. *Langmuir* **2007**, *23*, 6975–6982.

(153) Miller, A. F.; Richards, R. W.; Webster, J. R. P. *Macromolecules* **2000**, *33*, 7618–7628.

(154) Tomlinson, M. R.; Cousin, F.; Geoghegan, M. *Polymer (Guildf).* **2009**, *50*, 4829–4836.

(155) Peace, S. K.; Richards, R. W.; Taylor, M. R.; Webster, J. R. P.; Williams, N. *Macromolecules* **1998**, *31*, 1261–1268.

(156) Barentin, C.; Muller, P.; Joanny, J. F. *Macromolecules* **1998**, *31*, 2198–2211.

(157) Besheer, A.; Vogel, J.; Glanz, D.; Kressler, J.; Groth, T.; Mäder, K. *Mol. Pharm.* **2009**, *2*, 407–415.

(158) Williams, C. K. *Chem. Soc. Rev.* **2007**, *36*, 1573–80.

(159) Rieger, J.; Van Butsele, K.; Lecomte, P.; Detrembleur, C.; Jérôme, R.; Jérôme, C. *Chem. Commun.* **2005**, 274–6.

(160) Hu, J.; Gao, W.; Kulshrestha, A.; Gross, R. A. *Macromolecules* **2006**, *39*, 6789–6792.

(161) Yang, Y.; Lu, W.; Cai, J.; Hou, Y.; Ouyang, S.; Xie, W.; Gross, R. A. *Macromolecules* **2011**, *44*, 1977–1985.

(162) Kobayashi, S.; Makino, A. *Chem. Rev.* **2009**, *109*, 5288–353.

(163) Korupp, C.; Weberskirch, R.; Müller, J. J.; Liese, A.; Hilterhaus, L. *Org. Process Res. Dev.* **2010**, *14*, 1118–1124.

(164) Alvarez, S. G.; Alvarez, M. T. A Practical Procedure for the Synthesis of Alkyl Azides at Ambient Temperature in Dimethyl Sulfoxide in High Purity and Yield. *Synthesis.* **1997**, *1997*, 413–414.

(165) Ambade, A. V; Savariar, E. N.; Thayumanavan, S. *Mol. Pharm.* **2005**, *2*, 264–72.

(166) Azim, H.; Dekhterman, A.; Jiang, Z.; Gross, R. A. *Biomacromolecules* **2006**, *7*, 3093–7.

(167) Besheer, A.; Vogel, J.; Glanz, D.; Kressler, J.; Groth, T.; Mäder, K. *Mol. Pharm.* **2009**, *6*, 407–15.

(168) Bianco-Peled, H.; Dori, Y.; Schneider, J.; Sung, L.; Satija, S.; Tirrell, M. *Langmuir* **2001**, *17*, 6931–6937.

(169) Meng, W.; Parker, T. L.; Kallinteri, P.; Walker, D. a; Higgins, S.; Hutcheon, G. a; Garnett, M. C. *J. Control. Release* **2006**, *116*, 314–321.

(170) Puri, S.; Kallinteri, P.; Higgins, S.; Hutcheon, G. A.; Garnett, M. C. *J. Control. release* **2008**, *125*, 59–67.

(171) Meng, W.; Kallinteri, P.; Walker, D. a; Parker, T. L.; Garnett, M. C. *Exp. Biol. Med.* **2007**, *232*, 1100–1108.

(172) Brioude, M. D. M.; Guimarães, D. H.; Fiúza, R. D. P.; Prado, L. A. S. D. A.; Boaventura, J. S.; José, N. M. *Mater. Res.* **2007**, *10*, 335–339.

(173) Ebata, H.; Toshima, K.; Matsumura, S. *Chem. Lett.* **2001**, 798–799.

(174) Binns, F.; Roberts, S. M.; Taylor, A.; Williams, C. F. *J. Chem. Soc. Perkin Trans. 1* **1993**, 899.

(175) Mezoul, G.; MARECHAL, E.; Brigodiot, M. *J. Polym. Sci. Part A Polym. Chem.* **1995**, *33*, 2691–2698.

(176) Trusek-Holownia, A.; Noworyta, A. *J. Biotechnol.* **2007**, *130*, 47–56.

(177) Juais, D.; Naves, A. F.; Li, C.; Gross, R. a; Catalani, L. H. *Macromolecules* **2010**, *43*, 10315–10319.

(178) Uyama, H.; Inada, K.; Kobayashi, S. *Macromol. Rapid Commun.* **1999**, *20*, 171–174.

(179) Uyama, H.; Inada, K.; Kobayashi, S. *Macromol. Biosci.* **2001**, *1*, 40–44.

(180) Shi, H.; Zhao, Y.; Zhang, X.; Zhou, Y.; Xu, Y.; Zhou, S.; Wang, D.; Han, C. C.; Xu, D. *Polymer (Guildf).* **2004**, *45*, 6299–6307.

(181) Du, J.-Z.; Tang, L.-Y.; Song, W.-J.; Shi, Y.; Wang, J. *Biomacromolecules* **2009**, *10*, 2169–2174.

(182) Duncan, R. *Nat. Rev. Drug Discov.* **2003**, *2*, 347–360.

(183) Jiang, X.; Smith, M. R.; Baker, G. L. *Macromolecules* **2008**, *41*, 318–324.

(184) Kim, H.; Olsson, J. V.; Hedrick, J. L.; Waymouth, R. M. *ACS Macro Lett.* **2012**, 845–847.

(185) Naolou, T.; Weiss, V. M.; Conrad, D.; Busse, K.; Mäder, K.; Kressler, J. In *Tailored Polymer Architectures for Pharmaceutical and Biomedical Applications*; Scholz, C.; Kressler, J., Eds.; American Chemical Society: Washington, DC, 2013; Vol. 1135, pp. 39–52.

(186) Valdimir P. Torchilin *Nanoparticulates as drug carriers*; Imperial College Press, 2006; p. 65.

(187) Zhang, J.-F.; Ren, W.; Sun, X.; Meng, Y.; Du, B.; Zhang, X. *Macromolecules* **2011**, *44*, 9882–9886.

(188) Woodruff, M. A.; Hutmacher, D. W. *Prog. Polym. Sci.* **2010**, *35*, 1217–1256.

(189) Sinha, V. R.; Bansal, K.; Kaushik, R.; Kumria, R.; Trehan, A. *Int. J. Pharm.* **2004**, *278*, 1–23.

(190) Letchford, K.; Zastre, J.; Liggins, R.; Burt, H. *Colloids Surfaces B Biointerfaces* **2004**, *35*, 81–91.

(191) Du, Z.; Xu, J.; Fan, Z. *Macromolecules* **2007**, *40*, 7633–7637.

(192) Rajagopal, K.; Mahmud, A.; Christian, D. a; Pajerowski, J. D.; Brown, A. E. X.; Loverde, S. M.; Discher, D. E. *Macromolecules* **2010**, *43*, 9736–9746.

(193) Ahmed, F.; Discher, D. E. *J. Control. release* **2004**, *96*, 37–53.

(194) Kim, Y.; Dalhaimer, P.; Christian, D. a; Discher, D. E. *Nanotechnology* **2005**, *16*, S484–S491.

(195) Sugihara, S.; Blanazs, A.; Armes, S. P.; Ryan, A. J.; Lewis, A. L. *J. Am. Chem. Soc.* **2011**, *133*, 15707–13.

(196) Blanazs, A.; Ryan, A. J.; Armes, S. P. *Macromolecules* **2012**, *45*, 5099–5107.

(197) Cai, S.; Vijayan, K.; Cheng, D.; Lima, E. M.; Discher, D. E. *Pharm. Res.* **2007**, *24*, 2099–2109.

(198) Geng, Y.; Dalhaimer, P.; Cai, S.; Tsai, R.; Tewari, M.; Minko, T.; Discher, D. E. *Nat. Nanotechnol.* **2007**, *2*, 249–255.

(199) Geng, Y.; Discher, D. E. *J. Am. Chem. Soc.* **2005**, *127*, 12780–12781.

(200) Geng, Y.; Discher, D. E. *Polymer.* **2006**, *47*, 2519–2525.

(201) Ishizu, K.; Kakinuma, H. *J. Polym. Sci. Part A Polym. Chem.* **2005**, *43*, 63–70.

(202) Beers, K. L.; Gaynor, S. G.; Matyjaszewski, K.; Sheiko, S. S.; Möller, M. *Macromolecules* **1998**, *31*, 9413–9415.

(203) Ferrari, R.; Yu, Y.; Morbidelli, M.; Hutchinson, R. A.; Moscatelli, D. *Macromolecules* **2011**, *44*, 9205–9212.

(204) Cheng, X.; Ma, J.; Zhi, J.; Yang, X.; Hu, A. *Macromolecules* **2010**, *43*, 909–913.

(205) Hans, M.; Xiao, Y.; Keul, H.; Heise, A.; Moeller, M. *Macromol. Chem. Phys.* **2009**, *210*, 736–746.

(206) Xie, M.; Dang, J.; Han, H.; Wang, W.; Liu, J.; He, X.; Zhang, Y. *Macromolecules* **2008**, *41*, 9004–9010.

(207) Li, C.; Ge, Z.; Fang, J.; Liu, S. *Macromolecules* **2009**, *42*, 2916–2924.

(208) Hoogenboom, R.; Moore, B. C.; Schubert, U. S. *Chem. Commun.* **2006**, 4010–4012.

(209) Lendlein, A.; Sisson, A. *Handbook of Biodegradable Polymers: Isolation, Synthesis, Characterization and Applications*; Wiley-VCH, 2011; p. 432.

(210) Giacomelli, C.; Lafitte, G.; Borsali, R. *Macromol. Symp.* **2005**, *229*, 107–117.

(211) Luo, L.; Tam, J.; Maysinger, D.; Eisenberg, A. *Bioconjug. Chem.* **2002**, *13*, 1259–1265.

(212) Wu, C.; Siddiq, M.; Bo, S.; Chen, T. *Macromolecules* **1996**, *29*, 3157–3160.

(213) Cau, F.; Lacelle, S. *Macromolecules* **1996**, *29*, 170–178.

(214) Riess, G. *Prog. Polym. Sci.* **2003**, *28*, 1107–1170.

(215) Kyeremateng, S. O.; Henze, T.; Busse, K.; Kressler, J. *Macromolecules* **2010**, *43*, 2502–2511.

(216) Ma, J.; Guo, C.; Tang, Y.; Liu, H. *Langmuir* **2007**, *23*, 9596–9605.

(217) Dalhaimer, P.; Bates, F. S.; Discher, D. E. *Macromolecules* **2003**, *36*, 6873–6877.

(218) Jain, S.; Bates, F. S. *Science.* **2003**, *300*, 460–464.

(219) Liu, F.; Hu, J.; Liu, G.; Hou, C.; Lin, S.; Zou, H.; Zhang, G.; Sun, J.; Luo, H.; Tu, Y. *Macromolecules* **2013**, *46*, 2646–2657.

(220) He, W.-N.; Zhou, B.; Xu, J.-T.; Du, B.-Y.; Fan, Z.-Q. *Macromolecules* **2012**, *45*, 9768–9778.

(221) Matharu, Z.; Bandodkar, A. J.; Gupta, V.; Malhotra, B. D. *Chem. Soc. Rev.* **2012**, *41*, 1363–402.

(222) Reuter, S.; Amado, E.; Busse, K.; Kraska, M.; Stühn, B.; Tschierske, C.; Kressler, J. *J. Colloid Interface Sci.* **2012**, *372*, 192–201.

(223) Schief, W. R.; Antia, M.; Discher, B. M.; Hall, S. B.; Vogel, V. *Biophys. J.* **2003**, *84*, 3792–3806.

(224) Everaars, M. D.; Marcelis, A. T. M.; Sudhölter, E. J. R. *Thin Solid Films* **1994**, *242*, 78–82.

(225) Joachimi, D.; André, Ö.; Rettig, W.; Tschierske, C. *J. Chem. Soc. Perkin Trans. 2* **1994**, 2011–2019.

(226) Janietz, D. *J. Mater. Chem.* **1998**, *8*, 265–274.

(227) Mussone, P. G.; Ip, A. W. F.; Schroeder, S. L. M.; Murray, B. S.; Miller, A. F. *Langmuir* **2007**, *23*, 3766–3773.

(228) Yim, K. S.; Brooks, C. F.; Fuller, G. G.; Winter, D.; Eisenbach, C. D. *Langmuir* **2000**, *16*, 4325–4332.

(229) Wang, M.; Braun, H.-G.; Meyer, E. *Polymer.* **2003**, *44*, 5015–5021.

(230) Reiter, G.; Sommer, J.-U. *J. Chem. Phys.* **2000**, *112*, 4376–4383.

(231) Reiter, G.; Sommer, J.-U. *Phys. Rev. Lett.* **1998**, *80*, 3771–3774.

(232) Beers, K. L.; Douglas, J. F.; Amis, E. J.; Karim, A. *Langmuir* **2003**, *19*, 3935–3940.

(233) Sommer, J.-U.; Reiter, G. *J. Chem. Phys.* **2000**, *112*, 4376–4383.

(234) Mareau, V. H.; Prud'homme, R. E. *Macromolecules* **2002**, *35*, 5338–5341.

(235) Schönherr, H.; Frank, C. W. *Macromolecules* **2003**, *36*, 1188–1198.

(236) Schönherr, H.; Frank, C. W. *Macromolecules* **2003**, *36*, 1199–1208.

(237) Mareau, V. H.; Prud'homme, R. E. *Macromolecules* **2003**, *36*, 675–684.

(238) Sakai, Y.; Imai, M.; Kaji, K.; Tsuji, M. *Macromolecules* **1996**, *29*, 8830–8834.

(239) Mareau, V. H.; Prud'homme, R. E. *Macromolecules* **2005**, *38*, 398–408.

(240) Reiter, G.; Castelein, G.; Sommer, J.-U. *Phys. Rev. Lett.* **2001**, *86*, 5918–5921.

(241) Ferreiro, V.; Douglas, J. F.; Warren, J.; Karim, A. *Phys. Rev. E Stat. Nonlinear, Soft Matter Phys.* **2002**, *65*, 051606.

(242) Galán, M.; Valle, E. Del *Chemical engineering: trends and developments*; Galán, M. A.; Del Valle, E. M., Eds.; John Wiley & Sons, Ltd: Chichester, UK, 2005.

(243) Li, B.; Esker, A. R. *Langmuir* **2007**, *23*, 2546–2554.

(244) Amado, E.; Kerth, A.; Blume, A.; Kressler, J. *Langmuir* **2008**, *24*, 10041–53.

(245) Mareau, V. H.; Prud'homme, R. E. *Macromolecules* **2005**, *38*, 398–408.

(246) Berrill, S. A.; Heatley, F.; Collett, J. H.; Attwood, D.; Booth, C.; Fairclough, J. P. A.; Ryan, A. J.; Viras, K.; Dutton, A. J.; Blundell, R. S. *J. Mater. Chem.* **1999**, *9*, 1059–1063.

(247) Qiao, C.; Zhao, J.; Jiang, S.; Ji, X.; An, L.; Jiang, B. *J. Polym. Sci. Part B Polym. Phys.* **2005**, *43*, 1303–1309.

(248) Kressler, J.; Wang, C.; Kammer, H. W. *Langmuir* **1997**, *13*, 4407–4412.

(249) Chen, H.-L.; Li, L.-J.; Ou-Yang, W.-C.; Hwang, J. C.; Wong, W.-Y. *Macromolecules* **1997**, *30*, 1718–1722.

(250) Yu-Su, S. Y.; Sheiko, S. S.; Lee, H.; Jakubowski, W.; Nese, A.; Matyjaszewski, K.; Anokhin, D.; Ivanov, D. a. *Macromolecules* **2009**, *42*, 9008–9017.

(251) Li, B.; Esker, A. R. *Langmuir* **2007**, *23*, 574–581.

(252) Li, B.; Wu, Y.; Liu, M.; Esker, A. R. *Langmuir* **2006**, *22*, 4902–4905.

(253) Kressler, J.; Wang, C.; Kammer, H. W. *Langmuir* **1997**, *13*, 4407–4412.

(254) Leiva, A.; Farias, A.; Gargallo, L.; Radic´, D. *Eur. Polym. J.* **2008**, *44*, 2589–2598.

(255) Joncheray, T. J.; Denoncourt, K. M.; Meier, M. A. R.; Schubert, U. S.; Duran, R. S. *Langmuir* **2007**, *23*, 2423–2429.

(256) De Samaniego, M. S. S.; Miller, a. F. *Macromol. Symp.* **2007**, *256*, 167–174.

(257) Naolou, T.; Meister, A.; Schöps, R.; Pietzsch, M.; Kressler, J. *Soft Matter* **2013**, *9*, 10364.

(258) Peetla, C.; Graf, K.; Kressler, J. *Colloid Polym. Sci.* **2006**, *285*, 27–37.

(259) Hu, H.; Dorset, D. L. *Macromolecules* **1990**, *23*, 4604–4607.

(260) Bittiger, H.; Marchessault, R. H.; Niegisch, W. D. *Acta Crystallogr. Sect. B Struct. Sci.* **1970**, *26*, 1923–1927.

(261) Kundu, S.; Datta, A.; Hazra, S. *Langmuir* **2005**, *21*, 5894–900.

(262) Parazak, D. P.; Uang, J. Y.-J.; Turner, B.; Stine, K. J. *Langmuir* **1994**, *10*, 3787–3793.

(263) Kundu, S.; Datta, a.; Hazra, S. *Phys. Rev. E* **2006**, *73*, 1–7.

(264) Vaknin, D.; Bu, W.; Satija, S. K.; Travesset, A. *Langmuir* **2007**, *23*, 1888–1897.

(265) Bu, W.; Vaknin, D. *Langmuir* **2008**, *24*, 441–447.

(266) Rabinovitch, W.; Robertson, R. F.; Mason, S. G. *Can. J. Chem.* **1960**, *38*, 1881–1890.

(267) Pfefferkorn, D.; Pulst, M.; Naolou, T.; Busse, K.; Balko, J.; Kressler, J. *J. Polym. Sci. Part B Polym. Phys.* **2013**, n/a–n/a.

(268) Yan, Q.; Yuan, J.; Zhang, F.; Sui, X.; Xie, X.; Yin, Y.; Wang, S.; Wei, Y. *Biomacromolecules* **2009**, *10*, 2033–42.

(269) Anderson, P. M.; Wilson, M. R. *J. Chem. Phys.* **2004**, *121*, 8503–8510.

(270) Miller, A. F.; Richards, R. W.; Webster, J. R. P. *Macromolecules* **2001**, *34*, 8361–8369.

Acknowledgments

I would like first to express my deepest gratitude and sincere appreciation to my Ph.D. supervisor, Prof. Dr. Jörg Kressler, for his valuable guidance, motivation, suggestions and for giving me the opportunity to work under his mentorship. He always encouraged me to develop myself as an instructor and independent researcher which I strongly believe will help me throughout the rest of my scientific career. It was a privilege for me to work in his laboratory at Martin Luther University.

I am indebted to Dr. Karsten Busse for his assistance and guidance in the field of physical chemistry of polymers. I am also grateful to Dr. Samuel Kyeremateng and Dr. Christian Albrecht who helped me tremendously at the early phase of this work to develop my chemical synthesis skills.

I would also like to acknowledge all current and previous members of Prof. Jörg Kressler's group including Dr. Henning Kausche, Dr. Zofia Funke, Dr. Regina Scöps, Dr. Sacha Reuter, Dr. Dirk Pfefferkorn, Dr. Zheng Li, Dr. Elkin Amado, Frau Claudia Hochbach and Frau Elvira Stark. Many thanks go to Frau Susanne Tanner for the GPC measurements, Frau Otten in Physics Department, for the IR and Raman spectroscopy and for Mr. Xiaopeng Li for the SEM measurements.

I offer my thanks to Prof. Dr Karsten Mäder from the Pharmacy Institute and his students Dr. Andreas Schädlich and Dipl.-Pharm. Verena Weiss for the interesting scientific cooperation. The collaboration with Prof. Mäder group has indeed helped strengthen my research work and made it of more value.

I would also like to thank Dr. Mohamed Farag for his encouragement and always inspiring instructions.

I am deeply grateful to my parents who devoted and sacrificed their life to reach this point of my study. They always raised me with a love of science and supported me in all my scientific pursuits.

Finally, I come to address my appreciation to my wife for her love, moral support, and kind indulgence over the years of this thesis.

Curriculum Vitae

Personal Details:

Name: Toufik Naolou
Date of Birth: August 1st 1979
Place of Birth: Aleppo, Syria
Nationality: Syrian
Marital Status: Married

Educational Details:

06/2007 - 10/2013   Ph.D. student at the Institute of Chemistry Martin-Luther-Universität Halle-Wittenberg, Halle (Saale), in the groups of Prof. Dr. Jörg Kreßler (Physical Chemistry of Polymers).

09/2002 - 06/2004   Diploma of "Organic Chemistry", Aleppo University, Aleppo, Syria.

09/1998-06/2002   Bachelor of "Applied Chemistry", Aleppo University, Aleppo, Syria.

Work experience

2010-2013   Teaching Assistant, the Institute of Chemistry, Martin-Luther-Universität, Halle-Wittenberg.
- Teaching the practice of "Physikalische Chemie für Pharmazeuten" course for Pharmacy students.
- Teaching practice of "physical chemistry" for Master student

2006-2007   Teaching Assistant, Faculty of Agricultural Engineering, Al-Furate University, Dayr az-Zawr, Syria.

- Teaching "General Chemistry" and "Organic Chemistry" (Practice)

2005-2007   Senior Ink Development Chemist, "Mix Colour" to prepare inkjets, Aleppo, Syria

2004-2005   In Charge of Fertilizer Production Unit, Al Tahhan Institution for Manufacturing Pesticides & Fertilizers

Publications

1. Naolou, T.; Busse, K.; Kressler, J. Synthesis of well-defined graft copolymers by combination of enzymatic polycondensation and "click" chemistry. *Biomacromolecules* **2010**, *11*, 3660–3667.

2. Schädlich, A.; Naolou, T.; Amado, E.; Schöps, R.; Kressler, J.; Mäder, K. Noninvasive in vivo monitoring of the biofate of 195 kDa poly(vinyl alcohol) by multispectral fluorescence imaging. *Biomacromolecules* **2011**, *12*, 3674–3683.

3. Weiss, V. M.; Naolou, T.; Hause, G.; Kuntsche, J.; Kressler, J.; Mäder, K. Poly(glycerol adipate)-fatty acid esters as versatile nanocarriers: From nanocubes over ellipsoids to nanospheres. *J. Control. Release* **2012**, *158*, 156–164.

4. Weiss, V. M.; Naolou, T.; Amado, E.; Busse, K.; Mäder, K.; Kressler, J. Formation of structured polygonal nanoparticles by phase-separated comb-like polymers. *Macromol. Rapid Commun.* **2012**, *33*, 35–40.

5. Weiss, V. M.; Naolou, T.; Groth, T.; Kressler, J.; Mäder, K. *J.* In vitro toxicity of stearoyl-poly(glycerol adipate) nanoparticles. *Appl. Biomater. Funct. Mater.* **2012**, *10*, 163–169.

6. Naolou, T.; Jbeily, M.; Scholtysek, P.; Kressler, J. Synthesis and Characterization of Stearoyl Modified Poly (Glycerol Adipate) Containing ATRP Initiator on its Backbone. *Adv. Mater. Res.* **2013**, *812*, 1–11.

7. Pfefferkorn, D.; Pulst, M.; Naolou, T.; Busse, K.; Balko, J.; Kressler, J. Crystallization and melting of poly(glycerol adipate)-based graft copolymers with single and double crystallizable side chains. *J. Polym. Sci. Part B Polym. Phys.* **2013**, DOI: 10.1002/polb.23373.

8. Naolou, T.; Meister, A.; Schöps, R.; Pietzsch, M.; Kressler, J. Synthesis and characterization of graft copolymers able to form polymersomes and worm-like aggregates. *Soft Matter* **2013**, 9, 10364.

9. Jbeily, M.; Naolou, T.; Bilal, M.; Amado, E.; Kressler, J. Enzymatically synthesized polyesters with pendant OH-groups as macroinitiators for the preparation of well-defined graft copolymers by ATRP. *Polym. Int.* Accepted.

Book Chapter

1. Naolou, T.; Weiss, V. M.; Conrad, D.; Busse, K.; Mäder, K.; Kressler, J. Fatty acid modified poly(glycerol adipate) - polymeric analogues of glycerides, In *Tailored Polymer Architectures for Pharmaceutical and Biomedical Applications*; Scholz, C.; Kressler, J., Eds.; American Chemical Society: Washington, DC, 2013; Vol. 1135, pp. 39–52.

Meeting Abstracts

1. Jang, Y.; Schaedlich, A.; Schoeps, R.; Maeder, K.; <u>Naolou, T.</u>; Kressler, J. Poly(vinyl alcohol) hydrogel for postsurgical adhesion prevention. *240th ACS National Meeting*, Boston, MA, United States, August 2010.

2. <u>Naolou, T.</u>; Busse, K.; Pietzsch, M.; Kressler, J. Modification of poly(glycerol adipate) and its surface activity. *240th ACS National Meeting*, Boston, MA, United States, August 2010.

3. <u>Naolou, T.</u>; Busse, K.; Pietzsch, M.; Kressler, J. Modification of poly(glycerol adipate) and its surface activity. *Polymeric Materials (P.2010)*, Halle (Saale), September 2010.

4. <u>Naolou, T.</u>; Busse, K.; Kressler, J. Synthesis and characterization of amphiphilic graft copolymer by combination of enzymatic polycondensation and "click" chemistry. *Polymers in Biomedicine and Electronics*, Berlin, October 2010.

5. Kressler, J.; <u>Naolou, T.</u>; Conrad, D.; Busse, K.; Amado, E.; Weiss, V.; Mader, K. Fatty acid modified poly(glycerol adipate)- polymeric analogues of glycerides. *243rd ACS National Meeting*, San Diego, CA, United States, March 2012.

6. <u>Naolou, T</u>.; Busse, K.; Kressler, J. Biocompatible graft copolymer based on Poly(glycerol adipate). *243rd ACS National Meeting*, San Diego, CA, United States, March, 2012.

7. <u>Naolou, T</u>.; Kressler, J.; Schops, R. Preparation of stable worm-like aggregates using amphiphilic biodegradable graft copolymers. *245th ACS National Meeting*, New Orleans, LA, United States, April 2013.

Oral Presentation

<u>Naolou, T</u> Enzymatic Synthesis of Amphiphilic Polyesters and Their Application in Pharmacy, *Polymerwerkstoffe (P2012)*, Halle (Saale) 2012.

Erklärung

Hiermit erkläre in an Eides statt, dass ich die vorliegende Arbeit selbständig und ohne fremde Hilfe verfasst habe. Ich habe keine anderen Quellen und Hilfsmittel als die angegebenen verwendet und anderen Werken wörtlich oder inhaltlich entnommene Stellen als solche gekennzeichnet. Diese Arbeit habe ich an keiner anderen Hochschule vorgelegt und mich zu keinem früheren Zeitpunkt um den Doktorgrad beworben.

Toufik Naolou

Halle (Saale), 10.12.2013